Enhancing Freeway Merge Section Operations via Vehicle Connectivity

Kyungwon Kang

Dissertation submitted to the faculty of the
Virginia Polytechnic Institute and State University
in partial fulfillment of the requirements for the degree of

Doctor of Philosophy
in
Civil Engineering

Hesham A. Rakha, Chair
Kathleen L. Hancock
Hao Chen
Hao Yang

September 25, 2019
Blacksburg, VA

Keywords: Freeway merge section, Decision-making, Merging behaviors, Game theory, Cooperative maneuver planning, Optimal lane selection, Connected and automated vehicles

Enhancing Freeway Merge Section Operations via Vehicle Connectivity

Kyungwon Kang

ABSTRACT

Driving behavior considerably affects the transportation system, especially lane-changing behavior occasionally cause conflicts between drivers and induce shock waves that propagate backward. A freeway merge section is one of locations observed a freeway bottleneck, generating freeway traffic congestion. The emerging technologies, such as autonomous vehicles (AVs) and vehicle connectivity, are expected to bring about improvement in mobility, safety, and environment. Hence the objective of this study is to enhance freeway merge section operations based on the advanced technologies. To achieve the objective, this study modeled the non-cooperative merging behavior, and then proposed the cooperative applications in consideration of a connected and automated vehicles (CAVs) environment. As a tactical process, decision-making for lane-changing behaviors is complicated as the closest following vehicle in the target lane also behaves concerning to the lane change (reaction to the lane-changing intention), i.e., there is apparent interaction between drivers. To model this decision-making properly, this study used the game theoretical approach which is the study of the ways in which interacting choices of players. The game models were developed to enhance the microscopic simulation model representing human driver's realistic lane-changing maneuvers. The stage game structure was designed and payoff functions corresponding to the action strategy sets were formulated using driver's critical decision variables. Furthermore, the repeated game concept which takes previous game results into account was introduced with the assumption that drivers want to maintain initial decision in competition if there is no significant change of situations. The validation results using empirical data provided that the developed stage game has a prediction accuracy of approximately 86%, and the superior performance of the repeated game was verified by an agent-based simulation model, especially in a competitive scenario. Specifically, it helps a simulation model to not fluctuate in decision-making. Based on the validated non-cooperative game model, in addition, this study proposed the cooperative maneuver planning avoiding the non-cooperative maneuvers with prediction of the other vehicle's desired action. If a competitive action is anticipated, in other words, a CAV changes its action to be cooperative without selfish driving. Simulation results showed that the proposed cooperative maneuver planning can improve traffic flow at a freeway merge section. Lastly, the optimal lane selection (OLS) algorithm was also proposed to assist lane selection in consideration of real-time downstream traffic data transferred via a long-range wireless communication. Simulation case study on I-66 highway proved that the proposed OLS can improve the system-wide freeway traffic flow and lane allocation. Overall, the present work addressed developing the game model for merging maneuvers in a traditional transportation

system and suggesting use of efficient algorithms in a CAV environment. These findings will contribute to enhance performance of the microscopic simulator and prepare the new era of future transportation system.

Enhancing Freeway Merge Section Operations via Vehicle Connectivity

Kyungwon Kang

GENERAL AUDIENCE ABSTRACT

Driving behaviors considerably affect the traffic flow; especially a lane change occasionally forces rear vehicles in a target lane to decrease speed or stop, hence it is considered as one of primary sources causing traffic congestion. U.S. Department of Transportation (DOT) announced that freeway bottleneck including merge section contributes to freeway traffic congestion more than 40 percent while traffic incidents count for only 25 percent of freeway congestion. This study, therefore, selected a freeway merge section, where mandatory lane changes are required, as a target area for the study. The emerging technologies, such as autonomous vehicles (AVs) and vehicle connectivity, are expected to bring about improvement in mobility, safety, and environment. Based upon these backgrounds, the objective of this study was determined to enhance freeway merge section operations based on the advanced technologies.

To achieve the objective, first this study focused on understanding driving behaviors of human drivers. Decision-making for lane-changing behaviors is complicated as the closest following vehicle in the target lane also behaves concerning to the lane change (reaction to the lane-changing intention), i.e., there is apparent interaction between drivers. For example, the vehicle sometimes interferes the merging vehicle's lane-changing by decreasing a gap. To model the decision-making properly, this study modeled the non-cooperative merging behaviors using a game theoretical approach which mathematically explains the interaction (e.g., cooperation or conflict) between intelligent decision-makers. It was modeled for two vehicles, i.e., the merging vehicle in acceleration lane and a following vehicle in freeway rightmost lane, with possible actions of each vehicle. This model includes how each vehicle chooses an action in consideration of rewards. The developed model showed prediction accuracy of approximately 86% against empirical data collected at a merge section on US 101 highway. This study additionally evaluated the proposed model's rational decision-making performance in various merging situations using an agent-based simulation model. These evaluation results indicate that the developed model can depict merging maneuvers based on practical decision-making. Since most existing lane-changing models were developed from the standpoint of the lane-changing vehicle only, this study anticipates that a lane-changing model including practical decision-making process can be used to precisely analyze traffic flow in microscopic traffic simulation. Additionally, an AV should behave as a human-driven vehicle in order to coexist in traditional transportation system, and can predict surrounding vehicle's movement. The developed model in this study can be a part of AV's driving strategy based on perception of human behaviors.

In a future transportation environment, vehicle connectivity enables to identify the surrounding vehicles and transfer the data between vehicles. Also, autonomous driving behaviors can be programmed to reduce competition by predicting behaviors of surrounding human-driven vehicles. This study proposed the cooperative maneuver planning which future connected and automated vehicles (CAVs) avoid choosing the non-cooperative actions based on the game model. If a competitive action is anticipated, in other words, a CAV changes its action to be cooperative without selfish driving. Simulation results showed that the proposed cooperative maneuver planning can improve traffic flow at a freeway merge section. Lastly, the optimal lane selection (OLS) algorithm was also proposed to provide a driver the more efficient lane information in consideration of real-time downstream traffic data transferred via a long-range wireless communication. Simulation case study on I-66 highway proved that the proposed OLS can improve the system-wide freeway traffic flow and lane allocation. Overall, the present work addressed developing the game model for merging maneuvers in a traditional transportation system and suggesting use of efficient algorithms in a CAV environment. These findings will contribute to enhance performance of the microscopic simulator and prepare the new era of future transportation system.

Acknowledgements

I would like to express most sincere gratitude to my advisor, Dr. Hesham A. Rakha, for his continuous support and encouragement to finish my studies. His warm-hearted and careful guidance helped me to enhance my Ph.D. research in all the time. I also want to thank my committee members, Dr. Kathleen Hancock, Dr. Hao Chen, and Dr. Hao Yang, for their insightful advisories. This dissertation would have not been completed without their guidance.

I have had very grateful experience in Blacksburg, VA, USA. I really thank to my friends and colleagues who share happy memories I have. I am going to step forward based on this achievement.

Lastly, I am very grateful to my wife, Yoonmi Yang, for her encouragement during my studies at Virginia Tech. I cannot forget our start as a married couple in this peaceful and beautiful place. I also would like to thank to my family for their endless love and support throughout my life.

Table of contents

List of Figures

List of Tables

Chapter 1. Introduction

The first chapter introduces the research objectives followed by the problem statement related to lane-changing model. Thereafter, the contributions and layout of this dissertation are presented.

1.1 Background

Driving behavior highly affects the safety and throughput of the transportation system [1]. In particular, lane-changing behavior, which can occasionally cause conflicts between drivers, induce shock waves that propagate backward, especially in congested traffic streams [2]. In addition, merging area is one of locations observed a freeway bottleneck if added merging traffic leads to exceeding the lane capacity. It generates congestion starting at the bottleneck location and then spills back while the upstream arriving flow maintains sufficiently high [3]. U.S. Department of Transportation (DOT) announced that freeway bottleneck is a major source which contributes to freeway traffic congestion more than 40 percent while traffic incidents count for only 25 percent of freeway congestion [4]. Empirical observations show that whenever a bottleneck is activated, moreover, lane-changing maneuvers cause capacity drop by discharge flow may be 5% to 20% lower than the roadway capacity [5-8]. In order to precisely analyze traffic flow, therefore, development of the state-of-the-art lane-changing model is considerably important.

The applications of lane-changing models can be broadly classified into two groups: adaptive cruise control and microscopic traffic simulation [1]. Driving assistance models for adaptive cruise control consist of collision prevention models and automation models [9]. In addition, driving decision models focus on drivers' lane changing decisions under different traffic conditions and under different situational and environmental characteristics [9]. Lane-changing models were proposed based on various methodologies, which are reviewed in the next section, and calibrated based on field data collected on freeways. These models are an important component of microscopic traffic simulation [10]. Most models, however, focus on only lane-changing vehicle in decision-making and vehicle control. It could be a weakness to be used in microscopic traffic simulation because interaction with surrounding vehicles is critical in lane-changing. In detail, drivers of surrounding vehicles, especially the closest following vehicle in target lane, react after recognition of lane-changing intention. For example, a human driver occasionally does not allow a lane change. Even though competitive lane-changing case is barely observed, decision-making considering drivers' interaction should be studied in order to develop a precise lane-changing model.

Today, the automobile industry is on the cusp of a technological transformation that holds promise to catalyze an unprecedented advance in safety and mobility on roads and highways. The development of advanced automated vehicle technologies, including fully self-driving cars, may prove to be the greatest personal transportation revolution since the popularization of the personal automobile nearly a century ago [11]. The development of advanced vehicle technologies is expected to bring about new transportation paradigms by increase in safety, mobility, system efficiency, and decrease in negative environmental impacts. In this context, automated vehicles (AVs) have been developed by automotive and information technology (IT) industry. In order to successfully transform transportation systems from traditional systems to the connected and

automated systems, government and administration of worldwide countries are establishing comprehensive plan for AV initiatives [12].

Researchers have studied to equip sensors for detection of surrounding objects and road infrastructure, to process the earned data, and to develop driving strategies based on appropriate decision-making process, that is, the AV has been developed to substitute a human driver. It is recently tested/operated in roadways as a self-driving car, although many challenges to driving performance, ethical dilemmas, and responsibility of unexpected accidents still remain. A potential advantage of the AV is to prevent human errors arisen from incautious and aggressive (or selfish) driving behavior. To harmonize AVs with human drivers in mixed traffic, driving strategies of AVs should be developed in consideration of prediction of human driver's non-cooperative driving behavior. It will contribute to ensure the safe interoperation of AVs with human operated vehicles by minimization of potential competition.

Prospective benefits within a connected and automated environment come from connectivity through vehicle-to-vehicle (V2V) and vehicle-to-infrastructure (V2I) communication. It implies that the connected and automated vehicle (CAV) can broadcast real-time data and use data shared by downstream traffic to determine its own driving strategy. Therefore, it enables to not only decide to be cooperative with surrounding vehicles but also consider system performance, not focusing on individual benefits only. As a part of lane-changing maneuvers, for example, the CAV can select a target lane in consideration of both speed performance of each lane and downstream traffic. It helps to minimize negative effect on traffic flow and improve lane allocation for CAVs in freeway. Furthermore, research efforts have been devoted to developing and testing cooperative strategies, such as platooning, eco-cooperative adaptive cruise control (Eco-CACC), cooperative lane-changing, and traffic flow control. As likewise previous efforts which prepare new transportation system, more practical applications based on the connectivity should be proposed for improving transportation system performance in freeway.

1.2 Problem Statement

1.2.1 Lack of Understanding of Decision-Making in Lane-Changing Models

Lane-changing models describe the practice of lane-changing at the microscopic level. Lane-changing consists of a defined trigger to change lanes (e.g., motivation, attractiveness, or incentive), a target lane choice, a decision-making for vehicle control and a rule to accept a gap. In addition, most lane-changing models do not consider decision-making process of a human driver. These models only focus on a subject vehicle which wants to merge onto the freeway. For example, the lag vehicle in the rightmost lane (i.e., target lane) of a freeway is affected by the driver’s awareness of the merging vehicle in the auxiliary lane. The driver of the following vehicle can decide to increase or decrease his or her speed. The driver of the merging vehicle can choose

to use the forward gap ahead of the lead vehicle or the backward gap behind the following vehicle in the target lane depending on relative speed, although the current gap distance is sufficient to merge. Consequently, the tactical merging decision-making behavior should be modeled as a part of a lane-changing model, which represents realistic human driving behaviors.

1.2.2 Need to Model Realistic Lane-Changing Maneuvers for Microscopic Traffic Simulation

Microscopic traffic simulator should represent realistic driving behavior in traffic flow. Capturing real life lane-changing scenarios greatly increases the difficulty of model specification. In order to increase the accuracy of microscopic traffic simulation models, it is important to ensure that lane-changing models are clearly understood, appropriately designed, and carefully calibrated. It is expected that the decision-making model for non-cooperative lane-changing, which was proposed in this study, improves performance of microscopic traffic simulation to be a robust simulation model.

1.2.3 Need to Develop the Driving Strategy for CAVs (or AVs)

As a new future transportation mode, CAV, i.e., connected self-driving vehicle, which does not need human's intervention, is expected to save lives, prevent injuries, and make roads safer. To provide ride-sharing transportation services or be operated instead of a human driver, development of the state-of-the-art driving strategy which is implemented onto CAV is necessary. Especially, execution of lane-changing maneuvers should take surrounding vehicles into account to avoid unnecessary competition with a human driver or other CAV. Therefore, precisely understanding of decision-making process helps CAV to predict of human driver's behavior in competitive situation. Lane-changing process, including acceleration control and decision about the time turning a signal on, is integrated into the state-of-the-art self-driving strategy of the CAV is required.

1.2.4 Need to Propose Practical Applications for Improving Traffic Flow within a Connected Transportation System

As described in background, the connected and automated transportation system has potential benefits. In contrast with the traditional transportation system, the connected and automated transportation system will be able cooperative interaction. Also, traffic will be managed to focus on system performance, not considering individual benefit only. Therefore, practical applications which can be utilized in the future should be proposed in order to improve system performance. In the traditional transportation systems, excessive lane changes, which are conducted by human drivers for making individual travel faster, cause bottlenecks, resulting in severe congestion. The connectivity between vehicles helps to manage traffic flow at merging section considering real-

time traffic condition. In addition, it is possible to produce optimal lane information for the connected vehicles in consideration of downstream traffic condition and forward lane performance. It enables to avoid selfish driving behavior decided using instantaneous information earned by sight view only.

1.3 Research Objectives

The research aims to enhance freeway merge section operations within the connected transportation environment. In order to develop the state-of-the-art in related research topics, this study is expected to answer the following questions:

1. How to enhance freeway merge section operations by considering vehicle connectivity?
2. How to model realistic decision-making between human drivers for merging maneuvers in freeway?
3. How to prepare the observations in the natural driving data to evaluate the proposed model?
4. How to further develop the proposed model to be used in microscopic traffic simulation?
5. How to develop the proposed decision-making model for cooperative behavior of the CAV in mixed traffic?
6. How to develop an algorithm to select the optimal lane for an individual CAV to improve system performance in freeway?
7. What are the potential performances of cooperative maneuver planning and lane selection in a connected environment?

To achieve the research objectives, the entire research scope is constituted, as shown in Figure 1-1. This study focuses on lane-changing, which is one of the most significant driving maneuvers. In this research, decision-making, which decides how control the vehicle to conduct lane-changing or react about other vehicle's lane-changing intention, is modeled using a game theoretical approach. Game theory is the study of mathematical models of conflict and cooperation between decision makers [5]. In this study, decision-making between human drivers in merging situations is validated using empirical driving data, and also the repeated game model is evaluated through a simulation study. Based on the developed game model, cooperative maneuver planning is proposed by consideration of CAVs. Moreover, the useful application related to lane selection is additionally proposed to minimize the number of lane changes and optimize distribution of vehicles on a freeway in the connected environment.

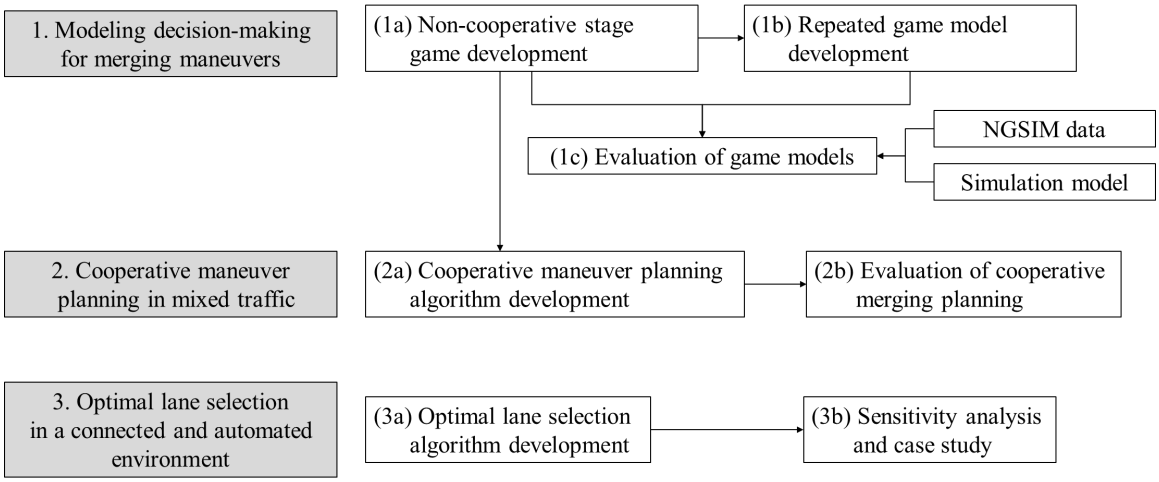

Figure 1-1. Research scope.

1.4 Research Contributions

The main contributions of the proposed works in this dissertation are listed below.

1. Modeling a decision-making for merging maneuvers on freeways

- Most existing lane-changing models focused lane-changing behavior at standpoint of the lane-changing vehicle only. To enhance a microscopic simulation model, this study models decision-making considering interaction between drivers.
- This study uses a game theoretical approach to model merging decision-making. A stage game structure including the players who participate in the game and their action strategies is designed to mimic realistic driver's behaviors. Payoff functions for each action strategy of both players are formulated by considering drivers' efficient decision factors.
- This study, in particular, introduces a repeated game concept taking previous decision-making results into account. Both the one-shot stage game and repeated game models are evaluated using the field data. The data preparation and classification of drivers' behaviors are extracted from naturalistic driving data.
- In addition, the efficiency of the repeated game model for use in a microscopic simulation model is verified by comparison of the one-shot game model.

2. Cooperative maneuver planning for the CAV

- Cooperative maneuver planning based on the developed game model is proposed in consideration of the CAV. In the mixed traffic the CAV predicts human driver's behaviors and then make a cooperative decision responding to a non-cooperative action strategy.

- To evaluate the proposed model, the simulation model based on the agent-based model (ABM) is developed. The validation of the simulation model is provided and then efficiency of the cooperative maneuver planning is presented.

3. Optimal lane selection algorithm in the connected environment

- The optimal lane selection algorithm is proposed to optimize lane distribution in entire freeway system. By decrease of the number of unnecessary lane changes and consideration of downstream traffic condition, the advanced traffic systems based on connectivity between vehicles provide travel faster than the traditional transportation systems.

1.5 Dissertation Layout

This research is organized into seven chapters, beginning with the introduction of the problem statements, research objectives, and research scope as the first chapter. The second chapter provides a review of the relevant literature on lane-changing behaviors, lane-changing models based on various methodologies, game theory-based driver's decision models. The third chapter models a stage game for decision-making between human drivers at merging section on freeways and proposes the game model based on the repeated game approach. To provide the elaborate and appropriate model to use in a microscopic traffic simulation, this study exhibits the stage game structure, the payoff functions formulation in three-phase stage game development, and the repeated game model are introduced. Next, the fourth chapter describes model evaluation based on field data and conducts a sensitivity analysis of the developed stage game model. A simulation study is followed to validate performance of the repeated game model. The fifth chapter proposes the cooperative maneuver planning for CAVs in a connected and automated environment. As an additional application, in the sixth chapter, the optimal lane selection algorithm within the connected transportation systems and verifies its efficiency through a case study. Finally, the dissertation study draw concluding remarks on this work and point out recommendations for future study.

The body structure and contents of this dissertation are based on the papers which have been published or are under review in journals and conferences as listed below:

[Journal publications]

[1] Kang, K. and Rakha, H. A. (2019). A Repeated Game Theory Lane-Changing Model for Merging Maneuvers. Submitted to *Sensors*.

[2] Kang, K., & Rakha, H. A. (2018). Modeling driver merging behavior: a repeated game theoretical approach. *Transportation Research Record: Journal of the Transportation Research Board*, *2672*(20), 144-153. doi: 10.1177/0361198118792982

[3] Kang, K., & Rakha, H. A. (2017). Game theoretical approach to model decision making

for merging maneuvers at freeway on-ramps. *Transportation Research Record: Journal of the Transportation Research Board*, *2623*(1), 19-28. doi: 10.3141/2623-03

[Book chapter]

[1] Kang, K. and Rakha, H. A. (2019). Development of a Decision Making Model for Merging Maneuvers: A Game Theoretical Approach. *Traffic and Granular Flow '17* (Ed. Hamdar, Samer H.), Springer. doi: 10.1007/978-3-030-11440-4

[Conference proceedings]

[1] Kang, K., Bichiou, Y., Rakha, H. A., Elbery A., and Yang, H. (2019, October). *Development and Testing of a Connected Vehicle Optimal Lane Selection Algorithm*. Accepted to present at 22nd International Conference on Intelligent Transportation Systems (ITSC) 2019, Auckland, New Zealand.

[2] Kang, K., Elbery A., Rakha, H. A., Bichiou, Y., and Yang, H. (2018, November). Optimal Lane Selection on Freeways within a Connected Vehicle Environment. In *Proceedings of 21st International Conference on Intelligent Transportation Systems (ITSC) 2018*, Maui, HI, USA.

[3] Kang, K. and Rakha, H. A. (2018). Modeling Driver Merging Behavior: A Repeated Game-Theoretical Approach. In *Proceedings of 97th Transportation Research Board Annual Meeting*, Washington, DC., USA.

[4] Kang, K. and Rakha, H. A. (2017, July). *Development of a Decision Making Model for Merging Maneuvers: A Game Theoretical Approach*. In Conference on Traffic and Granular Flow, Washington, DC., USA.

[5] Kang, K. and Rakha, H. (2017). A Game Theoretical Approach to Model Decision Making for Merging Maneuvers at Freeway On-Ramps. In *Proceedings of 96th Transportation Research Board Annual Meeting*, Washington, DC., USA.

Chapter 2. Literature Review

This chapter presents comprehensive literature review to consider previous related studies and further address the research needs. First, human driving behavior in lane-changing on the freeway are reviewed. Secondly, the lane-changing models are introduced in order to examine previous research efforts and identify research needs. Third subchapter investigates connected and automated transportation systems. Finally, applications related to lane-changing in consideration of future transportation systems are presented.

2.1 Lane-changing Types and Lane-changing Impacts on Traffics

2.1.1 Classification of lane changes

Lane changes on freeway are generally categorized into two types: discretionary lane-changing (DLC) and mandatory lane-changing (MLC) [10, 13-16]. DLC generally occurs when a driver is unsatisfied with current driving situation in current lane while the target lane shows better driving conditions. In addition, it is also motivated to avoid potential collision with a merging vehicle or performed for yielding to a tailgating vehicle which drives at higher speed. MLC is coercively required according to route choice. Merging and diverging on freeways, by taking on-ramp and off-ramp respectively, are main examples of MLC. Additionally, lane-changing due to lane drop is categorized as MLC. Based on NHTSA (2004), lane changes can be classified into eleven types (Note that figures showing all lane-changing types were reproduced in this study, referred to [17].):

1. Merging: Lane change to merge onto freeway via on-ramp

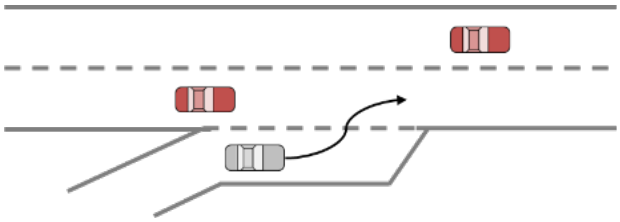

Figure 2-1. Lane change for merging.

2. Exiting (diverging) and preparation of exit: Lane changes associated with exiting (i.e., taking off-ramp or preparing to exit the freeway)

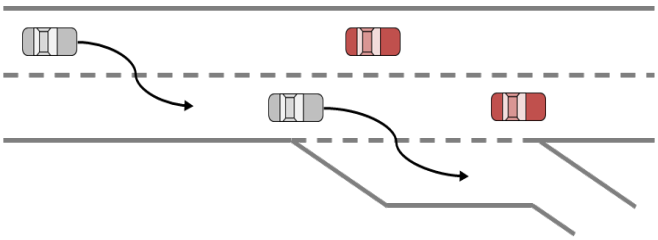

Figure 2-2. Lane changes to diverge and prepare exit.

3. Merging vehicle avoidance: Lane change to avoid potential collision (or expected deceleration) due to merging vehicle's lane-changing

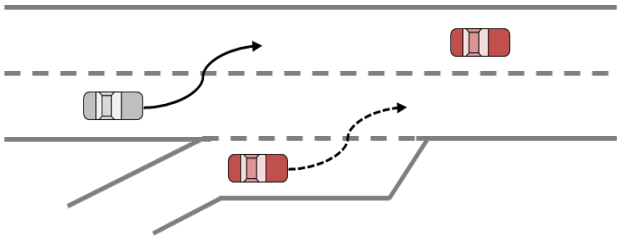

Figure 2-3. Lane change to avoid merging vehicle's entrance.

4. Passing a slow lead vehicle: Lane change to pass a vehicle which is moving slower than the lane-changing vehicle's preferred speed

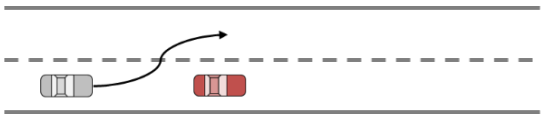

Figure 2-4. Lane change to pass a slow lead vehicle.

5. Returning to original lane: Lane change to return to original lane after deviating from it for any reasons

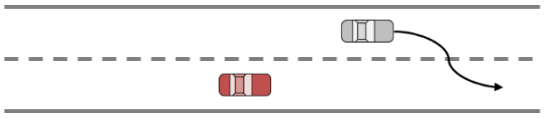

Figure 2-5. Lane change to return to original lane.

6. Yielding to a tailgating vehicle: Lane change due to a following vehicle approaching quickly; usually occurs while in the left lane. A driver of lane-changing vehicle may make lane change while the following vehicle is still at a considerable distance or time-to-collision (TTC) which is accounted for in the severity ratings.

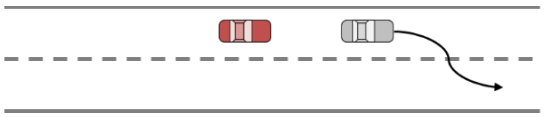

Figure 2-6. Lane change to yield to a tailgating vehicle

7. Rough roadway surface/obstacle avoidance: Lane change due to rough roadway surface or obstacle in road

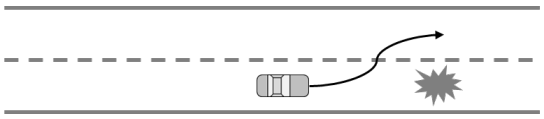

Figure 2-7. Lane change to avoid rough roadway surface or obstacle.

8. Lane drop: Lane change due to end of lane-changing vehicle's lane or work zone

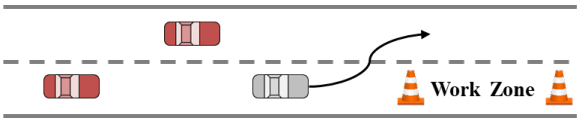

Figure 2-8. Lane change due to lane drop.

9. Added lane: Lane change due to addition of a lane

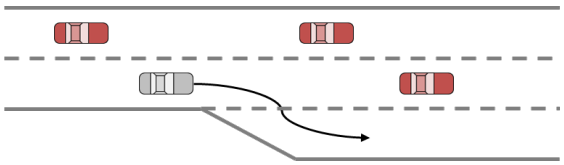

Figure 2-9. Lane change due to addition of a lane.

10. Unintended lane deviation: Unintended lane deviation due to distraction, drowsiness, poor driving, etc.; often only a partial lane change

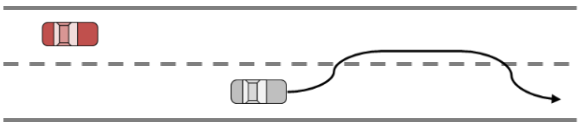

Figure 2-10. Unintended lane deviation.

11. Other lane-changing: Lane change for any other reasons or for no discernible reason

2.2 Lane-changing Behaviors on a Freeway

2.2.1 Lane-changing process

General lane-changing process can be categorized as a sequence of four steps: (1) the motivation to checking lane change necessity, (2) the lane selection to decide a target lane, (3) the gap choice in the target lane, and (4) the lane-changing execution through gap acceptance. To focus on research scope, this study reviews human driver's merging process in detail here. In merging, lane-changing motivation and lane selection are not required: lane-changing is definitely required to enter onto freeway and the target lane is already assigned (i.e., the rightmost lane). For the rest of lane-changing process, various factors (traffic condition, driver's characteristics, speed profile of the lane-changing vehicle and surrounding vehicles, spacing between vehicles, roadway design, and etc.) affect the gap choice and gap acceptance. Kondyli and Elefteriadou (2012) investigated merging process through field experiments in which thirty one people were participated. The

participants were asked to provide their thinking process as they were driving at merging area. Consequently, the observed merging process was summarized as following five steps [18]:

- Step 1: Drivers start accelerating on the on-ramp and first think about merging when they have a clear view of the freeway traffic.
- Step 2: Drivers evaluate the speed and the flow of traffic on the freeway, to assess how much they should adjust their own speed. They also account for the presence of other on-ramp vehicles ahead. If traffic is free-flowing, drivers leave a large gap to use later for acceleration. If the freeway is congested, they do not leave a large gap.
- Step 3: Drivers accelerate to a speed close to the freeway speed as they reach the acceleration lane. They also start looking at potential gaps.
- Step 4: This step includes the gap acceptance and merging process. In free-flowing conditions participants adjust their speed if necessary to fit a gap. Tasks such as actuating the turn signal and checking of the mirrors or blind spots follow. In congested conditions, drivers anticipate cooperation from the freeway vehicles.
- Step 5: After merging, most of the drivers move to the middle lane unless they need to exit at the next junction.

2.2.2 Merging maneuvers

As mentioned earlier, freeway mainline traffic and merging traffic streams compete at merging sections as bottlenecks, resulting in causing congestion observed in field [18]. Some studies mainly categorized the merging maneuvers as cooperative and forced merges [15, 19, 20], and free merge was considered as an additional category in other studies [19, 21]. The cooperative behavior generally indicates a yielding behavior by changing a lane to the left or decelerating to create gaps. In contrast, forced merge is defined when the SV compulsorily asks the LV to decelerate or change a lane for allowing the merge where the current gap is not acceptable. In [19, 21], free merge indicates a merging situation without apparent interactions between vehicles where the lead and lag gaps are sufficient for accepting a lane change.

In [21], participants answered which factors affects to each merging maneuver. They were asked to answer key factors related to cooperative merge at standpoint of the LV on the freeway mainline. Speed and acceleration capabilities of the merging vehicle is one of most important factors to perceive whether the merging vehicle can achieve a reasonable merging speed or not. If they think it can have acceptable speed, they would be willing to yield. Also, gap availability is important to show cooperative behavior by changing a lane to the left. Lastly, the merging vehicle's size and type is considered as well, e.g., they are reluctant to be cooperative for trucks. Regarding the forced merge, they chose main factors at standpoint of the SV on the freeway mainline, i.e., the merging vehicle. When the freeway is under congested traffic condition, they

are more likely to forcedly change a lane. In other words, average speed on the freeway, congestion level, and gap availability are key factors.

Besides traffic condition and both distance headway and relative speed profile with surrounding vehicles, individual characteristics, e.g., driver's aggressiveness, are important affecting to lane-changing behavior. It affects to choosing gap size, behaviors for cut-in, and reaction to the merging vehicle's lane change. In addition, geometric roadway design is a critical factor for deciding the driving behaviors.

2.2.3 Speed synchronization before merging

As the first step in merging process, one of features in merging process for the SV is to synchronize its speed with freeway vehicles [18]. Wan et al. (2013) analyzed the observed trajectories and they found that speed synchronization process exists before merging [22]. They classified merging vehicles based on a gap type, either original gap or forward gap, taken for merging into two categories, and compared absolute speed differences with the preceding and following vehicles on the target lane. The 97.7% of the merging cases which a forward gap was selected showed that the merging vehicle has a speed higher than the freeway mainline vehicles at the beginning of the acceleration lane, while the more than half of cases chosen an original gap showed similar speed with the freeway vehicles. As the results, they concluded that small differences of speeds are critical for successful merging. In addition, they found that speed synchronization process for merging consisted of two phases: 1) the SV maintained speed differences within 2 m/s and adjusted the location for merging; 2) they further synchronized the speed with the LV during lane-changing execution.

2.2.4 Gap acceptance in lane-changing

Gap acceptance is another critical issue in lane-changings studies. The principle of the gap acceptance models is to explain whether a driver accept a current gap or not. In this assessment, the gap will be accepted if the current gap is larger than a critical gap, otherwise it will be rejected. Regarding the merging behavior, gap acceptance models were modeled based on the assumption that the ramp traffic has no influence on the motorway traffic [23-25]. Ahmed (1999) modeled the lead and lag critical gap lengths using a binary logit model based on the assumption that they are log-normally distributed [15]. In addition, simulation models used a simplified gap acceptance model [26]. The critical gap has generally been modeled considering the driver's characteristics, roadway design, relative speed, traffic condition, and so on. In particular, the remaining distance to the end of the acceleration lane is a critical factor used for the MLC in comparison to the gap acceptance model for the DLC. At near the end of the acceleration lane, the accepted gap is smaller than that used at the beginning of the acceleration lane [27]. Also Wan et al. analyzed that the SV takes the relatively short gap for merge after overtaking the freeway vehicles in comparison to the merging cases which the original gaps are accepted [22].

2.3 Lane-changing Models

To represent lane-changing behaviors, lane-changing models were developed using various methodologies, and these can be classified into four groups: rule-based model, discrete-choice-based model, artificial intelligence model, and incentive-based model [1].

2.3.1 Rule-based models

Rule-based model is one of most popular methodologies based on the perspective of drivers [1]. Driver's decision-making in lane-changing process are simply defined as independent stage. Gipps (1986) initially introduced the lane-changing model covering various urban driving situations, intended for microscopic traffic simulation tools [13]. Gipps' model represented the lane-changing process as a decision tree with a series of fixed condition, and final output of this rule-based triggered event is a binary choice (i.e., change or not change) [1]. CORSIM model classified lane changes into two types: discretionary lane-changing (DLC) which occurs when a driver is unsatisfied with current driving situation in current lane while the target lane shows better driving conditions; mandatory lane-changing (MLC) which is coercively required according to route choice (i.e., lane change toward on-ramp or off-ramp) [16, 28]. Rahman et al. categorizes the game theory-based model, which explains lane-changing when a traffic conflict arises between the merging vehicle and closest following vehicle in the target lane, as rule-based model. Game theory, which is used in this paper, is the study of mathematical models of conflict and cooperation between decision-makers [29]. It focuses on decision-making in consideration of interaction between intelligent drivers. An advantage to use a game theoretical approach in that behaviors of a driver of following vehicle in the target lane take into account, while other approaches introduced above focused on only lane-changing vehicle's decision.

2.3.2 Discrete choice-based models

Second, discrete-choice-based-model is based on logit or probit model to explain lane-changing maneuvers. It decides lane-changing based on probabilistic results instead of binary answers. Ahmed modeled lane-changing motivation (i.e., trigger to change a lane), target lane choice, and gap acceptance, and this study modeled three categories of lane-changing: DLC, MLC, and forced merging (FM) which a gap is not sufficient but is conducted by a driver to execute a lane-changing maneuver in heavily congested traffic conditions [15]. Ahmed assumed that critical gaps follow a lognormal distribution to guarantee that they are nonnegative. Toledo et al. (2007) developed a probabilistic lane-changing decision model by combining MLC and DLC through a single utility function [30]. Both models developed by Ahmed and Toledo et al. considered drivers' heterogeneity, such as aggressiveness and driving skill level, by using random term as one of explanatory variables.

2.3.3 Fuzzy models

Next, Fuzzy model and Artificial neural network (ANN) model are representatives of artificial intelligence model. The former model considers human's imprecise perception and decision base, and incorporates more variables than the common mathematical models [31]. However, fuzzy model has disadvantage like unexpected difficulties and complexity in the fuzzy rules [31]. ANN model processes information using functional architecture and mathematical models that are similar to the neuron structure of the human brain [1]. Hunt and Lyons (1994) modeled the lane-changing decisions of drivers on dual carriageways [32]. Since neural network model is completely data-driven and requires field-collected traffic data, Hunt and Lyons used interactive driving simulation to train the model. Like this, a major disadvantage of artificial intelligence model is to require huge amount of data to be optimized and it needs training period.

2.3.4 Incentive-based models

Lastly, incentive-based model explains lane-changing desire by utilizing the defined incentive. In other words, this model has an assumption that a driver chooses to change lanes in order to maximize their benefits [1]. Minimizing overall braking induced by lane change (MOBIL) model, which were developed in [10], is based on the idea that to measure both the attractiveness and the risk associated with lane changes in terms of accelerations. Therefore, both the incentive criterion and the safety constraint are formed using the acceleration function of the underlying car-following model. In addition, the model describes the degree of passive cooperativeness among drivers using the politeness factor as a weight on the term for total advantage of the surrounding vehicles.

2.3.5 Lane selection model

General lane-changing models used in traditional vehicle systems include a trigger to change lanes, a target lane choice, and a rule to accept a gap [10, 15]. This study focuses on the target lane choice process, termed "lane selection" here. During lane selection, drivers compare their driving conditions in the current lane to the driving conditions in the left and right adjacent lanes and make a decision about whether to change lanes and which lane to move to [15]. In previous studies, various types of models were introduced to determine a target lane if a lane change improves the local traffic situation of a driver. Ahmed developed a lane selection model based on a developed utility function and a nested logit model [15]. The MOBIL model introduced the expected acceleration level as an incentive criterion for lane selection [10]. The Freeway Lane Selection (FLS) algorithm, developed by the Federal Highway Administration's (FHWA's) Next Generation SIMulation (NGSIM) program, assigns an individual score to each lane to choose the lane showing the highest score [33].

2.4 Game Theory-based Lane-changing Models

2.4.1 What is game theory?

In 1921, the mathematician Emile Borel suggested a formal theory of games, then the mathematician John von Neumann develops and popularizes game theory after seven years [34]. The mathematical theory of games was invented by the J. von Neumann and the economist Oskar Morgenstern (1944) who provided the basic terminology and problem setup that is still in use today. In 1950, John Nash demonstrated that finite games always have an equilibrium point [34], known as Nash equilibrium, applicable to a wider variety of games. In the 1950s and 1960s, game theory was theoretically broadened and the concepts of the core were developed. Since the 1970s, it has driven a revolution in economic theory, and has been applied in various fields [34]. Nash, John Harsanyi, and Reinhard Selten, who worked on game theory, received the Nobel Prize in Economic Sciences in 1994.

Game theoretical approach applies whenever the actions of several agents are interdependent [34], i.e., there is interaction between decision makers. Game theory is the study of the ways in which *interacting choices* of *agents* produce *outcomes* with respect to the *preferences* (or *utilities*) of those agents, where the outcomes in question might have been intended by none of the agents [35]. Specifically, a game involves a *number of players (N)*, a *set of strategies for each player*, a *payoff* that quantitatively describes the outcome of each play of the game [36]. The mathematical foundations of game theory can be used for modeling and designing automated decision-making process in interactive environments. There are several characteristics, as described in [34] and [37], to establish types of games in game theory as follows.

1) Fundamentals of game theory

a) Cooperative games

A *cooperative* game is used for describing the cooperation of players or groups of players, i.e., when *coalitions* occurs. Cooperative game theory focuses on predicting the joint actions that group (or players) take and the collective payoffs. Formally, a cooperative game in which a finite set of players N participates can be defined with a characteristic cost function $c: 2^n \longrightarrow \mathbb{R}$ satisfying $c(\emptyset) = 0$. The characteristic function c represents the cost of a set of players accomplishing the task together. It is often assumed that communication among players is allowed, i.e., they have perfect information about opposite player's payoffs and previous decisions. In this case, there is no conflict between players because all the players perceive outcomes and agree with common preference.

For instance, a two-person bargaining situation involves two individuals who have the opportunity to collaborate for mutual benefit in more than one way [38]. A feasibility set F, a closed subset of $\mathbb{R}^2$ that is often assumed to be convex, the elements of which are interpreted as

agreements. A disagreement, or threat, point $d = (d_1, d_2)$, where d_1 and d_2 are the payoffs to player 1 and player 2, respectively. Nash proved that a solution is the points (x, y) in F which maximize the following expression:

$$\max \big(u(x) - u(d)\big)\big(v(y) - v(d)\big) \tag{2.1}$$

where u and v are the utility functions of player 1 and player 2, respectively, and d is a disagreement, or threat, point $d = (d_1, d_2)$, where d_1 and d_2 are the payoffs to player 1 and player 2, respectively.

b) Non-cooperative games

A *non-cooperative* game is a game with *competition* between players who make their decisions independently of the opposite player. In other words, each player wants to maximize their own outcomes to achieve their goal in the game. In this game type, generally, players cannot decide action strategies as a joint group because of the absence of binding commitments externally enforced (e.g. through contract law), i.e., they must compete independently. Non-cooperative game theory is more general, as cooperative games can be analyzed using the terms of non-cooperative game theory if an agreement for arbitration is assumed. In non-cooperative games, the Nash equilibrium concept is used to analyze the outcome of the strategic interaction of several decision makers, as described in a following subsection.

c) Simultaneous vs. sequential games

Simultaneous games are games where both players move simultaneously, or if they do not move simultaneously, the later players are unaware of the earlier players' actions (assuming that the game is simultaneously played). In contrast, *sequential* games (or dynamic games) are games where a leader takes action first and the other (the follower) makes a decision in view of the decision made by the leader. Sequential games hence are governed by the time axis, and represented in the form of decision trees. Regarding knowledge about earlier actions, this need not be perfect information about every action of earlier players. Sometimes it might be very little knowledge. For instance, a player may know that an earlier player chose one particular action which has not published yet. Therefore, they does not know which of the available actions the first player actually selected.

Repeated games, which this study introduced for decision-making in merging, are an example of sequential games. Players play a stage game and the result of this game will determine how the game continues. At every new stage, both players will have complete information on how the previous stages had played out.

d) Zero-sum vs. non-zero-sum games

According to the summation of players' payoffs, games are classified into two types, i.e., *zero-sum* and *non-zero-sum*. A zero-sum game is a mathematical representation of a situation in which each participant's gain or loss of utility is exactly balanced by the losses or gains of the utility of the other participants. If the total gains of the participants are added up and the total losses are subtracted, they will sum to zero. In this type of game, one side takes all the benefits while the other gains nothing. In contrast, a non-zero-sum game describes a situation in which the interacting parties' aggregate gains and losses can be less than or more than zero. It indicates that all players can receive a payoff, which varies with the choice of strategies (actions) taken by each player.

e) Pure vs. mixed strategy

In game theory, a strategy is a complete plan of action for the players and thus in principle determines the participants' behavior. A *pure strategy* provides a complete decision how a player will play a game. In particular, it determines the move a player will make for any situation they could face. In addition, a *mixed strategy* is an assignment of a probability to each pure strategy, which allows for a player to randomly select a pure strategy. One of available action strategies can regard a pure strategy as a case of a mixed strategy, in which that particular pure strategy is selected with probability 1 and every other strategy with probability 0.

2) Nash equilibrium

Finding the best strategy set has been a topic of interest since the introduction of game theory [39]. To the optimum strategy for both players, the Nash equilibrium is considered. The Nash equilibrium is a solution where neither player has motivation to change their own strategy as no player can improve their situation by individually switching to another strategy [37]. If Nash equilibrium exists, players use *pure strategies*, implying that each player will choose the strategy that maximizes their own payoff while considering an opponent who also wants to maximize their payoff. In a two-player game, for example, Player 1 and Player 2 have three and two possible strategies, respectively: $S_1 = \{a_1, a_2, a_3\}$ or $S_2 = \{b_1, b_2\}$. This means that each game has six possible sets of strategies. The utility functions U_1 and U_2 are the payoff for Player 1 and Player 2, respectively, when the players choose a set of strategies. Nash equilibrium defines the *pure strategy* specified as:

$$\begin{cases} U_1(a^*, b^*) \geq U_1(a, b^*), & \forall a \in S_1 \\ U_2(a^*, b^*) \geq U_2(a^*, b), & \forall b \in S_2 \end{cases} \tag{2.2}$$

where a^* and b^* represent the equilibrium strategy sets for players 1 and 2, respectively.

However, the Nash equilibrium does not always exist [37]. In the absence of a Nash equilibrium, the mixed strategy is used. A probability for each player's strategy is assigned with consideration of each player's expected payoff from the different strategies [37].

2.4.2 Game theory-based lane-changing models

In lane-changing, it is clear that not only a driver of subject vehicle (SV), who is motivated to change lanes, but also a driver of lag vehicle (LV) in target lane controls own vehicle after perceiving merging vehicle in acceleration lane. The driver of SV controls longitudinal and lateral movements to safely change a lane in consideration of surrounding vehicles, and also the driver of LV responds by showing acceptance or disapproval of the SV'slane-changing intention. This decision-making related to both drivers motivated previous studies to use a game theoretical approach. Game theory-based models, therefore, were modeled as a two-player non-cooperative game.

1) Kita (1999)

Kita modeled merging-giveway interaction between vehicles in a merging section based on a game theoretical approach [40]. This study assumed that the merging decision-making game is a one-shot game because the amount of decision-making time is not so long and each decision is not affected by preceding decisions. Kita also modeled interaction between drivers as a game under perfect information as the drivers recognize each other in the game and they know the strategy of the other player.

The action strategies of SV are merging or keeping the lane, while the strategies of LV in the target lane are giving way (i.e., yielding) or not. To formulate the payoffs, Kita mentioned that drivers' payoffs are highly affected by the gap size with surrounding vehicles. This study hence used time-to-collision (TTC) between the ego vehicle and a target vehicle for each action strategy and introduced constant parameters to represent tendency to maintain the current action, a kind of inertia payoffs.

Kita estimated the parameters using 25 samples with complete of sets of variables, which were extracted in 2-hour recorded video. The value of likelihood ratio, which is an index of the replicability of the mode, was 0.347. This study concluded that the proposed model demonstrates its capability to explain merging and giveway behaviors. However, perfect information in the game theory indicates that all players have perfect and instantaneous knowledge of their own utility and the events previously occurred. In consideration of traditional transportation environment which a driver becomes aware of surroundings through sight view only, this assumption would be irrational. Additionally, Kita's model assumed that vehicle speeds are constant during the merging process, but it is not realistic [2].

2) Liu et al. (2007)

Liu et al. modeled merging process as an independent game by taking the SV (or called a merging vehicle), which is the vehicle in acceleration lane trying to join the freeway, and the LV, which is the vehicle in the target lane just behind the merging vehicle, as players [2]. As a non-cooperative game, both vehicles have to decide a set of moves to maximize their respective rewards in the game. In [2], the SV can select either to merge into the mainline traffic immediately or to wait until the next available gap, while the LV has options whether to keep its current car-following state or decelerate to yield in order to facilitate a smooth merge.

This study assumed the player's objective: the SV's objective is to minimize the time spend in acceleration lane subject to safety constraints, whereas that of the LV is to minimize speed variation. The payoffs of the LV and SV were formulated using acceleration level (in ft/s^2) and time (in second) that the merging vehicle spends on acceleration lane for each action strategy, respectively.

To solve the game, Liu et al. proposed a bi-level calibration framework, which the upper level programming is an ordinary least square problem and the lower level programming is a linear complementarity problem for finding the Nash equilibrium. Based on this bi-level programming problem, this study calibrated and validated the proposed model using the field observation data obtained from *Freeway Data Collection for Studying Vehicle Interactions* (DCSVI) project conducted by FHWA in 1983 [41]. Through screening process of the data, a total of 86 merging cases were used in model evaluation (63 cases were used on calibrating model parameters and the rest of the data were used for validation). This study concluded that the proposed model has a good capability to replicate and predicate vehicle actions at merging sections, showing the Mean Average Error of 0.087.

There are two issues arising from the review of Liu et al.'s study. First, the SV occasionally show different behaviors with the assumption on the defined SV's objective. Kondyli and Elefteriadou (2009) found that all drivers want to reach a speed close to the freeway speed or the speed limit, if there is no vehicle in front [21]. This speed synchronization process to accelerate when arriving at the beginning of the acceleration lane were observed at merging section on freeway [22]. Hence the assumption on the SV's objective in [2] may be unrealistic.

Next, Liu et al. provide figures to represent their model's performance to predict merging behaviors in [2]. The left-hand side of Figure 2-11, figure shows the speed profile of vehicles in merging situation where the SV and LV chose 'Merge' and 'Not yield' action, respectively. The other figure shows the merging situation where the SV and LV chose 'Wait' and 'Yield' action, respectively. In this figure the first point in merging vehicle's speed profile represents the decision point for all the players. It is hard to agree that the LV chose 'Not yield' action in the first case. Prior to the decision-making point, the LV properly followed the lead vehicle's speed profile as car-following state. Then, it controlled the speed using smaller acceleration level than that of the

lead vehicle, causing increase of the gap distance between both vehicles in the target lane. It might be classified as yielding behavior to provide sufficient gap to the SV after perceiving the SV's higher acceleration level. Also, the second situation on the right-hand side of Figure 2-11 was provided as a 'Wait' and 'Yield' situation. At near decision-making point, the SV slightly decreased speed, then accelerate to enter onto the freeway. It can be interpreted as the 'Wait' action. Since they did not provide information about gap distance between vehicles, however, only using speed profile has a limitation to recognize the decision of the vehicle. These examples of non-cooperative decisions cause conflict between drivers who want to achieve their own goal. Thus, one of them should change their initial decision, resulting in a cooperative decision. Since decision-making point is not a static point, thus the decision-making model needs to represent appropriate drivers' decision at any decision-making points.

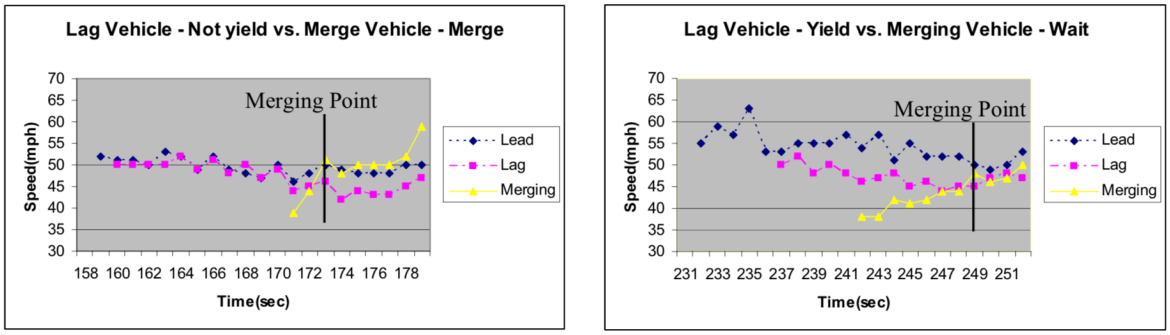

Figure 2-11. Vehicle speed profiles in competitive merging situations (in [2]).

3) Talebpour et al. (2015)

According to the development of advanced vehicle technologies (e.g., V2V communication), recent research efforts to focus on the cooperative interaction between vehicles have been led. Talebpour et al. modelled a game for lane-changing in consideration of both MLC and DLC within a connected environment [39]. In the absence of communication, there is the lack of accurate information about the surrounding traffic condition, causing in efficient and unsafe driving maneuvers. Therefore, they proposed the two types of game models depending on activation of V2V communication. The lane-changing behavior under active V2V communications was modeled as *two-person non-zero-sum non-cooperative game under complete information*, whereas a game model under inactive V2V communication was proposed as *two-person game under incomplete information*. To represent a game of imperfect information without V2V communication, they introduced the concept of *nature* as a player who chooses the type of each player, and adopted the Harsanyi transformation [42] to transform a game of incomplete information. In this transformation, from the LV's standpoint, nature moves first and chooses MLC with probability p and DLC with probability $1 - p$, as shown in Figure 2-12.

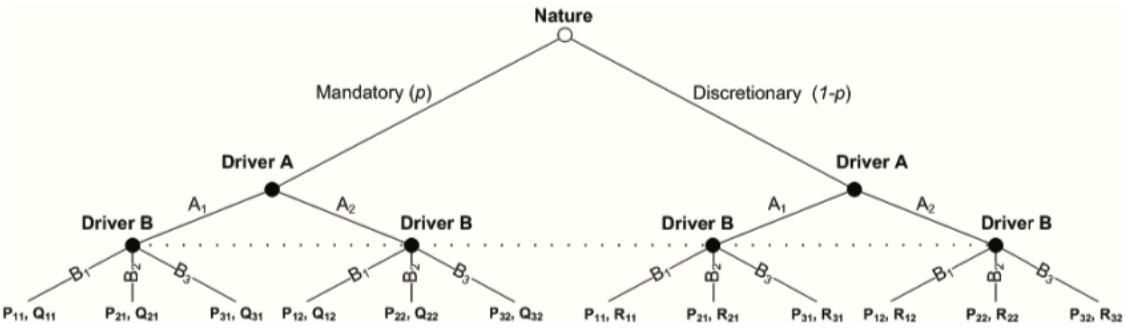

Note that discretionary lane-changing game with inactive V2V communication in normal form. *P* and *R* denote the payoff for target and lag vehicle, respectively. Mandatory lane-changing game with inactive V2V communication in normal form. *P* and *Q* denote the payoff for target and lag vehicle, respectively.

Figure 2-12. Lane-changing game with inactive V2V communication in extensive form (in [39]).

In their game models the SV has two pure strategies {Change lane and Wait} and the lag vehicle has three pure strategies {Accelerate, Decelerate, and Change Lane}. For the SV's payoffs, acceleration level, relative speed, and error term were used. In addition, acceleration level and error term were used for the LV's payoffs. To consider complicated functions using 58 parameters, this study simplified the proposed model by reducing the number of parameters based on assumptions. Then, they evaluated the proposed model using US 101 dataset in NGSIM data [43], and the validation results showed that the simplified model does not carry a prediction power and is not capable of accurately predicting lane-changing behavior. Their model focused on execution of a lane change, not including driver's behavior prior to lane-changing.

2.5 CAVs Environment

2.5.1 What are CAVs?

AVs are vehicles in which at least one element of vehicle control (e.g., steering, speed control) occurs without direct driver input [44]. They work by gathering information from various sensors (e.g., camera, radar, light detection and ranging (LIDAR), ultrasonic, and infrared sensors) equipped on the vehicles. They can detect and classify objects in their surroundings (e.g., other vehicles, pedestrians, and roadway objects), and predict how these surroundings are likely to behave. As mentioned previously, V2X communication can enhance the safety and efficiency of AVs by providing greater situational awareness and efficiency. FHWA defined that the CAV is an equipped vehicle sends basic safety messages (BSMs), transmitted 10 times per second [44]. Hence driver receive warnings and information to avoid potential crashes and improve mobility.

2.5.2 Connected transportation environment

Advanced information and communication technology (ICT) is expected to bring about significant improvements in mobility and safety in transportation systems. As the next generation of transportation solutions—connected and automated transportation systems—become a reality, various research efforts have been, and continue to be, devoted to developing and testing connected vehicle (CV) technologies. These CV technologies have the ability to exchange time-critical and safety-critical data, enabling cooperative control between vehicles and offering the potential to improve safety and mobility. The US Department of Transportation (USDOT), for example, has conducted field tests of several CV applications in test-beds [45]. Additionally, introducing state-of-the-art wireless communication can enhance traffic management by providing more and more timely data to CVs.

Wireless communication technologies have been developed and it will contribute to evolve transportation systems. For example, the next generation of wireless technology, known as 5G, will allow transmission of massive quantities of data in near real-time. The USDOT is preparing to integrate vehicle-to-everything (V2X) communications technologies into the transportation environment [46]. It is expected that vehicles will communicate both with one another and with physical transportation components. The dynamic wireless exchange of data offers the opportunity for significant safety improvements and a wide range of other mobility and environmental benefits. In addition, automobile and ICT enterprises have dedicated to propose interoperable solutions for cellular V2X, based on 5G and on the enhancement of Long-Term Evolution (LTE) [47]. The Third Generation Partnership Project (3GPP) is working on V2X standardization by identifying use cases and associated potential requirements for LTE support of V2X services [48]. It will support the cooperative transportation systems with stringent reliability, low latency, high data rates, and larger communication range even in the high density scenarios [48].

Chapter 3. Modeling a Decision-Making Game for Merging Maneuvers in the Traditional Transportation Systems

---

This chapter aims to model a stage game for human drivers' decision-making in merging and expands the model based on the repeated game approach. The following subsections describe a structure of the stage game, payoff functions formulation, and the repeated game design in detail.

This chapter is based on the papers listed below:

1. Kang, K. and Rakha, H. A. (2019). A Repeated Game Theory Lane-Changing Model for Merging Maneuvers. Submitted to *Sensors*.

2. Kang, K., & Rakha, H. A. (2018). Modeling driver merging behavior: a repeated game theoretical approach. *Transportation Research Record: Journal of the Transportation Research Board*, *2672*(20), 144-153. doi: 10.1177/0361198118792982

3. Kang, K. and Rakha, H. A. (2017, July). *Development of a Decision Making Model for Merging Maneuvers: A Game Theoretical Approach*. In Conference on Traffic and Granular Flow, Washington, DC., USA.

4. Kang, K., & Rakha, H. A. (2017). Game theoretical approach to model decision making for merging maneuvers at freeway on-ramps. *Transportation Research Record: Journal of the Transportation Research Board*, *2623*(1), 19-28. doi: 10.3141/2623-03

3.1 Introduction

Based on the literature review, this study demonstrates issues to be discussed and studied in this dissertation, as follows. First, a lane changing is a tactical process with some transitions [49]. The tactical merging decision-making behavior should be modeled as an entire process from the beginning of the decision-making impetus to the execution of the lane change. To realistically model a driver's lane-changing decision-making process, this study uses a game theoretical approach. When considering lane changes, it is assumed that a driver makes a trade-off between the expected advantage to him/herself and the disadvantage imposed on other drivers [10]. Drivers in the process of changing lanes converge to the equilibrium of a set of actions to maximize their advantages within an independent game. Typical lane-changing maneuvers are described as a non-cooperative decision-making process to achieve their own objectives.

To model merging maneuvers of drivers at a merging section on a freeway, this study proposes the stage game structure, and formulated the payoff functions through three-phase development [50-52]. In addition, the repeated game model, which a stage game is repeatedly played with consideration of previous game results, is introduced to depict realistic decision-making process. This chapter describes whole modeling process including the design of a stage game structure and payoff functions formulation, and concept of the repeated game model.

3.2 Design of a Stage Game for Merging Decision-making Game

The game model defines the number of players, action strategies of each player, and corresponding payoff functions to describe the outcome for each player throughout the game [53]. The merging decision-making process involves three vehicles: (1) the SV (i.e., merging vehicle), which makes a lane change to merge onto the freeway; (2) the LV, which is the closest following (lag) vehicle in the SV's target lane; and (3) the preceding vehicle (PV), which is the nearest preceding vehicle in the SV's target lane. In the absence of any connected vehicle technologies (e.g. V2V communication), drivers' perceptions of their surrounding traffic conditions are subjective [39]. When drivers of both the subject vehicle and lag vehicle perceive each other, they immediately choose a maneuver depending on individual judgment. The decision-making process for performing merging maneuvers is modeled here as a stage game based on a game theoretical approach.

A game consists of a number of players, a set of strategies for each player, and a payoff function to describe the outcome for each player throughout the game. The type of game proposed here is a *two-person non-zero-sum non-cooperative game under complete information.* In non-cooperative games, players decide their strategies independently since communication between them is not allowed. The game consists of two players: the driver of SV and that of LV, respectively. The driver of SVS, who wants merge onto the freeway, has three action strategies

(see Figure 3-1(a)): change a lane for merging (s_1), wait for the LV's overtaking maneuver in the acceleration lane (s_2), or overtake the PV and use a forward gap to merge (s_3). The opposite player the driver of LV has two action strategies (see Figure 3-1(b)): yield to allow the SV's lane change maneuver (l_1) or block the SV's merging maneuver by decreasing the spacing to the SV (l_2). In real life situations, the driver of LV can choose lane-changing to the left lane to avoid potential collision or considerable deceleration [18], and this lane-changing behavior was considered as a LV's action strategy in [39]. Freeway vehicles on the rightmost lane generally change lanes from the rightmost lane upstream of the merging section after perceiving the approach of the merging vehicle in order to maintain their speed. Since this mainline vehicle's lane change is conducted by independent behavior, not interaction with the merging vehicle, this study does not include a LV's lane-changing action as one of the pure action strategies of the driver of LV in the proposed merging game.

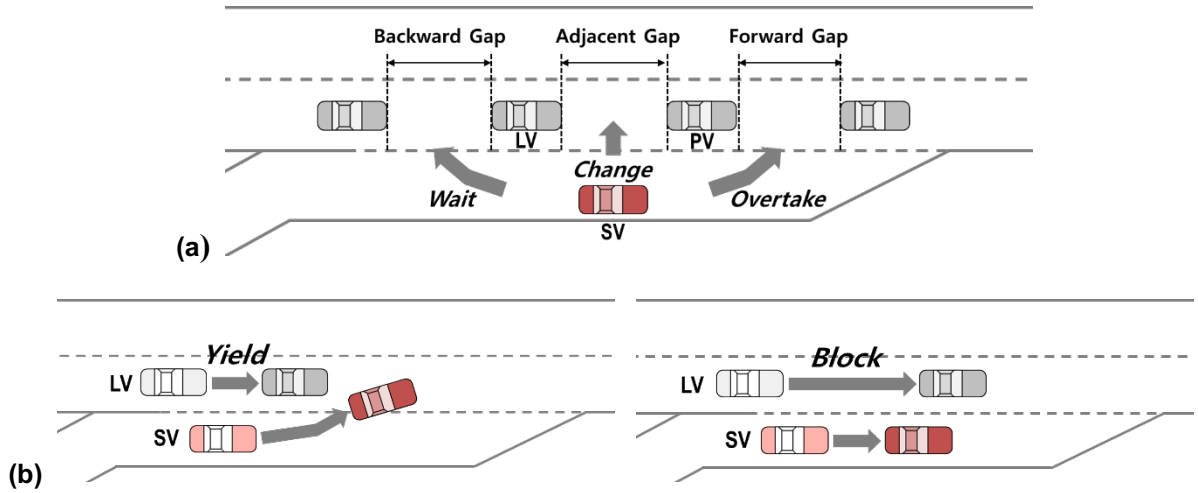

Figure 3-1. Players' strategies for merging maneuver: (a) the driver of SV and (b) the driver of LV.

Let $S = \{s_1, s_2, s_3\}$ and $L = \{l_1, l_2\}$ denote the set of pure strategies for the drivers of the SV and LV, respectively. In addition, $a_{ij} = (s_i, l_j)$ denotes a set of actions ($a_{ij} \in S \times L$) where i and j indicate the index of action strategies of each driver (i.e., i = 1, 2, 3 and j = 1, 2). Therefore, a total of six sets of action strategies were defined as the non-cooperative decision-making stage game for merging maneuvers. In these action strategies, (s_1,l_1), (s_2,l_2), and (s_3,l_1) are cooperative action strategies, whereas both (s_1,l_2) and (s_2,l_1) are non-cooperative strategies in which both players compete to achieve their objectives. The action strategy (s_3, l_2) is neither cooperative nor competitive. The proposed stage game with imperfect information, which captures the fact that players are simply unaware of the actions chosen by other players, is represented in the extensive form as shown in Figure 3-2. In the figure, a dashed line uniting three nodes, which implies imperfect information, indicates that the players do not know which node they are in. It means that there is no sequence to make a decision thus the driver of LV does not know SV's movement. Although there is no binding rule to make a decision together, players know who the opposite player is and what possible action strategies the other can choose. In other words, players choose

their action based on awareness of the other player and knowledge of the opposite player's possible action strategies. Thus, this game is assumed to be a complete information game. Moreover, P_{ij} and Q_{ij} denote the payoff of the drivers of the SV and LV for each action strategy a_{ij}, respectively. As a non-zero-sum game, the sum of their payoffs in the game cannot be zero, because all players receive a corresponding payoff. Table 3-1 shows the structure of the defined decision-making game for a merging maneuver in normal form.

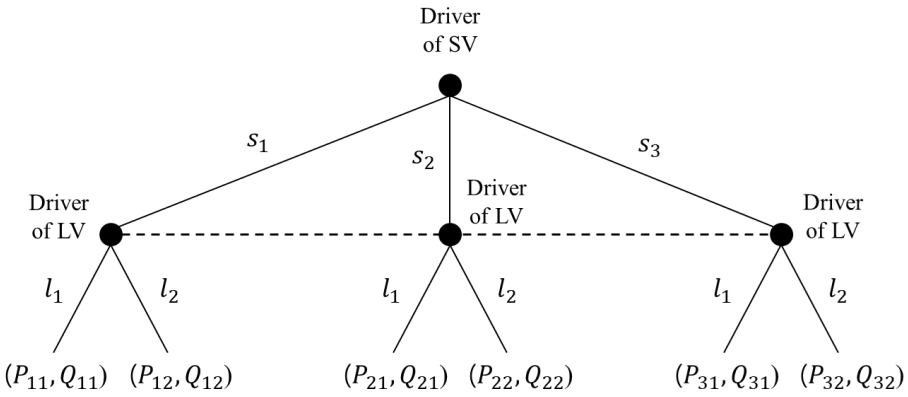

Figure 3-2. Merging decision-making game in the extensive form.

Table 3-1 Structure of the Merging Decision-Making Game in Normal Form

Player & Actions		Driver of LV	
		Yield, $l_1(q_1)$ [b]	Block, $l_2(q_2)$
Driver of SV	Change, $s_1(p_1)$ [a]	(P_{11}, Q_{11}) [c]	(P_{12}, Q_{12})
	Wait, $s_2(p_2)$	(P_{21}, Q_{21})	(P_{22}, Q_{22})
	Overtake, $s_3(p_3)$	(P_{31}, Q_{31})	(P_{32}, Q_{32})

[a] p_i in parentheses denotes the probability assigned to the pure strategy s_i of the driver of SV; $\sum_{i=1}^{3} p_i = 1$.
[b] q_j in parentheses denotes the probability assigned to the pure strategy l_j of the driver of LV; $\sum_{j=1}^{2} q_j = 1$.
[c] Note that *P* and *Q* denote the payoff for the drivers of the SV and LV, respectively.

This study defines the decision time as the time at which the merging decision-making game is played by the two players. Wan et al. concluded that small speed differences between the merging vehicle and surrounding vehicles (i.e., the PV and LV) are required for successful merging [22]. Therefore, it is assumed that the driver of SV focuses on speed synchronization before arriving in the acceleration lane. As illustrated in Figure 3-3(a), both drivers initially decide their action by playing the game at the beginning point of the acceleration lane, while taking traffic conditions and the traveling status of the PV and LV into consideration. Additional stage games are formed by overtaking the PV (see Figure 3-3(b)) or waiting to be overtaken by the LV (see Figure 3-3(c)). In other words, the stage game is newly built by identification change of the player, which drives in the target lane. This study also assumed that drivers control vehicles to perform the action strategy decided by playing the game until the next stage game is played.

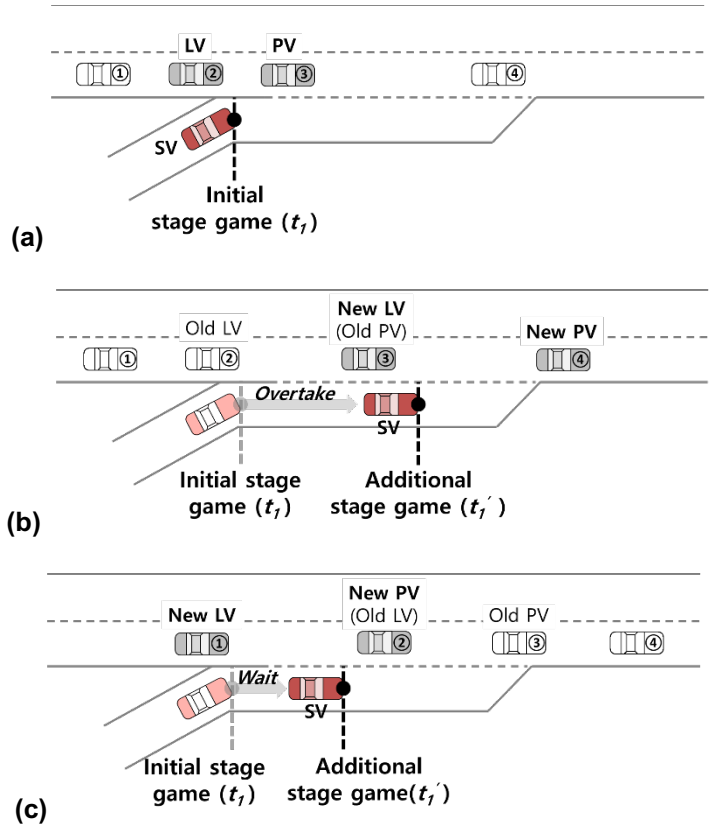

Figure 3-3. Defined game points in the merging decision-making game. (a) Initial game at the beginning point of an acceleration lane. (b) Additional game produced by the overtaking action of the driver of SV. (c) Additional game produced by the waiting action of the driver of SV (or the overtaking action of the driver of LV).

3.3 Payoff Functions Formulation

Prior to describe payoff function formulation, the process of game model development for this dissertation study is introduced first, as summarized in Table 3-2. The initial study proposed the stage game model to explain decision-making for merging maneuvers and formulated payoff functions using five decision factors: minimization of travel time, avoidance of collision (i.e., safety), travel efficiency, the LV's expected acceleration, and remaining distance [50]. Then, the model has been updated twice by reformulating payoff functions for drivers. In the first revision, this study simplified payoff functions in order to limit the number of observations for model calibration and correlation between decision factors. The payoffs of the driver of SV were formulated by the expected gap and remaining distance, and the expected relative speed was considered as the main decision variable of the driver of LV [51]. Using multiple variables having different units indicates that the payoffs are able to be only interpreted as qualitative outcome to represent player's preference. In addition, an error term utilized to capture unobserved variables was formulated as constant value, resulting in hardly consider driver's randomness. In the last

update, therefore, the payoff functions were reformulated using efficient decision variables including random error term and propose monotone (unitless) functions by transformation of quantitative variables. In following subsections, payoff functions formulation of each model is described.

Table 3-2. The Process of Model Development

Model type	Decision factors in payoff functions	Applied game type	References
1st Model	• Payoffs of the driver of SV: minimization of travel time, avoidance of collision (i.e., safety), travel efficiency, the LV's expected acceleration, and remaining distance • Payoffs of the driver of LV: safety, relative speed, and the expected acceleration	One-shot game (Single game)	[50]
2nd Model	• Payoffs of the driver of SV: the expected gap and remaining distance	One-shot game (Single game)	[51]
	• Payoffs of the driver of LV: the expected relative speed	Repeated game	[52]
3rd Model	• Payoffs of the driver of SV: safety and forced merging factor • Payoffs of the driver of LV: safety	Repeated game	

3.3.1 Payoff functions in the first model (in [50])

In the literature lane-changing game theoretical approaches considered different payoff functions for players based on assumptions of the player objectives. For example, Kita assumed that each player's behavior goal is to minimize their collision risk [40]. This assumption may result in trivial equilibrium solutions, as collision risks affect both players, and thus each player would have a similar magnitude of effects on game equilibrium [1] Liu et al. used the acceleration level for the payoff function of the driver of LV based on an assumption that the objective of the driver of LV is to minimize their speed variations [2]. They also assumed that the objective of the driver of SV is to minimize the time spent in an acceleration lane subject to safety constraints [2]. Talebpour et al. chose safety and speed gain as the main decision factors for driver's lane change decision [39].

It is hard to define a driver's objective as a single factor since the decision-making process is complicated considering the surrounding vehicles, vehicle dynamics, and the road design. Consequently, this study considers multi-decision factors to formulate payoff functions for both drivers using multivariate functions. As in the literature, safety is necessarily one of the major factors in the proposed model because drivers tend to avoid collisions. In addition, speed variation is also an important decision factor as declared in [2]. As mentioned in the previous paragraph, Liu et al. assumed that the driver of SV wants to minimize the time spent in an acceleration lane.

Under congested traffic conditions (i.e., critical density or jam density), however, the driver tends to overtake and stays longer in the acceleration lane after perceiving lower freeway traffic speeds [2]. To consider this case, the expected travel time is considered as one of the decision factors in this study. To consider a forced merging situation, moreover, the remaining distance to the end of the acceleration lane is used in the payoff function to influence the lane-changing behavior. A detailed explanation of these factors is provided in the following section.

1) Payoff Function of the driver of SV

Upon entering the acceleration lane, the driver of SV chooses an action strategy from among three actions in the proposed merging game. After choosing a type of gap for the merge, the driver tries to carry out the decision by creating a sufficient gap distance. In the study, the payoff is formulated by defining the rewards obtained by the game as a utility function. This means that the action showing the highest payoff value provides the player with the highest benefit.

Equation (3.1), (3.2), and (3.3) show the formulated payoff functions of the driver of SV for the three strategies—changing a lane, waiting, and overtaking, respectively—when the opposite player, i.e., the driver of LV, shows a yielding action. To interpret the terms included in the functions, the payoff function P_{11} is used here as an example. The first two terms on the right hand side of Equation (3.1) relate to the safety of the lag and lead vehicles, respectively. The third term comes from the expected travel time. The fourth term reflects travel efficiency as represented by the difference between the SV's actual speed and desired speed. The fifth term is the expected acceleration level of the LV in the corresponding action. The sixth term is related to a forced merging situation when the remaining distance to the end of acceleration lane is too short for smooth lane changing. The last term is an error term included to capture the unobserved decision variables [39]. For the driver of SV, the payoff functions when the driver of LV decides to yield, denoted by *P* (in Table 3-1), are specified as:

$$P_{11} = \alpha_{11}^{1}(\Delta x^{SV,LV} - x_j - x_s^{LV}) + \alpha_{11}^{2}(\Delta x^{PV,SV} - x_j - x_s^{SV}) + \alpha_{11}^{3} t_c + \alpha_{11}^{4}(v_d^{SV} - v^{SV}) + \alpha_{11}^{5} a_y^{LV} + \alpha_{11}^{6} \exp(x_0/x_{RD}) + \varepsilon_{11}^{SV} \quad (3.1)$$

$$P_{21} = \alpha_{21}^{1}(\Delta x^{SV,LV} - x_j - x_s^{LV}) + \alpha_{21}^{2} t_w + \alpha_{21}^{3} a_y^{LV} + \varepsilon_{21}^{SV} \quad (3.2)$$

$$P_{31} = \alpha_{31}^{1}(\Delta x^{PV,SV} - x_j - x_s^{SV}) + \alpha_{31}^{2} t_o + \alpha_{31}^{3}(v_d^{SV} - v^{SV}) + \varepsilon_{31}^{SV} \quad (3.3)$$

where

- $\Delta x^{SV,LV}$: Longitudinal spacing between the SV and LV;
- x_j: Jam density spacing;
- x_s^{LV}: Safe gap distance for the LV to avoid collision with the SV;
- $\Delta x^{PV,SV}$: Longitudinal spacing between the PV and SV;

- x_s^{SV}: Safe gap distance for the SV to avoid collision with the PV;
- t_c: Expected travel time when deciding 'change (s_1)' action strategy;
- v_d^{SV}: Desired speed (i.e., free-flow speed) of the SV to follow the PV in steady-state;
- v^{SV}: Speed of the SV;
- a_y^{LV}: Expected acceleration for the 'yield (l_1)' action of the driver of LV to avoid a collision with the SV;
- x_0: Distance threshold for forced lane-changing (= $10 \cdot x_j$);
- x_{RD}: Remaining distance in acceleration lane for the SV;
- t_w: Expected travel time if deciding on a 'wait (s_2)' action strategy;
- t_o: Expected travel time if deciding on an 'overtake (s_3)' action strategy;
- ε_{11}^{SV}, ε_{21}^{SV}, ε_{31}^{SV}: Error terms to capture the unobserved variables; and
- α_{11}^1, α_{11}^2, α_{11}^3, α_{11}^4, α_{11}^5, α_{11}^6, α_{21}^1, α_{21}^2, α_{21}^3, α_{31}^1, α_{31}^2, α_{31}^3: Parameters to be estimated. Note that it is expected that the driver of SV will have different weights on variables for each action strategy.

When the driver of LV chooses a blocking action, the payoff function of the driver of SV includes a different value and different weights on variables. The functions are organized in the same manner, and the meaning of each term is the same. In this paper, it is assumed that the expected acceleration of the LV in the function is affected only by the action of driver of LV. The payoff functions of the driver of SV when the opposite player decides to block are specified as:

$$P_{12} = \alpha_{12}^1\left(\Delta x^{SV,LV} - x_j - x_s^{LV}\right) + \alpha_{12}^2\left(\Delta x^{PV,SV} - x_j - x_s^{SV}\right) + \alpha_{12}^3 t_c + \alpha_{12}^4(v_d^{SV} - v^{SV}) + \alpha_{12}^5 a_b^{LV} + \alpha_{12}^6 \exp(x_0/x_{RD}) + \varepsilon_{12}^{SV} \quad (3.4)$$

$$P_{22} = \alpha_{22}^1(\Delta x^{SV,LV} - x_j - x_s^{LV}) + \alpha_{22}^2 t_w + \alpha_{22}^3 a_b^{LV} + \varepsilon_{22}^{SV} \quad (3.5)$$

$$P_{32} = \alpha_{32}^1(\Delta x^{PV,SV} - x_j - x_s^{SV}) + \alpha_{32}^2 t_o + \alpha_{32}^3(v_d^{SV} - v^{SV}) + \varepsilon_{32}^{SV} \quad (3.6)$$

where

- a_b^{LV}: Expected acceleration for the *'block'* action of the driver of LV to make a collision with the subject vehicle;
- ε_{12}^{SV}, ε_{22}^{SV}, ε_{32}^{SV}: Error terms to capture the unobserved variables; and
- α_{12}^1, α_{12}^2, α_{12}^3, α_{12}^4, α_{12}^5, α_{12}^6, α_{22}^1, α_{22}^2, α_{22}^3, α_{32}^1, α_{32}^2, α_{32}^3: Parameters to be estimated.

The detailed trade-off of each factor is specified as follows. The *safety* factor stems from a comparison of the actual gap distance and minimum gap to avoid a collision. Initially, the safe gap distance of the following vehicle is determined by the collision avoidance component in the Rakha-Pasumarthy-Adjerid (RPA) model [54]. A safe gap distance variable for the LV, x_s^{LV}, is computed as:

$$x_s^{LV} = \frac{v^{SV\,2} - v^{LV\,2}}{2d_{max}} \tag{3.7}$$

where v^{SV} and v^{LV} are the speed of the SV and LV, respectively, and d_{max} is the maximum deceleration rate observed in the field. A safe gap distance for the SV, x_s^{SV}, is computed as:

$$x_s^{SV} = \frac{v^{PV\,2} - v^{SV\,2}}{2d_{max}} \tag{3.8}$$

where v^{PV} is the speed of the PV. This safe gap distance is only applied when the following vehicle is traveling at a speed higher than the speed of the lead vehicle [54]. For example, in Equation (3.7), the LV and SV is the following and lead vehicle, respectively. The safe gap distance of the LV denoted as x_s^{LV} only occurs when $v^{SV} < v^{LV}$. Otherwise, a value of x_s^{LV} equals to zero. Note that when $\Delta x^{SV,LV} - x_j - x_s^{LV} < 0$, the driver of SV incurs a penalty for merging, which encourages the driver to choose a waiting action. Otherwise, the driver can merge without colliding with the LV. This is applied identically to the relationship between the PV and SV in Equation (3.8).

The *travel time* incentive factor implies that the driver of SV tends to minimize travel time. It is anticipated that travel time will be different depending on the chosen actions. The related terms have negative parameters to penalize for the SV's expected travel time, meaning the driver of SV gets a large penalty when the expected travel time resulting from the chosen action is long.

The *travel efficiency* is related to the deviation of the SV's speed from the desired speed. The desired speed is obtained by the RPA model [54]:

$$v_d^{SV} = \frac{-c_1 + c_3 v_d + \Delta x^{PV,SV} - \sqrt{(c_1 - c_3 v_d - \Delta x^{PV,SV})^2 - 4c_3(\Delta x^{PV,SV} v_d - c_1 v_d - c_2)}}{2c_3} \tag{3.9}$$

where

- c_1: Fixed distance headway constant in the RPA model ($= \frac{x_j v_d}{{v_c}^2}[2v_c - v_d]$);
- c_2: The first variable headway constant in the RPA model ($= \frac{x_j v_d}{{v_c}^2}[v_d - v_c]^2$);
- c_3: The second variable headway constant in the RPA model $\left(= \frac{x_c}{v_c} - \frac{x_j v_d}{{v_c}^2}\right)$;

- v_d: Free-flow speed (m/s);
- v_c: Speed at capacity (m/s); and
- x_c: Vehicle spacing at capacity (m).

When $v_d^{SV} - v^{SV} > 0$, it is efficient to merge. Otherwise, the driver of SV gets a penalty for changing a lane since the current vehicle speed is higher than the expected speed after merging.

The *acceleration of the LV* is considered as a trade-off factor. If the driver of the LV accelerates to block a lane change of the subject vehicle, the lane change incurs a penalty. On the other hand, if the driver of LV chooses the yielding action, the payoff for the changing action is increased.

The *remaining distance* is related to a forced merging maneuver. Close to the end of the lane, the *remaining distance* factor forces the subject vehicle to merge. This term was formulated using the *Hardwall* concept proposed by Rakha and Zhang (2004) and the exponential function suggested by Wang et al. (2015) as a route cost term for a cost function of lane-changing and car-following controller [55, 56]. The *Hardwall* is an imaginary lane-changing wall for mandatory lane-changing and it is located at 10 times vehicle spacing at standstill (i.e., jam density spacing), x_j [54]. When $x_0 > x_{RD}$, this term considerably increases the payoff of the driver of SV to undertake a lane change.

2) Payoff Function of the driver of LV

The objective of the driver of LV is to maintain its car-following status subject to safety constraints. The payoff functions consist of the safety, speed difference between the PV and LV, expected acceleration level of the LV, and error terms as described above. For the driver of LV, the payoff functions, denoted by *Q* (in Table 3-1), are specified as:

$$Q_{ij} = \beta_{11}^1\left(\Delta x^{SV,LV} - x_j - x_s^{LV}\right) + \beta_{11}^2 \Delta v^{PV,LV} + \beta_{11}^3 a_y^{LV} + \varepsilon_{11}^{LV}, \quad \forall\, i = 1,2,3,\ j = 1,2 \qquad (3.10)$$

where

- $\Delta v^{PV,LV}$: Speed difference between the PV and LV;
- $\varepsilon_{11}^{LV}, \varepsilon_{12}^{LV}, \varepsilon_{21}^{LV}, \varepsilon_{22}^{LV}, \varepsilon_{31}^{LV}, \varepsilon_{32}^{LV}$: Error terms to capture the unobserved variables; and
- $\beta_{ij}^1, \beta_{ij}^2$, and β_{ij}^3 for $\forall\, i = 1,2,3,\ j = 1,2$ are parameters to be estimated. Note that it is expected that the driver of LV will have different weights on variables for each action strategy.

3.3.2 Payoff functions in the second model (in [51])

Payoff functions in game models reveal the expected outcome (or reward) of each player when a specific action strategy set in the stage game is chosen at a time step t. In the first model, this study formulated the payoff functions for the both drivers by using five decision factors [50]. To reduce the number of parameters and decrease correlations between variables, this study uses the simplified payoff functions for both drivers. A detailed explanation of the payoff functions used here is provided in the following subsections.

1) Payoff Functions for the driver of SV

In the payoff functions for the driver of SV, the main decision factor is the expected gap based on the anticipated acceleration levels of the two vehicles in each set of action strategies; the forced merging factor is also considered. It is assumed that the driver of SV predicts whether there are available lag and lead gaps to merge onto a freeway at the next time step. If available gaps are difficult to assure, it should be assumed that the driver intends to either to overtake or wait. In addition, the third term in Equation (3.11) and (3.12) is the forced merging factor for considering the remaining distance in the decision-making process. If the driver is close to the end of the acceleration lane, they should merge onto the freeway due to the remarkable increase of the changed action's payoffs. In other words, the model outcome should result in the driver of SV deciding to merge if there is not sufficient distance in the current lane for an 'overtaking (s_3)' or 'waiting (s_2)' action. As consideration of the forced merging situation, this third term was identically formulated using the *Hardwall* concept proposed by Rakha and Zhang as the exponential function [55]. Lastly, the last term in Equations (3.11) to (3.16) is an error term included to capture the unobserved utility. The payoff functions of the driver of SV, denoted by P_{ij} ($i = 1,2,3$ and $j = 1,2$), are specified as:

$$P_{11} = \alpha_{11}^1 \Delta x_{11}^{SV,LV}(t+\Delta t) + \alpha_{11}^2 \Delta x_{11}^{PV,SV}(t+\Delta t) + \alpha_{11}^3 \exp(x_0/x_{RD}) + \varepsilon_{11}^{SV} \quad (3.11)$$

$$P_{12} = \alpha_{12}^1 \Delta x_{12}^{SV,LV}(t+\Delta t) + \alpha_{12}^2 \Delta x_{12}^{PV,SV}(t+\Delta t) + \alpha_{12}^3 \exp(x_0/x_{RD}) + \varepsilon_{12}^{SV} \quad (3.12)$$

$$P_{21} = \alpha_{21}^1 \Delta x_{21}^{SV,LV}(t+\Delta t) + \varepsilon_{21}^{SV} \quad (3.13)$$

$$P_{22} = \alpha_{22}^1 \Delta x_{22}^{SV,LV}(t+\Delta t) + \varepsilon_{22}^{SV} \quad (3.14)$$

$$P_{31} = \alpha_{31}^1 \Delta x_{31}^{PV,SV}(t+\Delta t) + \varepsilon_{31}^{SV} \quad (3.15)$$

$$P_{32} = \alpha_{32}^1 \Delta x_{32}^{PV,SV}(t+\Delta t) + \varepsilon_{32}^{SV} \quad (3.16)$$

where

- $\Delta x_{ij}^{SV,LV}(t+\Delta t)$ = the expected lag gap between the SV and LV in the action strategies set (s_i, l_j) at time $t+\Delta t$ (in m);

- $\Delta x_{ij}^{PV,SV}(t+\Delta t)$ = the expected lead gap between the PV and SV in the action strategies set (s_i, l_j) at time $t+\Delta t$ (in m);
- x_0 = the distance threshold for forced lane-changing (= $10 \cdot x_j$) (in m);
- x_{RD} = the remaining distance in the acceleration lane for the SV (in m);
- ε_{ij}^{S} = an error term to capture the unobserved payoffs; and
- α_{11}^1, α_{11}^2, α_{11}^3, α_{12}^1, α_{12}^2, α_{12}^3, α_{21}^1, α_{22}^1, α_{31}^1, α_{32}^1 = parameters to be estimated. Note that it is expected that the driver of SV will have different weights on variables for each action strategy.

2) Payoff Functions for the driver of LV

For the payoff function of the driver of LV, it is assumed that the driver evaluates the future driving condition according to the speed difference between the SV and LV. The expected relative speed is used for the decision factor of the driver of LV in this study. The driver wants to maintain the car-following status and also perceives the SV's intention to merge when there is available spacing. Therefore, it is assumed that a 'yield (l_1)' action has priority for the driver of LV if there is no considerable decrease of speed expected. In other words, if the driver of LV is not affected by a merging action of the driver of SV, the former generally chooses the 'yield (l_1)' action.

If the relative speed between two vehicles is positive or close to zero, the driver of LV will likely choose the 'yield (l_1)' action. Otherwise, the driver of LV will likely try to block the SV's merging due to an anticipated decrease of speed. The payoff functions of the driver of LV denoted by Q_{ij} are specified as:

$$Q_{ij} = \beta_{ij}^1 \Delta \dot{x}_{ij}^{SV,LV}(t+\Delta t) + \varepsilon_{ij}^{LV}, \qquad \forall\, i = 1,2,3, \qquad j = 1,2 \tag{3.17}$$

where

- $\Delta \dot{x}_{ij}^{SV,LV}(t+\Delta t)$ = the expected relative speed between the SV and LV in the action strategies set (s_i, l_j) at time $t+\Delta t$ (in m/s);
- ε_{ij}^{LV} = an error term to capture the unobserved payoffs; and
- β_{ij}^1 = a parameter to be estimated.

3.3.3 Payoff functions in the third model

In previous game theory-based-models, the payoff functions for two players were formulated using the significant decision factors, such as safety, spacing (or gap), relative speed, travel time, expected acceleration level, remaining distance to reach the end of acceleration lane, and so on [2, 39-40, 50-52, 57]. In the first model, this study initially proposed the payoffs using five decision

factors: minimization of travel time, avoidance of collisions (i.e., safety), travel efficiency, the LV's expected acceleration, and remaining distance [50]. In a following study, the payoffs of the driver of SV were formulated by the expected gap and remaining distance, and the expected relative speed was considered as the other driver's main decision variable [51]. Both previous studies used multiple dimensioned variables making the payoffs as only interpreted as qualitative outcome to represent player's preference. In addition, an error term was considered to capture unobserved variables was formulated as a constant value, resulting in minimal consideration of a driver's randomness. As described previously, therefore, this study updates the payoff functions to use efficient decision variables including a random error term and proposes monotone (unitless) functions by transformation of quantitative variables. This section introduces the decision variables, and then presents the reformulated payoff functions for each driver.

1) Decision variables

a) Safety payoff

Among various decision factors, safety is a key factor for human drivers' decisions to avoid a potential collision or not induce a dangerous situation. Yu et al. (2018) used time headway as a safety payoff [57], as presented in Equation (3.18):

$$h_{PV,SV}(t) = \frac{x_{PV}(t) - x_{SV}(t)}{v_{SV}(t)} \tag{3.18}$$

where $x_{PV}(t)$ and $x_{SV}(t)$ are positions of the (potential) PV and SV at instant time t, respectively; and $v_{SV}(t)$ is speed of the SV at time t. However, they did not take the speed of a PV into account. In [51], the expected spacing between vehicles, indicating a possibility to ensure safe distance with consideration of vehicles' speed and acceleration levels, was used. Additionally, Wang et al. (2018) used a penalty formulated using relative speed and gap distance [58]. Kita used TTC between vehicles as the main payoff [40] as defined in Equation (3.19):

$$TTC_{PV,SV}(t) = \frac{x_{PV}(t) - x_{SV}(t) - l_{PV}}{v_{SV}(t) - v_{PV}(t)} \qquad \text{if } v_{SV}(t) > v_{PV}(t) \tag{3.19}$$

where l_{PV} denotes the length of the PV; and $v_{PV}(t)$ is the speed of the PV at instant time t.

The interactive effects of relative speed and gap distance are contained in the single measure TTC [59]. Brackstone et al. (1999) collected realistic data using an instrumented vehicle equipped with relative distance- and speed-measuring sensors [60]. Observations of vehicle trajectories from five participants showed that TTC is a major factor in lane-changing decisions. Most collision avoidance systems (or pre-crash safety systems) applied in a vehicle use the instantaneous TTC to evaluate collision risk [61]. Moreover, Vogel (2003) recommended to use TTC for evaluation of safety because it indicates the actual occurrences of dangerous situations [62]. Vogel also noted that a situation with a small TTC is imminently dangerous, and that a situation with a small

headway and relatively large TTC is a potentially dangerous situation. Therefore, this study proposes the integrated safety payoff function A^S with consideration of not only TTC but also headway, which was formulated using the hyperbolic tangent function, as presented in Equation (3.20) and (3.21).

$$A^S_{PV,SV} = \begin{cases} \left(tanh\left(\frac{TTC_{PV,SV}(t)}{t^S} - 1\right) + tanh\left(\frac{h_{PV,SV}(t)}{t^S} - 1\right)\right) \times 0.5, & \text{if } v_{SV}(t) > v_{PV}(t) \\ \left(1 + tanh\left(\frac{h_{PV,SV}(t)}{t^S} - 1\right)\right) \times 0.5, & o.w. \end{cases} \quad (3.20)$$

$$A^S_{SV,LV} = \begin{cases} \left(tanh\left(\frac{TTC_{SV,LV}(t)}{t^S} - 1\right) + tanh\left(\frac{h_{SV,LV}(t)}{t^S} - 1\right)\right) \times 0.5, & \text{if } v_{LV}(t) > v_{SV}(t) \\ \left(1 + tanh\left(\frac{h_{SV,LV}(t)}{t^S} - 1\right)\right) \times 0.5, & o.w. \end{cases} \quad (3.21)$$

Here $t^S = \min\left(\frac{RD_{SV}}{v_{SV}(t)}, 3\right)$ denotes minimum safe time headway between the 3-second rule for the minimum safe following distance recommended by the National Safety Council [63] and the time headway to reach the end of the acceleration lane ($= \frac{RD_{SV}}{v_{SV}(t)}$).

The safety payoffs of both drivers for the action strategies were formulated to satisfy $U^S \in [-1,1]$, as shown in Equation (3.22) to (3.25).

$$U^S_{SV}(s_1) = 0.5\left(A^S_{PV,SV} + A^S_{SV,LV}\right) \quad (3.22)$$

$$U^S_{SV}(s_2) = -A^S_{SV,LV} \quad (3.23)$$

$$U^S_{SV}(s_3) = -A^S_{PV,SV} \quad (3.24)$$

$$U^S_{LV}(l_1) = A^S_{SV,LV} = -U^S_{LV}(l_2) \quad (3.25)$$

For the 'change (s_1)' action of the driver of SV, $U^S_{SV}(s_1)$ was formulated as the average of safety payoffs taking both the PV and LV in the target lane into account. For the 'wait (s_2)' and 'overtake (s_3)' action of the driver of SV, on the other hand, the driver's safety payoffs were formulated to consider only the corresponding vehicle related to each action strategy. Likewise, it was assumed that the driver of LV also evaluates their safety in consideration of the SV only.

As shown in the safety payoff formulation, the safety payoffs vary by spacing between vehicles and each vehicle's speed. Figure 3-4 shows the prospective safety payoffs of the driver of SV at various speeds of the three vehicles (i.e., PV, SV, and LV), with the SV in different positions between the PV and LV. In this example, spacing between the PV and LV is constant at 77 m.

Figure 3-4(a) presents the case in which the SV is located close to the PV. In other words, the lead gap $\Delta x_{PV,SV}$ is small and the lag gap $\Delta x_{SV,LV}$ is large. If $v_{PV} > v_{SV}$, $U_{SV}^{S}(s_1)$ is greater than $U_{SV}^{S}(s_3)$. Otherwise, the driver of SV is attracted to choose the 'overtake (s_3)' action in consideration of safety. In the second case described in Figure 3-4(b), the SV is located at the middle position between the PV and LV. Therefore, the 'change (s_1)' action is relatively attractive, i.e., $U_{SV}^{S}(s_1) > U_{SV}^{S}(s_2)$ and, $U_{SV}^{S}(s_1) > U_{SV}^{S}(s_3)$ even if v_{SV} is slightly less than v_{PV} and v_{LV}. The the 'overtake (s_3)' action is attractive when $v_{SV} \gg v_{PV}$, and $U_{SV}^{S}(s_2)$ is greater than $U_{SV}^{S}(s_1)$ when $v_{SV} \ll v_{LV}$. The last case, in which the SV is close to the LV, represents the case where the driver of SV is drawn to choosing the 'wait (s_2)' action if $v_{LV} > v_{SV}$. If $v_{SV} > v_{LV}$, the 'change (s_1)' action is more attractive. From these cases, transformed safety payoffs are reasonable to represent the general decision-making results of the driver of SV.

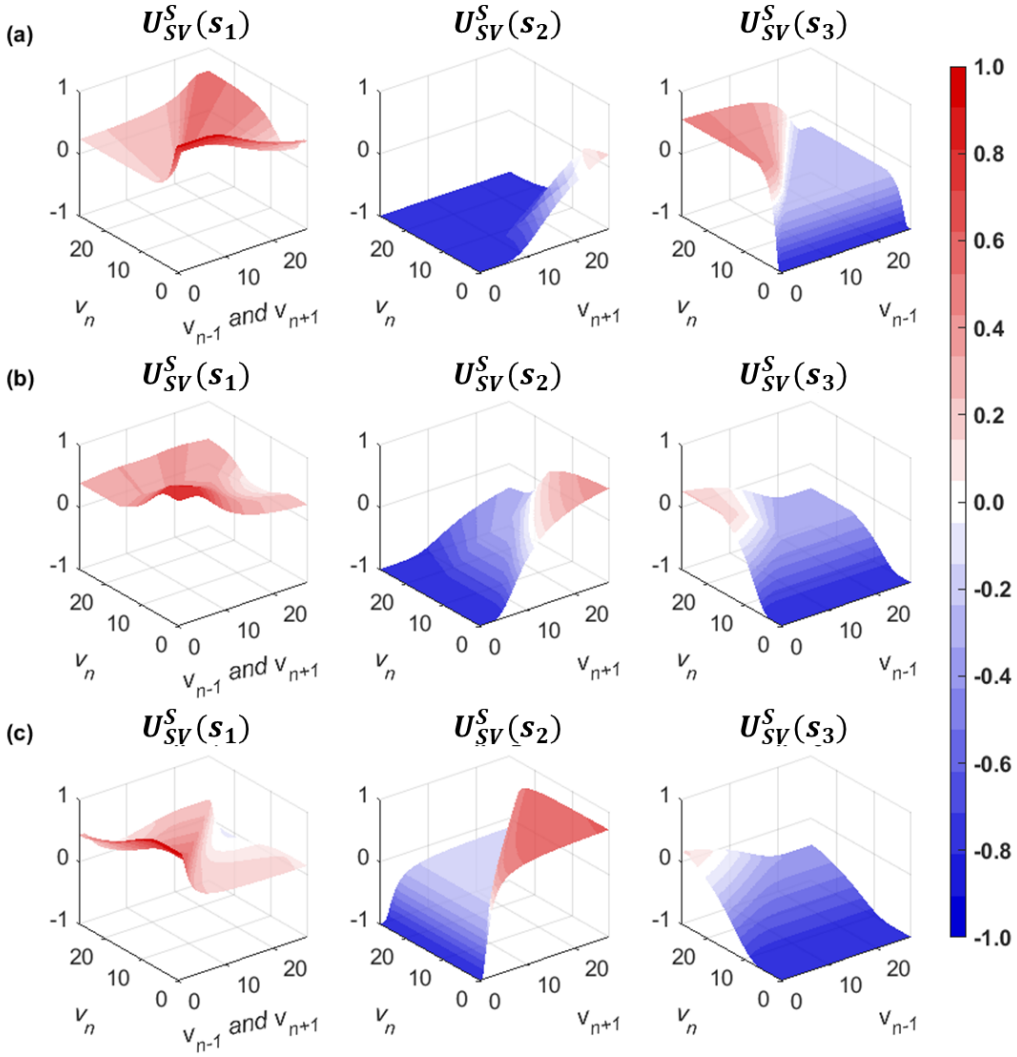

Figure 3-4. Safety payoffs of the driver of SV for the s_1, s_2, and s_3 action: (a) close to the PV ($\Delta x_{SV,LV} = 67\ m, \Delta x_{PV,SV} = 10\ m$); (b) middle position between PV and LV ($\Delta x_{SV,LV} = 38\ m, \Delta x_{PV,SV} = 39\ m$); (c) close to the LV ($\Delta x_{SV,LV} = 10\ m, \Delta x_{PV,SV} = 67\ m$).

Figure 3-5 presents the safety payoffs for the driver of LV in the three cases described above. In Figure 3-5(a), which shows that $\Delta x_{SV,LV}$ is considerably large, the driver of LV desires to choose the 'yield (l_1)' action, except in the case where $v_n \ll v_{n+1}$. These payoffs seem to be reasonable because the LV is far away from the SV. In the second case, the 'yield (l_1)' action is attractive as well. This case is similar to a real field situation, where the lane-changing action of the following vehicle in the target lane mostly shows cooperation in order to accept the merging vehicle's lane change. In the third case, the huge deceleration is expected to provide a gap to the SV because the LV is close to the SV. Therefore, the safety payoffs of the driver of LV for the 'block (l_2)' action is higher than that for the l_1 action if $v_{SV} < v_{LV}$. Otherwise, the safety payoff of the driver of LV for the 'yield (l_1)' action is slightly higher, except in a freeway congested traffic condition (i.e., $v_{SV} \gg v_{LV}$).

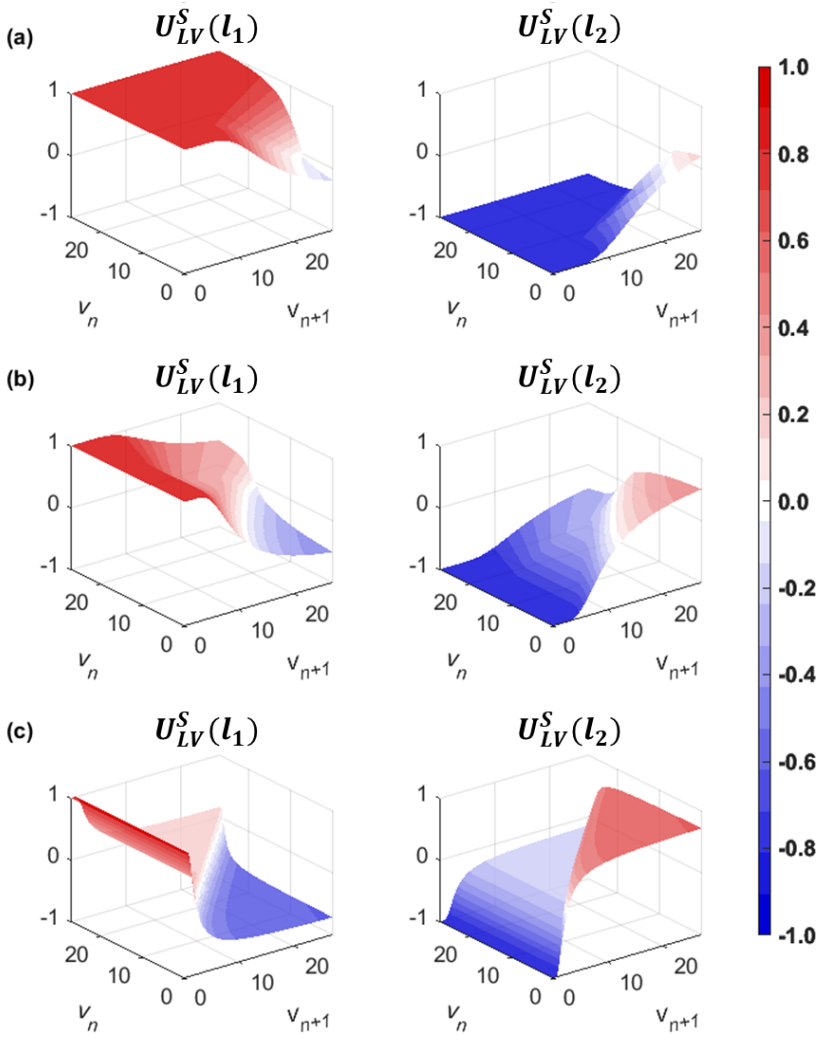

Figure 3-5. Safety payoffs of the driver of LV for the l_1 and l_2 action: (a) close to the PV ($\Delta x_{SV,LV} = 67\ m, \Delta x_{PV,SV} = 10\ m$); (b) middle position between PV and LV ($\Delta x_{SV,LV} = 38\ m, \Delta x_{PV,SV} = 39\ m$); (c) close to the LV ($\Delta x_{SV,LV} = 10\ m, \Delta x_{PV,SV} = 67\ m$).

b) Forced merging payoff for the driver of SV

According to the empirical field data collected at a freeway merging section, the driver of a vehicle entering through an on-ramp usually accelerates for speed-harmonization with freeway vehicles. The driver of SV then selects a gap to merge onto the freeway. In congested traffic conditions, however, the merging vehicles travel at a higher speed than the surrounding vehicles on the freeway. Thus, the driver occasionally rejects the initial gap and then uses a farther forward gap close to the end of the acceleration lane. Wan et al. found that merging vehicles pass freeway vehicles and try to find an acceptable gap to merge onto the freeway after traveling longer than the normal merging cases in congested traffic conditions [22]. Marczak et al. (2013) analyzed data collected at two sites to find variables related to gap acceptance, concluding that the distance to the end of the acceleration lane is a significant variable [64]. Also, Hwang and Park (2005) concluded that the remaining distance is the most important factor for determining gap acceptance; the driver will most likely accept a smaller gap if the remaining distance to the end of the acceleration lane is smaller [65]. In order to consider the case in which a vehicle merges close to the end of the acceleration lane, the payoff function of the driver of SV should include a term called the forced merging payoff, which relates the remaining distance to the end of the acceleration lane. It affects that the driver decides the 'change (s_1)' action at the decision point where the remaining distance is considerably short.

This study formulated the forced merging payoff as a function of the remaining distance and $v_{SV}(t)$. There is an assumption that the end of the acceleration lane is an imaginary preceding vehicle that is stopped. The presence of this imaginary vehicle, which is also considered as a hard wall, means the driver of SV cannot drive further due to the restricted length of the acceleration lane. Thus, the expected safety distance to maintain the instant speed of the SV, $v_{SV}(t)$, was estimated by a car-following model. This study used the RPA car-following model, which was first developed by Rakha et al. (2009) [66]. Performance of the RPA car-following model has been validated against naturalistic driving data [54]. This study estimated the safety distance for the SV, $x_{SV}^{CF}(t)$ using the RPA model's two components: steady-state traffic stream behavior and collision avoidance. The steady state modeling applies the Van Aerde's steady state car-following model [67, 68], which is a non-linear single regime function of vehicle speed and spacing. The first safe spacing (i.e., safety distance) provided by the steady-state model is

$$x_{SV}^{CF\_1}(t) = c_1 + c_3 \cdot v_{SV}(t) + \frac{c_2}{v_f - v_{SV}(t)}. \tag{3.26}$$

Here v_f indicates the free-flow speed. The model coefficients can be computed as

$$c_1 = \frac{v_f}{k_j {v_c}^2}\left(2v_c - v_f\right), \tag{3.27}$$

$$c_2 = \frac{v_f}{k_j {v_c}^2}\left(v_f - v_c\right)^2, \tag{3.28}$$

$$c_3 = \frac{1}{q_c} - \frac{v_f}{k_j {v_c}^2}, \tag{3.29}$$

where k_j, v_c, and q_c indicate the jam density, speed-at-capacity, and saturation flow rate, respectively. The detailed definition of these coefficients is described in [67].

As the second component of the RPA model, collision avoidance was modeled to avoid incidents at non-steady state conditions [54]. The second safe spacing estimated by collision avoidance is defined in Equation (3.30).

$$x_{SV}^{CF\_2}(t) = \frac{v_{SV}(t)^2}{2 \cdot a_{min}} + x_j \tag{3.30}$$

where a_{min} and x_j denote the minimum acceleration (i.e., maximum deceleration) and the jam spacing, respectively.

The maximum value of two safe spacings, $x_{SV}^{CF\_1}(t)$ and $x_{SV}^{CF\_2}(t)$, is considered as the expected safe spacing to maintain current speed.

$$x_{SV}^{CF}(t) = \max\left(x_n^{CF\_1}(t), x_n^{CF\_2}(t), x_{max}^{RD}\right) \tag{3.31}$$

where x_{max}^{RD} is the maximum of the remaining distance, i.e., the longitudinal length of the acceleration lane.

To balance each payoff, this study re-formulated the forced merging payoff of the driver of SV, U_{SV}^{FM}.

$$U_{SV}^{FM} = \left[\frac{\max\left(x_{SV}^{CF}(t) - x_{SV}^{RD}(t), 0\right)}{x_{SV}^{CF}(t)}\right]^2 \tag{3.32}$$

where $x_{SV}^{RD}(t)$ indicates the remaining distance for the SV in the acceleration lane at time t. This formulation satisfies $U_{SV}^{FM} \in [0,1]$ as shown in Figure 3-6. If the remaining distance is shorter than $x_{SV}^{CF}(t)$, U_{SV}^{FM} begins to have positive payoffs, inducing a preference for the 'change (s_1)' action. This term presents greater payoffs when $v_{SV}(t)$ is faster.

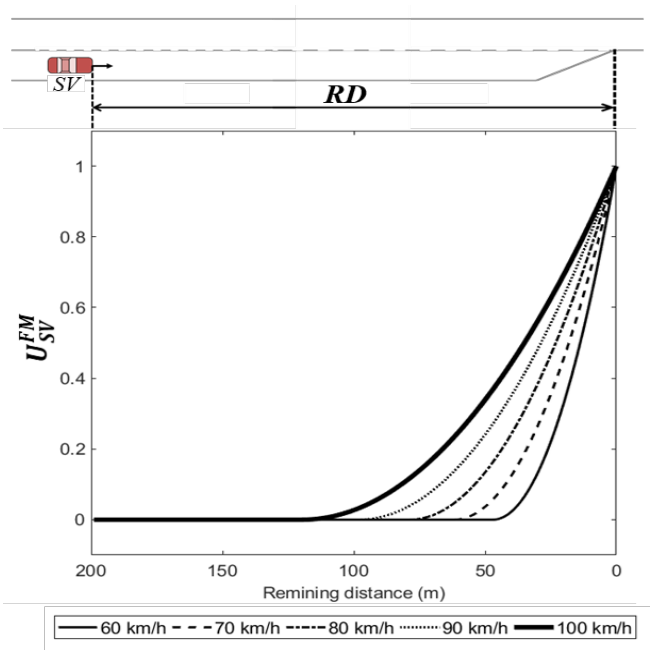

Figure 3-6. Forced merging payoff by the remaining distance at various speeds.

2) Payoff functions for the drivers of the SV and LV

Table 3-3 represents the updated merging decision-making model in normal form. The payoff functions of the driver of SV consist of both the safety and forced merging payoffs, and those of the driver of LV include the safety payoffs only. In order to capture unobserved utility, both players' payoff functions also have an error term, which was assumed to be normally distributed as $\varepsilon_{ij}^{SV\ or\ LV} \sim N(0,1)$. The parameters in the payoff functions, i.e., set of α_{ij} and β_{ij} (i = 1,2,3 and j = 1, 2), are parameters to be estimated.

Table 3-3. Game Structure and Payoff Functions of the Merging Decision-Making Game in Normal Form

Player & Actions		Driver of LV	
		Yield $[l_1(q_1)]$ [b]	Block $[l_2(q_2)]$
Driver of SV	Change $[s_1(p_1)]$ [a]	• $P_{11} = \alpha_{11}^1 + \alpha_{11}^2 U_{SV}^S(s_1) + \alpha_{11}^3 U_{SV}^{FM} + \varepsilon_{11}^{SV}$ • $Q_{11} = \beta_{11}^1 + \beta_{11}^2 U_{LV}^S(l_1) + \varepsilon_{11}^{LV}$	• $P_{12} = \alpha_{12}^1 + \alpha_{12}^2 U_{SV}^S(s_1) + \alpha_{12}^3 U_{SV}^{FM} + \varepsilon_{12}^{SV}$ • $Q_{12} = \beta_{12}^1 + \beta_{12}^2 U_{LV}^S(l_2) + \varepsilon_{12}^{LV}$
	Wait $[s_2(p_2)]$	• $P_{21} = \alpha_{21}^1 + \alpha_{21}^2 U_{SV}^S(s_2) + \varepsilon_{21}^{SV}$ • $Q_{21} = \beta_{21}^1 + \beta_{21}^2 U_{LV}^S(l_1) + \varepsilon_{21}^{LV}$	• $P_{22} = \alpha_{22}^1 + \alpha_{22}^2 U_{SV}^S(s_2) + \varepsilon_{22}^{SV}$ • $Q_{22} = \beta_{22}^1 + \beta_{22}^2 U_{LV}^S(l_2) + \varepsilon_{22}^{LV}$
	Overtake $[s_3(p_3)]$	• $P_{31} = \alpha_{31}^1 + \alpha_{31}^2 U_{SV}^S(s_3) + \varepsilon_{31}^{SV}$ • $Q_{31} = \beta_{31}^1 + \beta_{31}^2 U_{LV}^S(l_1) + \varepsilon_{31}^{LV}$	• $P_{32} = \alpha_{32}^1 + \alpha_{32}^2 U_{SV}^S(s_3) + \varepsilon_{32}^{SV}$ • $Q_{32} = \beta_{32}^1 + \beta_{32}^2 U_{LV}^S(l_2) + \varepsilon_{32}^{LV}$

[a] p_i in parentheses denotes the probability assigned to the pure strategy of the driver of SV, s_i; $\sum_{i=1}^{3} p_i = 1$.
[b] q_j in parentheses denotes the probability assigned to the pure strategy of the driver of LV, l_j; $\sum_{j=1}^{2} q_j = 1$.

3.4 Development of the Model Using a Repeated Game Concept

In the game model, one of the characteristics to be specified is the number of games to be repeated [40]. Aside from [52], none of the other game theory-based models reviewed in this study have used the repeated game approach. In the authors' previous study, a repeated game approach was used in order to depict a practical decision-making process for merging maneuvers. In real life, at a freeway merging section in a traditional transportation environment, a driver continuously makes a decision using the data taken in by sight and controls the vehicle to fulfill their decision. When the merging vehicle enters the acceleration lane, the driver of SV selects a gap type to change a lane and then directs their vehicle accordingly. The driver controls the acceleration level to synchronize vehicle speed with freeway vehicles and ensure a safe gap distance [18, 22]. During this lane-changing preparation process, the driver of SV repeatedly checks surroundings to judge if their decision can be fulfilled and tries to follow-up on their decision. In this study, therefore, this repetition in decision-making for merging maneuvers prior to lane-changing execution was regarded as playing the game repeatedly.

In game theory, the repeated game consists of a number of repetitions of a stage game. When players interact by playing a similar stage game numerous times, the game is called a dynamic, or repeated game. As shown in Figure 3-7, the repeated game concept implies that a stage game with identical structure is repeatedly played until termination of the game, which is divided into two classes: finite or infinite, depending on the players' beliefs about the number of repetitions. In this study, the decision-making game for merging was regarded as an infinitely repeated game because the players in the game do not know how many times the game will be repeated. Note that for an infinitely repeated game, the stage game will not necessarily be repeated an infinite number of times.

Furthermore, if the identity of the players changes, the base stage game is reset as a new stage game between the driver of SV and the fresh driver of LV at time step t_1. Each driver makes a decision at a given time step *t* in consideration of the entire history of play in previous time steps. Drivers do not know what the opponent will choose without any communication system at a given time step *t*, but recognize the other driver's decision made in previous time steps by observing the other vehicle's relative speed or acceleration level. Thus, this game is also regarded as an *imperfect information game* with *perfect recall* (or *monitoring*). It allows a player to condition their current action in consideration of their opponent's earlier actions.

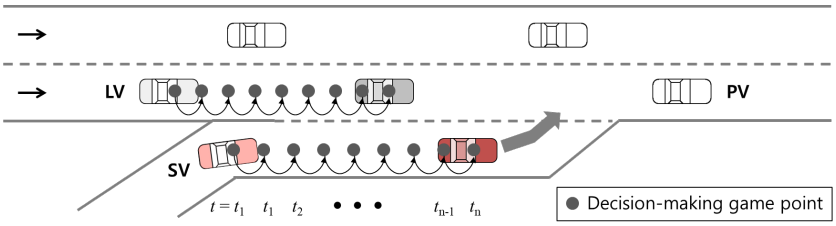

Figure 3-7. Conceptual diagram of a repeated game for merging decision-making (in [52]).

Drivers (i.e., players) interact by playing a stage game numerous times. As a summary of explanation about the game model type, the one-shot game model implies that previous game results do not affect the present game, while the decision-makers take previous game results into account in the repeated game model, as illustrated in Figure 3-8. This study uses the cumulative payoffs to prevent the repeated fluctuations in payoffs, as proposed in [52]. The stage decision-making game is conducted periodically and repeatedly over discrete time periods $T \in [t_1, t_n]$. Time preference is considered by assuming that future payoffs are weighted proportionately at rate δ, called the rate factor. Cumulative payoffs of the driver d for action strategy a_{ij}, i.e., $U_{ij}^d = P_{ij}$ or Q_{ij}, are presented in Equation (3.33).

$$U_{ij}^d(T) = \sum_{t_1}^{t_n} \delta^{t-1} u_{ij}^d(t) \tag{3.33}$$

Here $u_{ij}^d(t)$ is a utility of a driver d for an action strategy set (s_i, l_j) at time step t; T is the number of decision-making time steps; and d denotes a driver, i.e., player in a game, driver of SV or that of LV. The rate factor $\delta = 0$ implies that the present has no value [69]. Like the assumption in the previous study, in other words, players follow the action strategy decided at the initial game point without change of their former decisions. Otherwise $\delta = 1$ means that the present is just as important as the past [69]. In addition, $0 < \delta < 1$ indicates that the past more valuable than the present; $\delta > 1$ denotes that the current payoffs are more meaningful than the past payoffs.

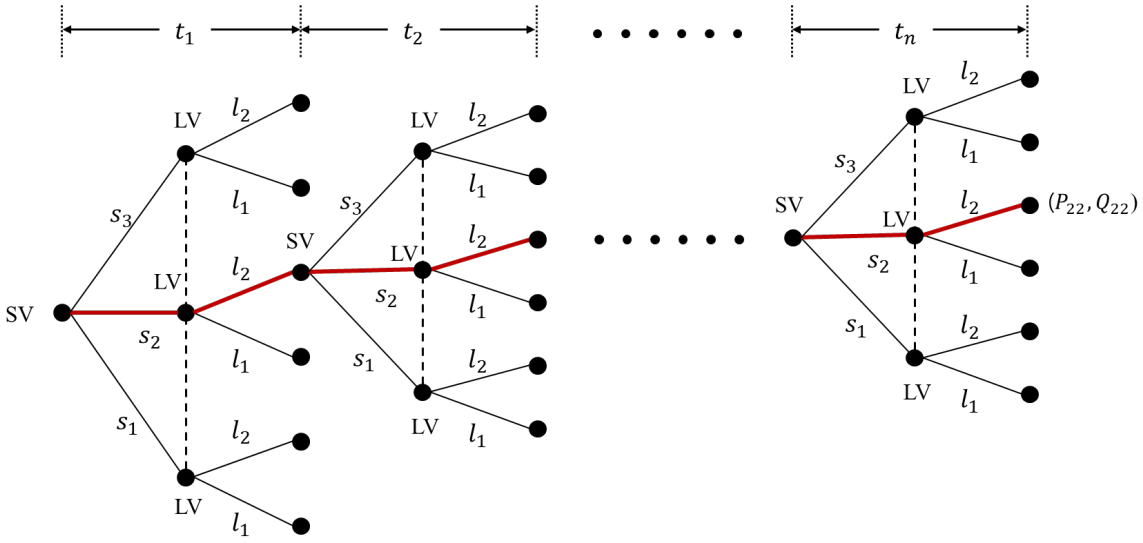

Figure 3-8. Decision-making game based on the repeated game approach in extensive form.

Chapter 4. Evaluation of Merging Decision-Making Game Models

This chapter presents evaluation of game models developed in previous chapter. The game models are calibrated using the Next Generation SIMulation (NGSIM) data, then the model validation results are provided. In addition, this study conducts a sensitivity analysis to evaluate whether the developed stage game model can depict rational merging decision-making according to variation of the related factors. Moreover, this study develops an agent-based model integrated with the game models. The case study compares simulation results based on each game model, i.e., the repeated game model or the one-shot game model, in cooperative and competitive merging scenarios. The results indicate evidence of benefit to use the repeated game approach that previous decision-making results take into account.

This chapter is based on the papers listed below:

1. Kang, K. and Rakha, H. A. (2019). A Repeated Game Theory Lane-Changing Model for Merging Maneuvers. Submitted to *Sensors*.

2. Kang, K., & Rakha, H. A. (2018). Modeling driver merging behavior: a repeated game theoretical approach. *Transportation Research Record: Journal of the Transportation Research Board*, *2672*(20), 144-153. doi: 10.1177/0361198118792982

3. Kang, K. and Rakha, H. A. (2017, July). *Development of a Decision Making Model for Merging Maneuvers: A Game Theoretical Approach*. In Conference on Traffic and Granular Flow, Washington, DC., USA.

4. Kang, K., & Rakha, H. A. (2017). Game theoretical approach to model decision making for merging maneuvers at freeway on-ramps. *Transportation Research Record: Journal of the Transportation Research Board*, *2623*(1), 19-28. doi: 10.3141/2623-03

4.1 Next Generation SIMulation (NGSIM) Data

To help achieve wider acceptance of the use of microsimulation systems and ensure the tools provide accurate results, the Next Generation SIMulation (NGSIM) program was launched as Traffic Analysis Tools Program of the Federal Highway Administration (FHWA) [43]. It was conducted through a public-private partnership between FHWA and commercial microsimulation software developers, the academic research community, and the traffic microsimulation community. One of objectives of the program is to collect real-word data for the research, development, and validation of behavioral algorithms. The vehicle trajectory data, which was recorded every one-tenth of a second, were collected using digital video cameras like the one shown in Figure 4-1.

Figure 4-1. A digital video camera mounted on top of a building that overlooks a highway is recording vehicle trajectory data.

One of several datasets collected under the NGSIM program is the US Highway 101 (US 101) dataset [43] which was used in this study for model evaluation. The vehicle trajectory data on a segment of U.S. Highway 101 (Hollywood Freeway) in Los Angeles, California collected between 7:50 a.m. and 8:35 a.m. on June 15th, 2005 [70]. The study area, as illustrated in Figure 4-2, was approximately 640 meters (2,100 feet) in length and consisted of five mainline lanes throughout the section. An auxiliary lane is present through a portion of the corridor between the on-ramp at Ventura Boulevard and the off-ramp at Cahuenga Boulevard and the lane length is approximately 212 m. Eight synchronized digital video cameras, mounted from the top of a 36-story building adjacent to the freeway, recorded vehicles passing through the study area. This vehicle trajectory data transcribed from the video provide the precise location of each vehicle within the study area every one-tenth of a second, resulting in detailed lane positions and locations relative to other vehicles. These data represent the buildup of congestion, or the transition between uncongested

and congested conditions, and full congestion during the peak period [70]. The vehicle speeds on the main lane varied from 32.18 to 49.88 km/h during the 45 minutes of data collection, while the average speed of the on-ramp merging vehicles when entering the auxiliary lane was around 50.01 km/h [22].

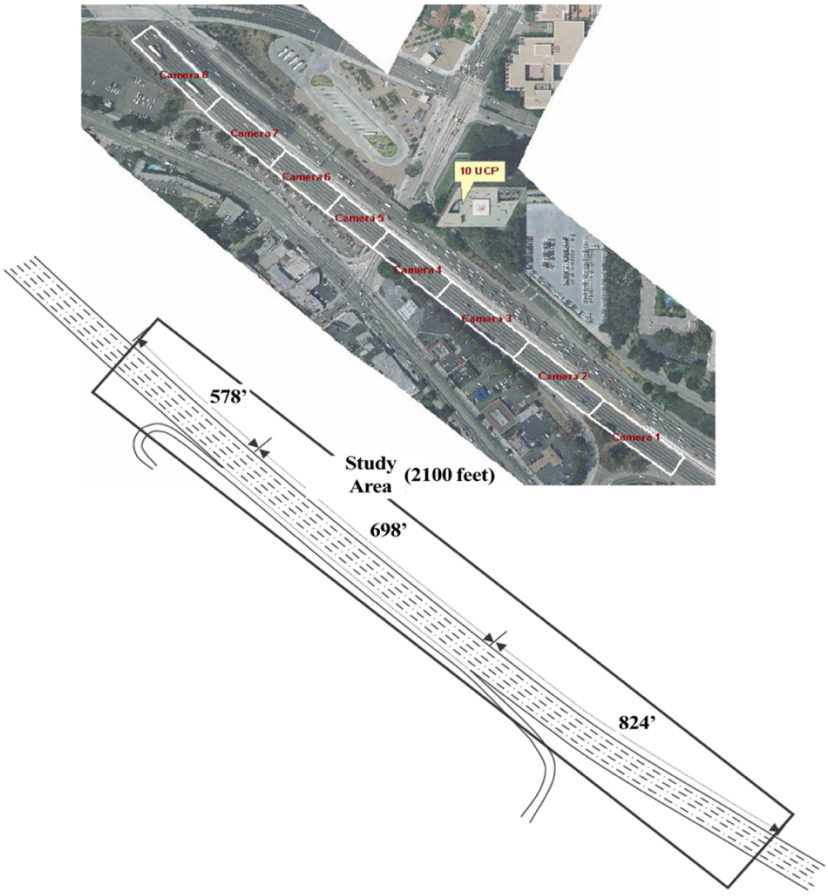

Figure 4-2. Study area schematic and camera coverage for vehicle trajectory data collected on US 101 (in [70]).

4.2 Evaluation of the First Model (in [50])

4.2.1 Preparation of Observation Dataset

To calibrate the proposed model, the observational data for each set of pure strategies were extracted and classified. It is important for model evaluation that the action strategies for the drivers of the SV and LV are identified for each case considering only vehicle trajectory data. Talebpour et al. proposed an identification method based on the visual observation; however, they noted that the method can induce significant error [39]. In addition, it is difficult to define the exact point at which a driver decides to initiate a merging maneuver, (i.e., the point the signal light is

turned on). This study suggests a simple method to categorize the observed data. In this work, it is assumed that the decision of the driver of SV is categorized by a comparison of the configuration of the surrounding vehicles (i.e., the PV and LV) during travel in the imaginary decision-making section of the acceleration lane (see Figure 4-3). If there is no change with both the PV and LV in the section, the driver of SV is considered to choose a 'change (s_1)' action at the beginning of the wall. On the other hand, if the potential PV and LV are replaced due to a change of circumstance (e.g., LV's 'block (l_2)' action and SV's 'overtake (s_3)' or 'wait (s_2)' action), the decision of the driver of SV will be a 'wait (s_2)' or 'overtake (s_3)' action, and a new decision point is considered.

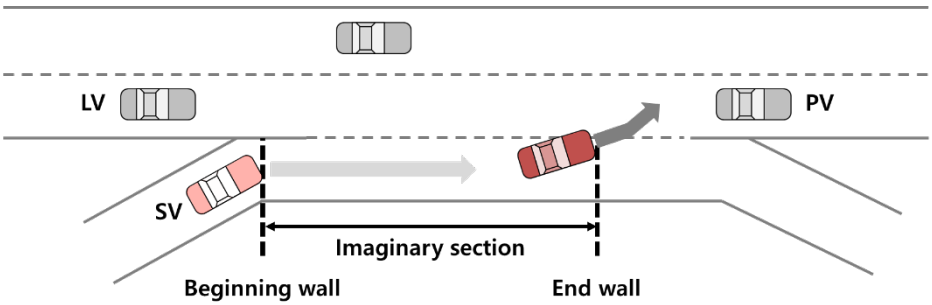

Figure 4-3. Imaginary section to extract data for model calibration and validation.

To identify the observed action strategies of the driver of LV, Liu et al. analyzed and screened the speed profiles of the SV and LV in each merging case [2]. In the NGSIM data, however, the acceleration data collected every 0.1 s showed fluctuations that were affected by the car-following situation. Using the acceleration level as a standard to classify the maneuvers chosen by the driver of LV is considerably challenging. Therefore, this study proposes the longitudinal spacing between the lead and lag vehicles, i.e., PV and LV, as the classification standard herein as shown in Figure 4-4. It is assumed that the gap distance between the two vehicles in the target lane reveals the LV's maneuvers considering the expected SV's lane change. In Figure 4-4(a), the gap distance between the SV and LV is less than 3 m at the beginning wall. Although the LV has a non-negative acceleration, it is regarded to reveal a 'yield (l_1)' action by increasing the gap distance between the PV and LV in the imaginary section. On the other hand, the action of the driver of LV is classified as a 'block (l_2)' action when the gap distance between the two vehicles on the target lane decreases in the section as shown in Figure 4-4(b).

In this study, a total of 378 cases, at the time to play the merging decision-making game, were extracted. All possible data were screened to test the model using a large number of data to capture various merging maneuvers. Nevertheless, the cases showing the 'wait (s_2)' action of the driver of SV were rare; only four cases were identified since the NGSIM data were collected during a peak hour.

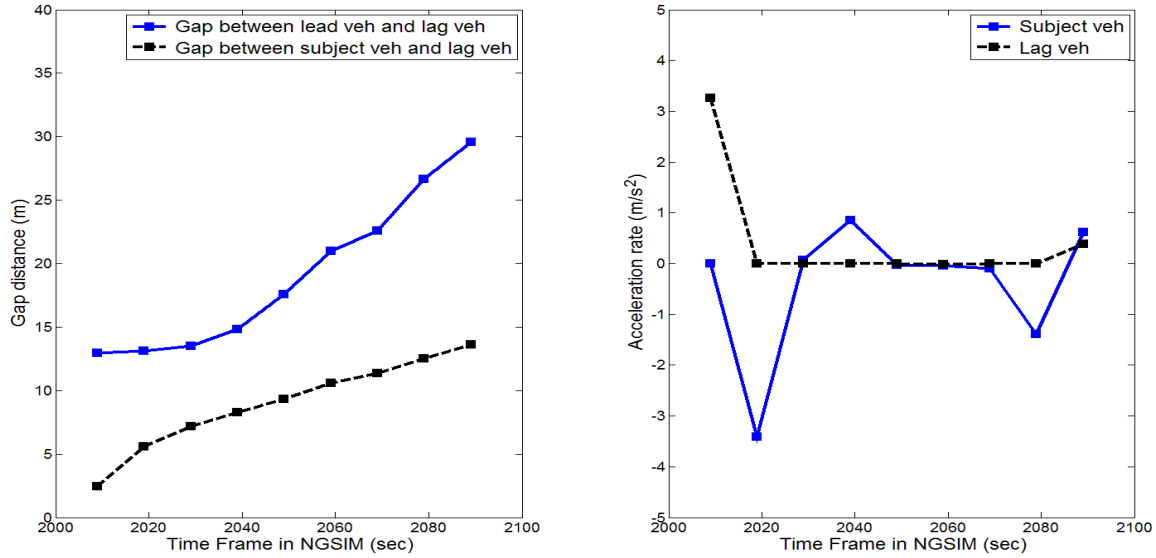

(a) SV (vehicle ID: 344) and LV (vehicle ID: 306) in yielding situation.

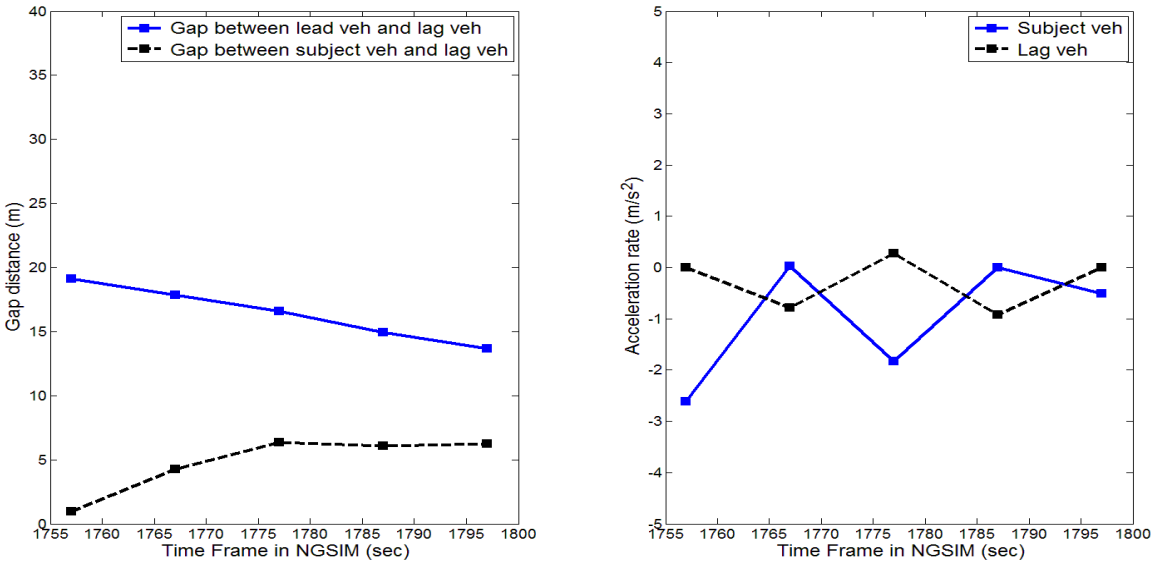

(b) SV (vehicle ID: 303) and LV (vehicle ID: 290) in blocking situation.

Figure 4-4. Gap distance and acceleration for a comparison of the action strategies of the driver of LV (in the observed data from 8:20 a.m. to 8:35 a.m.).

4.2.2 Model Calibration

To calibrate the merging decision-making model, this study followed the calibration method proposed by [2]. Figure 4-5 shows the schematic workflow used in model calibration. (A^k and B^k denotes all parameters to be estimated for the payoff functions of the drivers of the SV and LV, respectively.) Liu et al. proposed a parameter estimation method by solving a bi-level programming problem [2]. The upper level is a non-linear programming problem to minimize the system total deviation from actual observed action:

$$\min \sum_{i=1}^{n} (1 - x_i) \tag{4.1}$$

where i is the index of observations, n is the number of observations in the dataset. x_i denotes an indicator of model prediction. It indicates that the proposed model estimates correctly for both drivers' action, specified as:

$$x_i = \begin{cases} 1 & if\ S_i = \hat{S}_i(p_1^i, p_2^i, p_3^i)\ and\ L_i = \hat{L}_i(q_1^i, q_2^i) \\ 0 & otherwise \end{cases} \tag{4.2}$$

where S_i and $\hat{S}_i$ are the observed action and predicted action of the driver of SV (1: change, 2: wait, and 3: overtake), and L_i and $\hat{L}_i$ are the observed action and predicted action of the driver of LV (1: yield and 2: block).

For lower level programming, the estimated parameters should satisfy the Nash equilibrium for the observations. As stated above, to solve the two-player non-cooperative game, the study used the algorithm developed by Chatterjee [71].

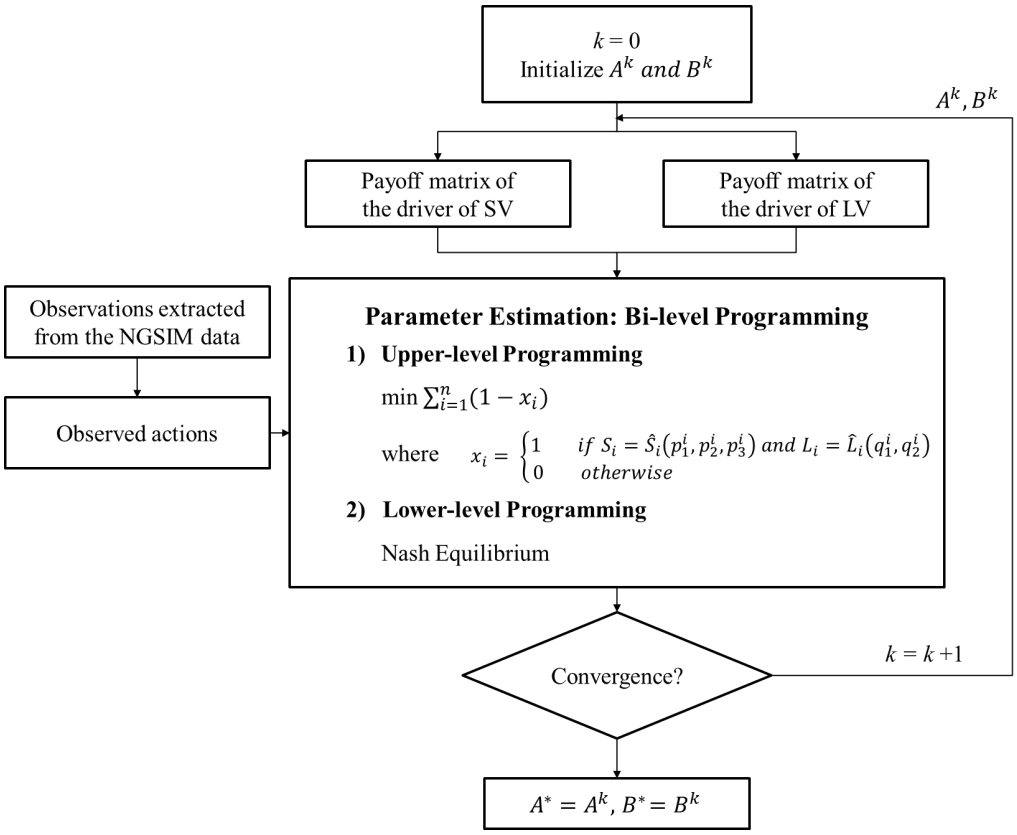

Figure 4-5. Schematic workflow for calibration approach based on bi-level programming.

In addition, the RPA model needed to be calibrated herein since the defined payoff functions include variables related to the car-following model. The macroscopic parameters, i.e., x_j, v_d, and v_c, were calibrated by using a heuristic automated tool (SPD-CAL), described by Rakha and Arafeh [72]. To calibrate the RPA model, all 45 minutes of NGSIM data were used. The parameters estimated by SPD-CAL were x_j = 6.35 m, v_d = 80.4 km/h, and v_c = 40.6 km/h. The estimated parameters for the RPA model were used in model calibration and validation.

A total of 201 cases (out of 378) collected between 7:50 a.m. and 8:20 a.m. was used in model calibration. Tables 4-1 and 4-2 show the estimated parameters for the payoff functions of the drivers of the SV and LV, respectively. The mean absolute error (MAE) was calculated by Equation (4.3). The MAE for the calibrated model is 0.104. This demonstrates that the proposed model correctly captures 89.6% of decision-making for merging maneuvers.

$$MAE = \frac{1}{n}\sum_{i=1}^{n}(1 - x_i) \tag{4.3}$$

Table 4-1. Calibration Results for the Payoff Functions of the Driver of SV

Function	Parameter	Calibrated Value	Parameter	Calibrated Value
P_{11}	α_{11}^1	2.019	α_{11}^5	-6.723
	α_{11}^2	1.991	α_{11}^6	16.225
	α_{11}^3	-4.931	ε_{11}^{SV}	28.740
	α_{11}^4	7.145		
P_{12}	α_{12}^1	2.780	α_{12}^5	-7.507
	α_{12}^2	11.751	α_{12}^6	9.071
	α_{12}^3	-2.965	ε_{12}^{SV}	-2.399
	α_{12}^4	1.989		
P_{21}	α_{21}^1	-8.416	α_{21}^3	3.582
	α_{21}^2	-7.625	ε_{21}^{SV}	1.251
P_{22}	α_{22}^1	-5.513	α_{22}^3	3.700
	α_{22}^2	-25.911	ε_{22}^{SV}	-35.591
P_{31}	α_{31}^1	-4.336	α_{31}^3	-5.345
	α_{31}^2	-9.617	ε_{31}^{SV}	-3.786
P_{32}	α_{32}^1	-6.016	α_{32}^3	-4.463
	α_{32}^2	-8.916	ε_{32}^{SV}	-16.331

Table 4-2. Calibration Results for the Payoff Functions of the Driver of LV

Function	Parameter	Calibrated Value	Parameter	Calibrated Value
Q_{11}	β_{11}^{1}	0.165	β_{11}^{3}	0.000
	β_{11}^{2}	14.214	ε_{11}^{LV}	3.166
Q_{12}	β_{12}^{1}	-0.024	β_{12}^{3}	0.000
	β_{12}^{2}	-9.293	ε_{12}^{LV}	3.871
Q_{21}	β_{21}^{1}	8.154	β_{21}^{3}	6.517
	β_{21}^{2}	8.572	ε_{21}^{LV}	2.404
Q_{22}	β_{22}^{1}	-8.999	β_{22}^{3}	-4.643
	β_{22}^{2}	-7.196	ε_{22}^{LV}	11.268
Q_{31}	β_{31}^{1}	0.028	β_{31}^{3}	7.418
	β_{31}^{2}	13.813	ε_{31}^{LV}	8.805
Q_{32}	β_{32}^{1}	-0.272	β_{32}^{3}	-6.539
	β_{32}^{2}	-53.247	ε_{32}^{LV}	4.687

4.2.3 Model Validation

The proposed model was evaluated to validate the prediction capability of the calibrated model. This study used the MAE and root mean square error (RMSE) for model validation, as shown in Equations (4.3) (as presented above) and (4.4), respectively:

$$\mathrm{RMSE} = \sqrt{\frac{1}{\mathrm{n}}\sum_{\mathrm{i}=1}^{\mathrm{n}}(1 - x_i)} \tag{4.4}$$

A total of 177 cases (out of 378) collected between 8:20 a.m. and 8:35 a.m. was used for model validation purposes. The MAE, which captures the false alarm rate as stated by Liu et al., is 0.158. This reveals the model successfully predicted vehicle actions in merging cases for 84.2 % of all cases. The RMSE of model predictions is 0.398. This shows that the model has the capability to predict the decision-making of both vehicles in the on-ramp section. Due to the lack of observational data for the 'wait (s_2)' action strategy of the driver of SV, the proposed model is expected to reveal better prediction capacity for merging maneuvers if a balanced dataset for all sets of strategies is used in model calibration.

4.3 Evaluation of the Second Model

4.3.1 Evaluation of the One-Shot Game Model Based on the Second Stage Game (in [51])

1) Preparation of Observation Dataset

As described previously, the US 101 data collected between 7:50 a.m. and 8:35 a.m. on June 15th, 2005 were used for calibration of the developed merging decision-making model. To extract observations properly from the field data, as shown in Figure 4-6, all moments of the game were selected in the decision-making period between the beginning point of the acceleration lane and the lane change execution point. Figure 4-6 demonstrates how the point of lane change execution time is defined by the lateral movement of the subject vehicle in the vehicle trajectory data. Specific observed cases where the initial lag spacing at stage t_1 was greater than twice the jam density spacing $2x_j$ were eliminated from the datasets. Specific observed cases where the initial lag gap at time step t_1 was greater than twice the jam density spacing, $2x_j$, were eliminated from the dataset. In these cases, it was assumed that the merging action did not affect the acceleration level of the lag vehicles because of sufficient gap size. To apply a conservative length of lag gaps in model evaluation, therefore, this study used a constant threshold ($2x_j$) by considering a length of average accepted lag gaps in the NGSIM data [43].

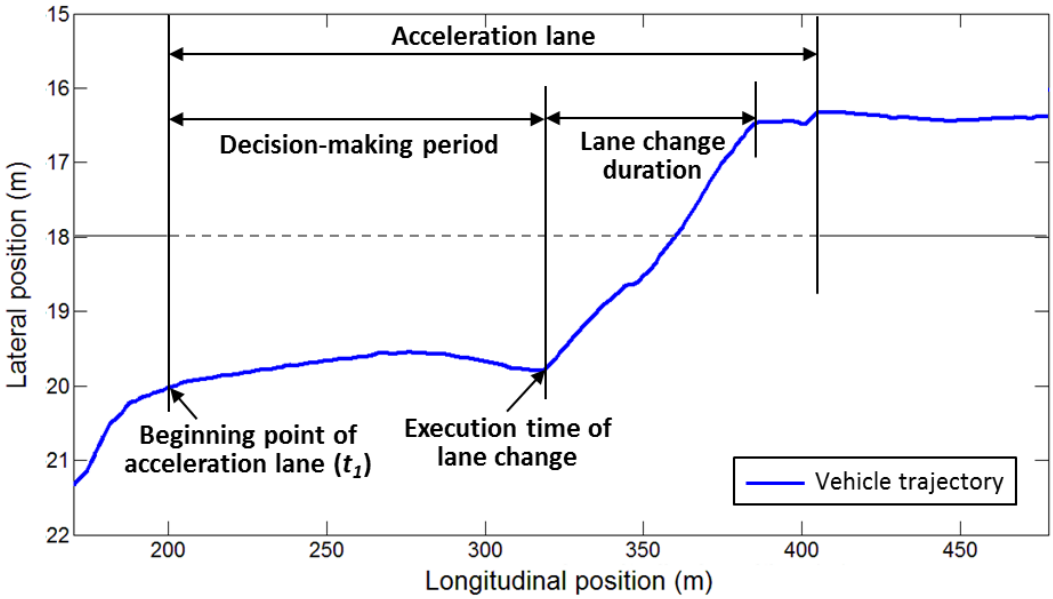

Figure 4-6. Definition of decision-making period and a point of lane change execution (subject vehicle 1302 in the 8:20 a.m. ~ 8:30 a.m. data).

Reasonable classification of the action strategies chosen by the drivers of the SV and LV is a critical issue, as it is directly related to the game model's results. Following an approach described in subsection 4.2.1, for classification of the SV's actions observed in the field, this study used one of the three following gap types: a) forward gap, b) original (current) gap, or c) backward gap). This approach, however, is limited in defining the initial decision of the driver of SV and the exact point where the initial (or previous) decision was changed, as it only focuses on the type of the gap in the final game result (i.e., final choice of action). As mentioned in introduction of NGSIM data, the data were collected in traffic congestion during the peak period, showing that the speed of merging vehicles is higher than that of the freeway traffic [22]. To take the NGSIM data features into consideration, therefore, this study assumed that the driver of SV has a priority to preserve the initial decision and the opposite player, i.e., the driver of LV, loses in the competitive game. This allowed for use of the merging gap types for classification of the observed actions of the driver of SV.

For classification of the actions of the driver of LV, the spacing between the SV and LV was used. Only data which showed a continuous increase or decrease in lag spacing was collected. It was assumed that an increase in lag spacing occurred as a result of a 'yield (l_1)' action and that lag space otherwise decreased. Fluctuation of lag spacing caused by instantaneous vehicle acceleration and relative speed affects the quality of the dataset in the model's evaluation. Consequently, this study considered instantaneous fluctuations below a certain range as noise when classifying the actions of the driver of LV, meaning that that the driver's action did not change. Therefore, data showing a variation below than the noise cancellation range (η) were collected as observations for the model evaluation. Table 4-3 shows the number of observations depending on the noise cancellation range.

Table 4-3. Number of Observations Depending on Noise Cancellation Range

Dataset	Set 1	Set 2	Set 3	Set 4	Set 5	Set 6
Noise cancellation range, η (*m/0.5s*)	$\pm$ 0.0	$\pm$ 0.2	$\pm$ 0.4	$\pm$ 0.6	$\pm$ 0.8	$\pm$ 1.0
Number of observations	383	392	397	403	409	413

2) Model Calibration Approach

In the game model, each player decides on one of the pure strategies to achieve the goal of the game [37]. To find the best strategies for both drivers, the Nash equilibrium was used in this study. The Nash equilibrium is a solution where neither player has motivation to change their own strategy, as no player can improve their situation by individually switching to another strategy [37].

If the Nash equilibrium exists, players use *pure strategies*. This means that each player will choose the strategy that maximizes their own payoff while considering an opponent who also wants to maximize their payoff. The Nash equilibrium defines a *pure strategy* as:

$$\begin{cases} P(s^*, l^*) \geq P(s_i, l^*), \ \forall s_i \in S, & i = 1,2,3 \\ Q(s^*, l^*) \geq Q(s^*, l_j), \ \forall l_j \in L, & j = 1,2 \end{cases} \tag{4.5}$$

where s^* and l^* indicate the equilibrium action strategy of the drivers of the SV and LV, respectively.

If a *pure strategy Nash equilibrium* is absent, however, a *mixed strategy Nash equilibrium* is considered. A mixed strategy Nash equilibrium involves at least one player playing a randomized strategy and no player being able to increase his or her expected payoff by playing an alternate strategy. A probability for each player's strategy is assigned with consideration of each player's expected payoff from the different strategies [37]. In the defined game, each driver's best response is the set of probabilities that maximizes their own payoff according to the set of probabilities chosen by the other driver [39]. For this model, this study used the MATLAB function NPG developed by Chatterjee to solve a two-player finite non-cooperative game [71]. Chatterjee's algorithm solves the game by computing the Nash equilibrium in mixed strategies based on the estimated parameters and expected payoffs (i.e., P_{ij} and Q_{ij}). The algorithm provides probabilities of choice of pure action strategies for each driver (i.e., p_i and q_j) in each observation.

In order to calibrate the merging decision-making model, this study followed the calibration method proposed by Liu et al. [2]. Liu et al. proposed a parameter estimation method by solving a bi-level programming problem [2]. As illustrated in Figure 4-7, the lower-level programming is to find Nash equilibrium by Chatterjee's function. This study also defined that the upper level is a non-linear programming problem to minimize the total deviation of probabilities in the system to choose actual observed actions by the following function:

$$\min \sum_{k=1}^{N} (1 - p_{a^k} \cdot q_{a^k}) \tag{4.6}$$

where k denotes the index of observations; a^k is the observed action strategies set $({s_i}^k, {l_j}^k)$ in observation k; and p_{a^k} and q_{a^k} are the probabilities of the drivers of the SV and LV, respectively, choosing the observed action in a_k. Here, A^k and B^k denote all parameters to be estimated for each driver's payoff functions.

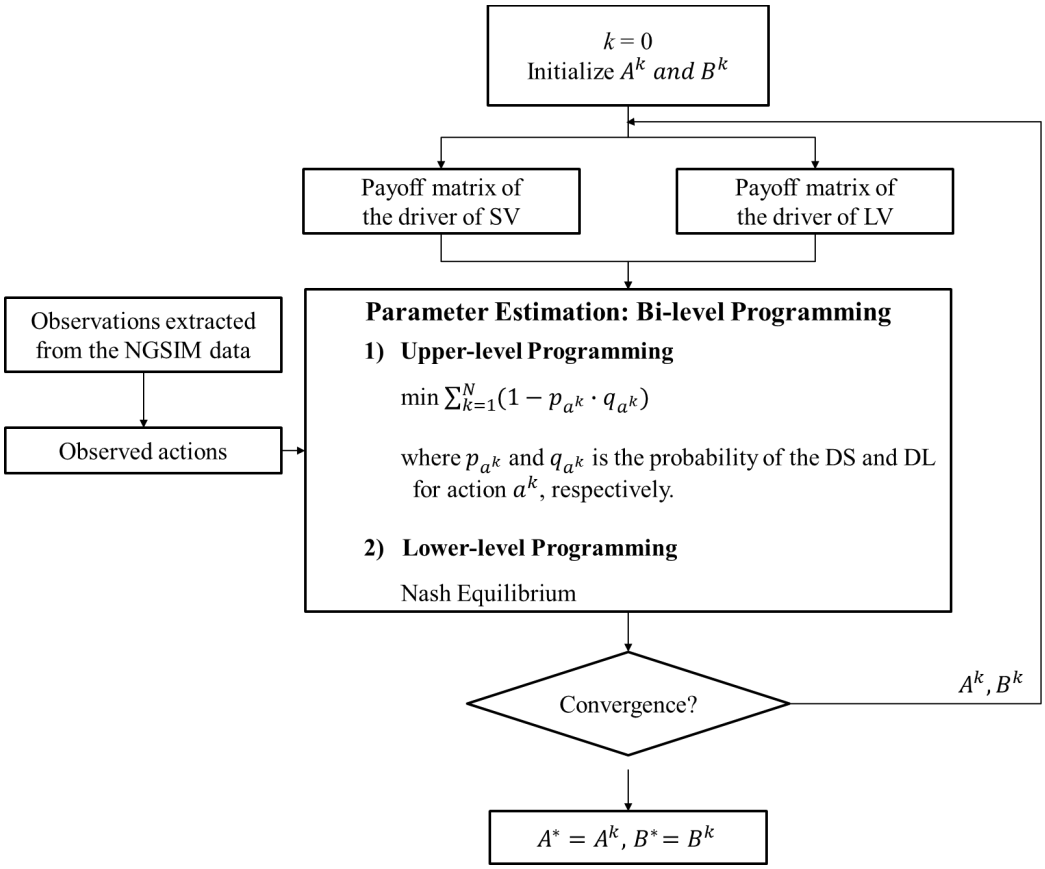

Figure 4-7. Schematic workflow for calibration approach based on bi-level programming.

3) Model Calibration Results

The proposed model was calibrated to estimate parameters depending on the noise cancellation range η (between $\pm$0.0 *m/0.5s* and $\pm$1.0 *m/0.5s*). A dataset collected between 7:50 a.m. and 8:20 a.m. was used in model calibration. Table 4-4 and 4-5 show the estimated parameters for the payoff functions of the drivers of the SV and LV, respectively.

The mean absolute error (MAE) was calculated using Equation (4.7) as follows:

$$MAE = \frac{1}{n}\sum_{k=1}^{n}|1 - 1(\hat{x}_k - x_k)| \tag{4.7}$$

where n, $\hat{x}_k$, and x_k denote the number of observations, model prediction, and actual observation, respectively. Note that $1(\hat{x}_k - x_k)$ is equal to one if $\hat{x}_k = x_k$, and is zero otherwise. The model prediction $\hat{x}_k$ was estimated by probabilities calculated using Chatterjee's algorithm. Table 4-5 reveals the calibration results. The MAE of the models is less than 0.17.

Table 4-4. Estimated Parameters for the Payoff Functions of the Drivers of the SV and LV

Function	Parameters	Calibrated values of the model parameters					
		Model 1 ($\eta = \pm 0.0$)	Model 2 ($\eta = \pm 0.2$)	Model 3 ($\eta = \pm 0.4$)	Model 4 ($\eta = \pm 0.6$)	Model 5 ($\eta = \pm 0.8$)	Model 6 ($\eta = \pm 1.0$)
P_{11}	α_{11}^{1}	2.809	1.990	2.292	2.213	4.460	0.680
	α_{11}^{2}	6.480	14.264	6.154	12.746	14.028	8.050
	α_{11}^{3}	11.354	4.511	5.695	-1.892	6.625	1.470
	ε_{11}^{SV}	7.151	2.044	0.979	0.197	12.502	9.767
P_{12}	α_{12}^{1}	6.001	2.947	6.946	10.238	9.784	8.987
	α_{12}^{2}	4.285	4.083	2.472	1.675	2.754	3.454
	α_{12}^{3}	4.032	6.178	5.167	5.191	1.173	3.499
	ε_{12}^{SV}	4.038	15.074	-2.855	0.155	2.208	8.238
P_{21}	α_{21}^{1}	-1.020	-0.227	-0.304	0.444	-3.599	-2.271
	ε_{21}^{SV}	0.900	-9.046	-10.130	-2.216	-15.550	-14.528
P_{22}	α_{22}^{1}	-4.502	-0.901	-3.205	-4.739	-17.494	-8.698
	ε_{22}^{SV}	-3.840	-5.136	-9.868	-5.394	-14.255	5.523
P_{31}	α_{31}^{1}	-4.483	-9.749	-7.268	-10.855	-12.003	-5.907
	ε_{31}^{SV}	10.508	17.433	-4.399	-0.693	-9.370	-0.195
P_{32}	α_{32}^{1}	-5.048	-2.641	-7.838	-5.377	-3.168	-11.330
	ε_{32}^{SV}	-5.292	2.053	-6.590	-11.026	11.839	-14.432
Q_{11}	β_{11}^{1}	-0.523	-3.129	-3.836	-6.490	-3.797	-0.261
	ε_{11}^{LV}	3.004	18.425	17.042	16.157	8.588	-0.953
Q_{12}	β_{12}^{1}	1.869	6.377	8.366	1.302	10.002	3.146
	ε_{12}^{LV}	-3.334	-6.661	-16.305	-4.569	-28.639	-10.082
Q_{21}	β_{21}^{1}	-9.717	-8.224	-4.697	-3.382	-8.151	-13.609
	ε_{21}^{LV}	3.045	10.832	10.634	13.289	6.250	18.583
Q_{22}	β_{22}^{1}	4.044	8.419	0.366	6.694	1.427	9.595
	ε_{22}^{LV}	1.488	6.590	6.265	-13.679	-6.862	-0.184
Q_{31}	β_{31}^{1}	-2.324	-5.514	-2.898	-3.718	-11.553	-2.049
	ε_{31}^{LV}	-4.316	19.527	-1.049	-2.132	26.902	-5.923
Q_{32}	β_{32}^{1}	8.090	12.136	2.506	9.908	3.206	11.649
	ε_{32}^{LV}	-12.938	-14.174	0.072	5.102	1.208	-16.047

Table 4-5. Calibration Results

Models	Model 1	Model 2	Model 3	Model 4	Model 5	Model 6
Noise cancellation range, η (*m/0.5s*)	$\pm$ 0.0	$\pm$ 0.2	$\pm$ 0.4	$\pm$ 0.6	$\pm$ 0.8	$\pm$ 1.0
MAE[a]	0.1595 (84.05%)	0.1420 (85.80%)	0.1570 (84.30%)	0.1600 (84.00%)	0.1564 (84.36%)	0.1648 (83.52%)

[a] The number in parentheses indicates prediction accuracy of the calibrated model.

4) Model Validation Results

The rest of the data collected between 8:20 a.m. and 8:35 a.m. was used for model validation purposes. Table 4-6 shows the model validation results. The models that considered the noise cancellation range η from $\pm 0.0\ m/0.5s$ to $\pm 1.0\ m/0.5s$ show prediction accuracy of 83.48 % to 87.44 % for each observation dataset. These results reveal that the developed model shows greater prediction accuracy than the previous model.

Table 4-6. Validation Results

Models	Model 1	Model 2	Model 3	Model 4	Model 5	Model 6
Noise cancellation range, η (*m/0.5s*)	$\pm$ 0.0	$\pm$ 0.2	$\pm$ 0.4	$\pm$ 0.6	$\pm$ 0.8	$\pm$ 1.0
MAE[a]	0.1273 (87.27%)	0.1256 (87.44%)	0.1422 (85.78%)	0.1447 (85.53%)	0.1652 (83.48%)	0.1429 (85.71%)

[a] The number in parentheses indicates prediction accuracy of the calibrated model.

4.3.2 Evaluation of the Repeated Game Model Based on the Second Stage Game (in [52])

1) Preparation of Observation Dataset

To evaluate the repeated game model based on the second stage game (as described in section 3.3.2), this study basically used the US 101 data collected between 7:50 a.m. and 8:35 a.m. to extract observations properly. As the same with previous model evaluation, specific observed cases where the initial lag gap at time step t_1 was greater than twice the jam density spacing, $2x_j$, were eliminated from the dataset. To evaluate the proposed model, all game points were selected between the beginning point of the acceleration lane and the lane change execution points every 0.5 s (see Figure 3-7). Moreover, entire game points were considered as individual observations within a historical sequence. This study assumed that the merging decision-making game was terminated at the execution point in each lane change.

To classify the action strategies chosen by the both drivers, this study follows an approach proposed by previous data extraction, for classification of the observed actions of the drivers of the SV and LV, this study used the type of gap and lag spacing, respectively. Due to the feature of the NGSIM data as described earlier, the decision of the driver of SV was assumed to maintain the initial decision. In classification of the LV's maneuvers, fluctuation of the lag spacing caused by instantaneous vehicle acceleration and relative speed affects the quality of the dataset in the model's evaluation. Consequently, this study considered instantaneous fluctuations below a certain range as noise when classifying the LV's maneuvers. The noise-cancellation range $\pm 1.0\ m$ was used here; any variation smaller than the defined range was ignored and treated as if the LV's maneuver did not change. Following this method, only 50 cases in entire data were observed shown change of the initial decision of the driver of LV. Although a suitable number of observations in each combination of action strategies are needed to evaluate the proposed model, there were some data composition limitations in the dataset (e.g., the cases showing a 'wait (s_2)' action of the driver of SV were rarely observed.).

Figure 4-8 shows the sets of action strategies identified by the proposed approach: 4-8(a) and 4-8(b) show the cooperative action strategies sets (s_1, l_1) and (s_2, l_2), respectively. These cases reflect no conflict between both drivers. The former set, (s_1, l_1), shows that the driver of SV drove at a higher speed than the driver of LV, and the latter driver decreased speed slightly and then maintained the original car-following speed. In Figure 4-8(b), there was a smaller gap than x_j and the LV had a higher speed then the SV, thus the driver of SV chose the 'wait (s_2)' action and decreased its speed. Otherwise 4-8(c) and 4-8(d) show non-cooperative cases, including the action strategies sets (s_2, l_1) and (s_1, l_2), respectively. These cases show instances where there was competition between two players at early decision-making period, which culminated in cooperative action strategies through a consecutive decision-making process. Case 4-8(c) reflects a case where both drivers decreased their speed through a waiting and yielding decision (s_2, l_1), and then the driver of SV revised its initial decision to change lanes in recognition of the 'yield (l_1)' action of the driver of LV. In Figure 4-8(d), both drivers accelerated initially. After a while having competition between drivers, the driver of LV decelerated to yield. On the other hand, the driver of SV maintained their initial decision to change a lane. A total of 1,504 similar cases were extracted within the time parameters to play the repeated merging decision-making game.

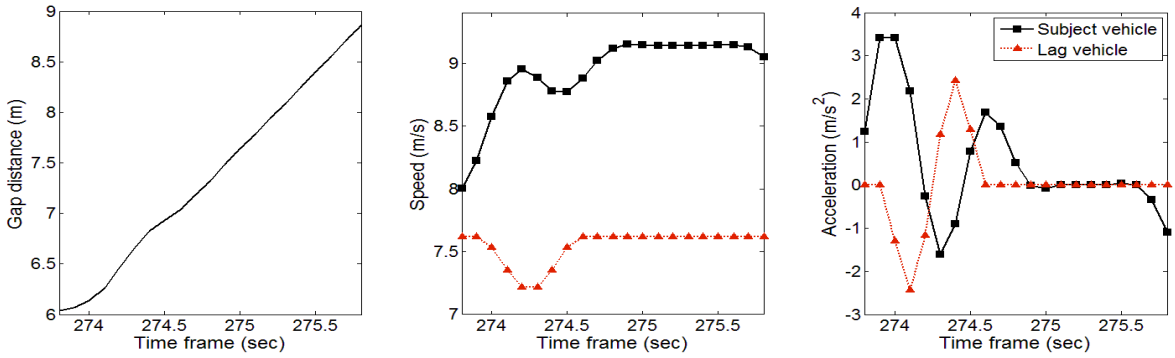

(a) Cooperative case: *change* (s_1) and *yield* (l_1) (subject vehicle 559 in the 8:05 a.m. ~ 8:20 a.m. data).

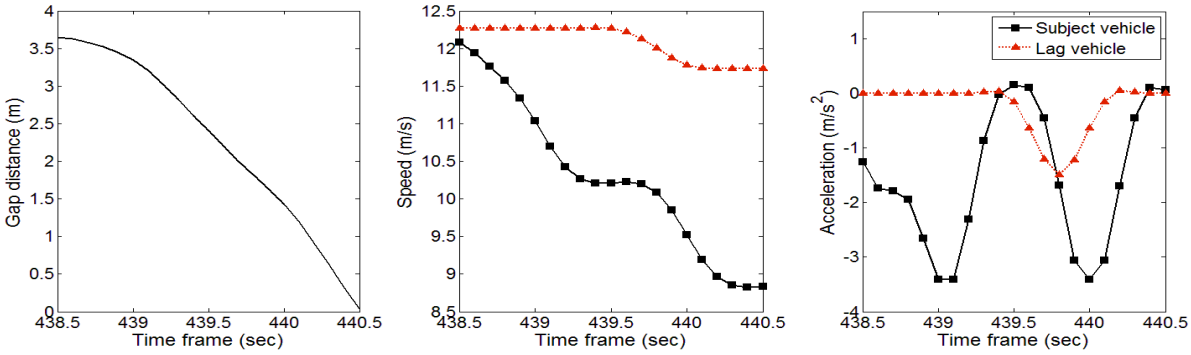

(b) Cooperative case: *wait* (s_2) and *block* (l_2) (subject vehicle 879 in the 8:20 a.m. ~ 8:35 a.m. data)

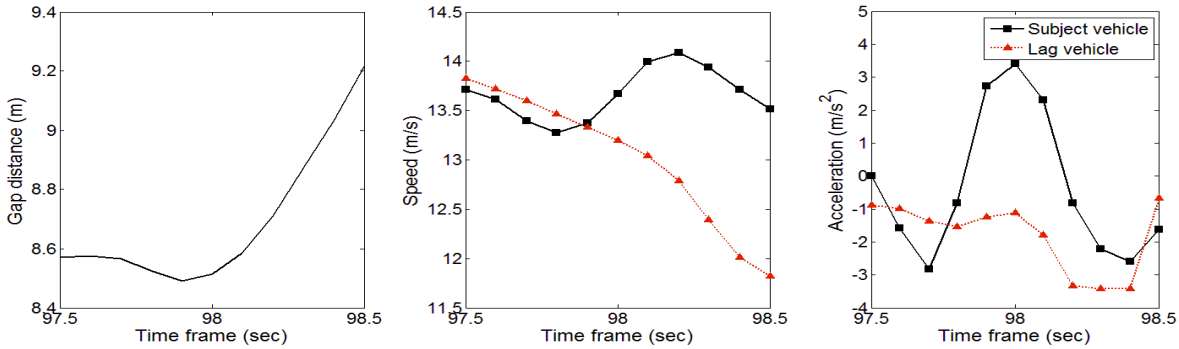

(c) Competitive case: *wait* (s_2) and *yield* (l_1) (subject vehicle 157 in the 8:20 a.m. ~ 8:35 a.m. data)

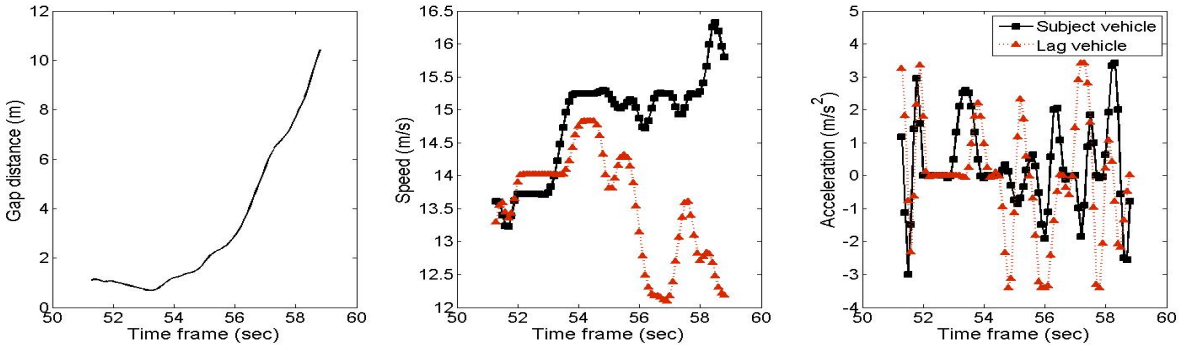

(d) Competitive case: *change* (s_1) and *block* (l_2) (subject vehicle 35 in the 8:20 a.m. ~ 8:35 a.m. data)

Figure 4-8. Classification of the drivers' action strategies.

2) Model Evaluation Results

The proposed repeated game model was calibrated using the calibration approach described in one-shot game model evaluation. To calibrate the repeated game model, the five rate factors are prepared as: $\delta = \{0.6, 0.8, 1.0, 1.2, 1.4\}$. To prove the performance of the repeated game model based on the second stage game, the base game model that drivers chose an action strategy based solely on the initial payoff value, as denoted the Model 0 with δ = 0.0, was also calibrated and validated. It followed the assumption that the drivers decide once and just follow their initial decisions. A total of 685 cases (out of 1,504) collected between 7:50 a.m. and 8:20 a.m. were used for model calibration. Table 4-7 shows the estimated parameters for the payoff functions of the drivers of the SV and LV in all alternatives of the model.

The model prediction about decision-making results were estimated by probabilities calculated using Chatterjee's algorithm. Table 4-8 reveals the calibration results of the proposed models based on the estimated parameters. The MAE, calculated by Equation (4.7), of all repeated games models (i.e., Model 1 to 5) is less than that of the base game Model 0, implying that the repeated game models were calibrated to capture more drivers' decision-making results in comparison to the previous game model.

The rest of the data, a total of 819 cases (out of 1,504) collected between 8:20 a.m. and 8:35 a.m., were used for model validation purposes. Table 4-8 also includes the model validation results. First, Model 1 to 5, which considered the rate 0.6 to 1.4, explained 75.09 % to 77.29 % of the observation dataset. On the other hand, Model 0 showed a prediction accuracy of 71.92 %. Consequently, the proposed repeated game in this study shows the better prediction ability than the previous game model as Model 0 does not capture changes in the driver's decision-making. It is therefore expected Model 0 would have lower prediction ability if there were more competitive cases in the dataset. In addition, these results indicate that consideration of not only instantaneous data but also previous game results is required to depict drivers' decisions. Consequently, it shows why using the repeated game has an advantage.

Furthermore, a microscopic traffic simulator integrated the repeated game model is expected to represent stable car-following status and non-cooperative decision-making. In contrast, the one-shot game model may challenge to represent stable vehicle trajectories in competitive merging scenarios even if it has a capacity to explain cooperative merging scenarios. In comparison results between Model 0 and Model 4, the latter shows the higher prediction accuracy for decisions at initial game point in each stage game. It demonstrates that the one-shot game model can induce improper vehicle speed profiles in microscopic traffic simulation due to impractical game results. This might depict unnatural car-following and driving behaviors in a microscopic simulation model.

Table 4-7. Estimated Parameters for the Payoff Functions of the Driver of the SV and LV

Payoff Functions	Parameters	Calibrated values of the model parameters					
		Model 0 (δ=0.0)	Model 1 (δ=0.6)	Model 2 (δ=0.8)	Model 3 (δ=1.0)	Model 4 (δ=1.2)	Model 5 (δ=1.4)
P_{11}	α_{11}^{1}	-0.589	-0.416	-0.425	-0.023	-0.680	-0.927
	α_{11}^{2}	0.330	0.522	0.409	0.434	0.497	0.632
	α_{11}^{3}	0.436	0.887	2.075	0.590	1.916	0.721
	ε_{11}^{SV}	-2.307	-1.926	-1.236	-1.582	-2.364	-1.998
P_{12}	α_{12}^{1}	0.426	1.186	-0.641	0.090	-0.577	-0.248
	α_{12}^{2}	1.303	0.471	1.727	0.811	1.265	0.758
	α_{12}^{3}	1.157	1.007	0.834	0.802	0.849	1.299
	ε_{12}^{SV}	3.142	0.736	2.735	-0.679	0.684	0.424
P_{21}	α_{21}^{1}	-0.191	-0.863	-0.915	-0.386	-1.572	-1.201
	ε_{21}^{SV}	-2.487	-2.253	-1.875	-0.287	2.065	0.206
P_{22}	α_{22}^{1}	-0.548	-2.092	-1.243	-1.014	-1.110	-0.223
	ε_{22}^{SV}	0.269	1.692	-0.817	-1.849	1.218	-1.000
P_{31}	α_{31}^{1}	0.015	0.377	-0.003	0.129	-0.209	-0.160
	ε_{31}^{SV}	3.121	1.052	4.814	2.212	4.164	1.983
P_{32}	α_{32}^{1}	-1.035	-0.660	-0.629	-0.624	-1.237	-0.796
	ε_{32}^{SV}	-2.274	0.514	-2.484	-0.422	-1.320	1.005
Q_{11}	β_{11}^{1}	-1.013	-0.289	0.239	-0.089	-1.733	-0.855
	ε_{11}^{LV}	0.235	0.474	-2.457	-0.279	-0.549	1.166
Q_{12}	β_{12}^{1}	1.496	0.862	2.135	0.981	0.791	0.544
	ε_{12}^{LV}	0.344	0.525	-4.342	-0.903	1.292	1.685
Q_{21}	β_{21}^{1}	-0.199	-0.973	-2.400	-1.172	-0.659	-1.007
	ε_{21}^{LV}	0.746	0.120	3.192	0.401	-1.113	-0.404
Q_{22}	β_{22}^{1}	1.196	1.310	0.866	0.360	0.486	0.940
	ε_{22}^{LV}	-0.842	0.591	1.041	1.081	-1.298	-1.135
Q_{31}	β_{31}^{1}	-0.167	-1.192	0.903	-0.036	-0.396	-1.214
	ε_{31}^{LV}	1.554	-1.335	-1.377	0.271	3.459	-1.232
Q_{32}	β_{32}^{1}	1.503	0.568	2.758	1.091	0.933	0.535
	ε_{32}^{LV}	0.988	-0.039	0.914	0.370	2.803	1.965

In conclusion, the repeated game Model 1 to 5 show considerable prediction accuracy of more than 75 %. Only minor differences between models using the various rates were observed due to issues with the data. Specifically, because of lack of cases showing changes of driver's initial decisions, these cases might be excluded in parameter estimation. Nevertheless, validation results of Model 3 to 5, i.e., models with $\delta \geq 1.0$, show higher than the other repeated models using $\delta < 1.0$. It means that decisions made at previous time steps is important, but present condition may be more critical to make a decision. This study concludes that the repeated game model is an appropriate approach to predict realistic driver merging behavior along an on-ramp section.

Table 4-8. Model Evaluation Results

Models	Model 0	Model 1	Model 2	Model 3	Model 4	Model 5
Rate factor, δ	0.0	0.6	0.8	1.0	1.2	1.4
Calibration results[a]	0.2686 (73.14%)	0.2102 (78.98%)	0.2175 (78.25%)	0.2321 (76.79%)	0.2204 (77.96%)	0.2146 (78.54%)
Validation results	0.2808 (71.92%)	0.2454 (75.46%)	0.2491 (75.09%)	0.2271 (77.29%)	0.2357 (76.43%)	0.2418 (75.82%)

[a] The number in parentheses indicates prediction accuracy.

4.4 Evaluation of the Third Model

4.4.1 Observations extraction for the repeated game calibration

Model evaluation was conducted to prove efficiency of the game models using the stage game based on the newly formulated payoff functions. This section introduces the observation dataset for model evaluation and calibration methodology. In addition, calibration and validation results of the second stage game mode [51] and the updated repeated game models are presented.

This study used same US 101 vehicle trajectory data. Reasonable classification of the action strategies chosen by both drivers is a critical issue, as it is directly related to the results of the game model. There is a limitation on the classification of drivers' decisions based on trajectories and speed profile data. This study extracted a total of 1,504 observations from NGSIM data using a method in Section 4.3.2. For classification of the SV's maneuvers observed in the field, this study used the type of gaps that were selected at game playing moments among the three following gap types (as illustrated in Figure 3-1(a)): (1) forward (lead) gap, (2) adjacent (current) gap, or (3) backward (lag) gap. In addition, the spacing between the SV and LV was used for classification of the LV's maneuvers. Detailed classification methodology is described in Section 4.3.2. Next, all data were reviewed to judge whether the classification results were reasonable to show drivers' intentions. If the specific data were regarded as improper classification, these data were modified. Decisions made by drivers in all observations were classified using this process.

4.4.2 Model Calibration Results

a total of two types of game models: (1) the one-shot game model, in which the developed stage game is played independently at every game point based on instantaneous status only; (2) the repeated game model using the cumulative payoffs with factor δ of various rates. To verify performance of the updated payoff functions in predicting human-drivers' decisions in merging situations, the first type of the models was subdivided into two models according to the payoff functions used in model calibration as below.

- One-shot game model based on the second stage game using the payoff functions developed in [51]
- One-shot game model based on the third stage game using the reformulated payoff functions

Herein the former and latter models were called as the '2nd stage one-shot game model' and the 'one-shot game model', respectively. For model calibration, a NGSIM dataset observed between 7:50 a.m. and 8:20 a.m. was used. The number of observations used in model calibration was 685 (out of 1,504). Table 4-9 shows the estimated parameters of the payoff functions of the drivers of the SV and LV.

As the calibration results, the MAEs of three types of models are shown in Table 4-10. In comparison with previous model [51], the one-shot game model based on the third stage game using the reformulated payoff functions shows better calibration results. It indicates that the game model using the third stage game has higher prediction capacity than that using the second stage game in merging decision-making. In the repeated game models, the models with $\delta > 1.0$ show lower MAEs than those with $\delta \leq 1.0$.

Table 4-9. Estimated Parameters of the Payoff Functions for the Game Models

Payoff Function	Parameters	One-shot Game Model	Repeated Game Models					
			Model 1 (δ=0.6)	Model 2 (δ=0.8)	Model 3 (δ=1.0)	Model 4 (δ=1.2)	Model 5 (δ=1.4)	Model 6 (δ=1.6)
P_{11}	α_{11}^1	9.64	5.10	2.88	6.69	-1.77	7.08	7.11
	α_{11}^2	23.51	74.83	48.38	96.45	9.20	27.34	8.38
	α_{11}^3	32.69	59.51	69.45	1.00	5.16	97.08	2.75
P_{12}	α_{12}^1	9.43	8.83	3.58	7.87	8.64	7.27	-6.26
	α_{12}^2	87.57	77.60	44.40	86.30	3.11	50.13	4.25
	α_{12}^3	10.98	43.84	1.80	71.19	5.73	84.75	7.34
P_{21}	α_{21}^1	0.63	-9.78	-7.49	-6.91	-8.88	-6.65	-8.13
	α_{21}^2	3.35	26.60	10.68	62.49	3.18	31.94	1.75

Payoff Function	Parameters	One-shot Game Model	Repeated Game Models					
			Model 1 (δ=0.6)	Model 2 (δ=0.8)	Model 3 (δ=1.0)	Model 4 (δ=1.2)	Model 5 (δ=1.4)	Model 6 (δ=1.6)
P_{22}	α_{22}^1	-7.88	-8.50	-3.42	-6.19	9.73	-8.98	5.56
	α_{22}^2	42.64	20.75	5.21	65.72	6.22	19.43	7.16
P_{31}	α_{31}^1	-0.66	6.07	-9.38	-6.21	-2.84	-5.18	6.41
	α_{31}^2	67.24	48.05	78.92	94.59	11.19	25.08	7.53
P_{32}	α_{32}^1	-0.53	-3.10	-5.39	-0.44	2.75	-3.69	8.35
	α_{32}^2	16.91	52.79	95.22	59.86	2.21	30.06	4.79
Q_{11}	β_{11}^1	9.93	3.78	6.96	9.80	-1.99	7.97	-3.75
	β_{11}^2	13.30	17.29	6.64	25.06	6.88	5.86	10.22
Q_{12}	β_{12}^1	-1.26	-8.39	-6.24	-5.83	-7.03	-8.90	-8.36
	β_{12}^2	3.70	0.29	19.40	23.84	10.20	18.49	1.89
Q_{21}	β_{21}^1	5.78	7.64	8.05	8.74	5.52	8.25	0.27
	β_{21}^2	89.18	57.76	58.65	78.06	2.76	82.45	4.12
Q_{22}	β_{22}^1	7.73	-4.36	-4.36	0.63	0.34	-8.66	-5.95
	β_{22}^2	57.97	6.64	55.26	14.12	7.43	38.74	7.61
Q_{31}	β_{31}^1	3.88	-4.02	-6.99	6.38	9.39	-0.82	3.68
	β_{31}^2	55.87	96.95	98.01	1.12	4.35	46.49	9.22
Q_{32}	β_{32}^1	4.26	-9.75	1.08	-8.01	6.78	1.53	-4.85
	β_{32}^2	27.87	26.74	22.93	74.89	2.20	86.19	7.83

Note that the second stage one-shot game model was calibrated using the same calibration methodology, but the estimated parameters are not shown in the table because of the different formulation for payoff functions.

Table 4-10. Calibration Results of the Game Models

Models	2nd Stage One-shot Game Model	One-shot Game Model	Repeated Game Models					
			Model 1	Model 2	Model 3	Model 4	Model 5	Model 6
Rate factor, δ	*na*[a]	*na*	0.6	0.8	1.0	1.2	1.4	1.6
MAE[b]	0.2555 (74.45 %)	0.1241 (87.59 %)	0.1708 (82.92 %)	0.1606 (83.94 %)	0.1606 (83.94 %)	0.1372 (86.28 %)	0.1358 (86.42 %)	0.1460 (85.40 %)

[a] Not applicable.
[b] The number in parentheses indicates prediction accuracy.

4.4.3 Model Validation Results

The rest of the data, 819 observations out of 1,504, collected between 8:20 a.m. and 8:35 a.m., were used for validating the model, and the validation results are shown in Table 4-11. Model validation results, which show the same trends as the calibration results, are summarized as follows. First, as the comparison results of the stage game developed in the previous study [51] and this study, the prediction accuracy increase by about 12% when the third stage game is used. Thus, this study enhances the decision-making game model's performance by using the reformulated payoff functions to represent merging maneuvers. Next, in the validation results, the repeated game models with $\delta \geq 1.0$ show prediction accuracy of higher than 85%. In particular, the repeated game model shows the highest prediction accuracy when $\delta = 1.4$. Both the one-shot game and repeated game model with $\delta = 1.4$ show considerably high prediction accuracy of more than 86%. Due to limitations of unbalanced observation data, nevertheless, model validation using field data cannot provide evidence to be beneficial using the repeated game. It is also hard to show the apparent difference between the one-shot game and the repeated game model. In the following sections, therefore, the game models are additionally evaluated through sensitivity analysis and simulation study.

Table 4-11. Validation Results of the Game Models

Models	2nd Stage One-shot Game Model	One-shot Game Model	Repeated Game Models					
			Model 1	Model 2	Model 3	Model 4	Model 5	Model 6
Rate factor, δ	*na*	*na*	0.6	0.8	1.0	1.2	1.4	1.6
MAE[a]	0.2418 (75.82 %)	0.1197 (88.03 %)	0.1954 (80.46 %)	0.1758 (82.42 %)	0.1465 (85.35 %)	0.1368 (86.32 %)	0.1307 (86.94 %)	0.1355 (86.45 %)

[a] The number in parentheses indicates prediction accuracy.

4.5 Sensitivity Analysis of the Game Model

In this section, this study describes the sensitivity analysis conducted to observe how factor changes related to the proposed payoffs impact the stage game results. In reality, drivers' merging behavior to select an acceptable gap size and speed difference between the freeway mainline vehicles and the merging vehicle is different depending on the merging point [22, 64]. Hence, this sensitivity analysis is required to demonstrate whether the developed stage game model represents merging behaviors observed in the field in various conditions. To show the decision-making model's sensitivity, the stage game is independently played in diverse scenarios varied by three input factors: game location, relative speed, and spacing. Preparation for the sensitivity analysis is presented first in the following sections, then results and corresponding discussions are provided.

4.5.1 Sensitivity Analysis Setting

As shown in Figure 4-9, a freeway segment that included an on-ramp was used for the analysis, with locations to play a game classified into two areas: the beginning of the acceleration lane and the end of the acceleration lane. For the spacing factor test, the SV changed its position between the PV and LV. For the speed profile test, the freeway mainline vehicles' speed was basically categorized into five scenarios: 60 km/h, 70 km/h, 80 km/h, 90 km/h, and 100 km/h. In each speed scenario, the SV's speed varied from 60 km/h to 100 km/h. The freeway testbed and calibrated stage game were modeled on MATLAB, and other simulation settings are described below.

- The length of the acceleration lane was 250 m.
- Based on initial longitudinal coordination, $n-1$, n, and $n+1$ denote the PV, SV, and LV, respectively.
- It was assumed that spacing between the PV and LV, $\Delta x_{n-1,n+1}$, was constant as 40 m: In the game played at the beginning of the acceleration lane, the PV and LV were located at 70 m and 30 m from the beginning of the acceleration lane, respectively. In the game played at the end of the acceleration lane, the longitudinal position of the PV and LV were 230 m and 190 m from the beginning point, respectively.
- The length of all vehicles was assumed as constant at 4.8 m.
- Link properties for the freeway are as follows. Saturation flow rate was 2,400 $veh/h/lane$. Jam density was 160 $veh/km/lane$. Free-flow speed and speed-at-capacity were 100 km/h and 80 km/h, respectively.
- Calibrated parameters of payoff functions for the repeated game model with $\delta = 1.4$ were used.

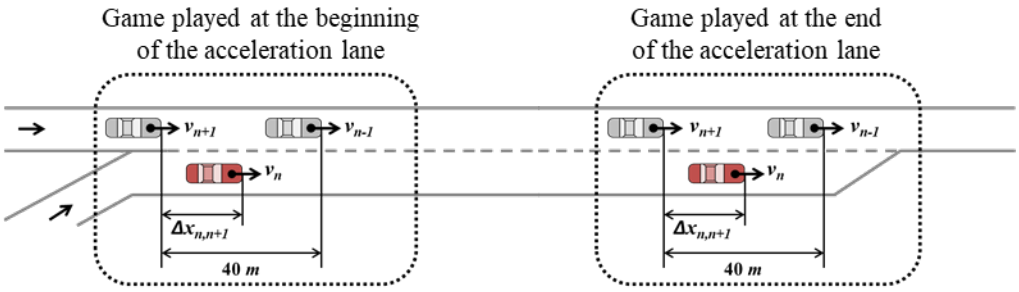

Figure 4-9. Topology of freeway merging section for sensitivity analysis.

4.5.2 Sensitivity Analysis Results

Based on the results of the stage game played at two locations in various lag spacing and relative speed scenarios, the impact of input factors and other findings revealed by the sensitivity analysis

are provided. Figure 4-10(a) to 4-10(e) show the results after playing games near the beginning of the acceleration lane, and Figure 4-10(f) to 4-10(j) reveal the game results after playing the game near the end of the acceleration lane. The Chatterjee function for finding the Nash equilibrium was used to decide these game results [71]. If the game result in each case is a pure strategy Nash equilibrium, the corresponding action set is a dominant decision made by two drivers, i.e., the probability of one of six action strategies ($p_{ij} \times q_{ij}$) is one. Otherwise, when a mixed strategy Nash equilibrium exists, the game result is randomly chosen by probabilities.

Differences in drivers' behaviors based on the merging point are distinct in merging maneuver decisions. At near the beginning of the acceleration lane, a merging vehicle driver usually passes a lead vehicle when $v_n > v_{n-1}$ and when lead spacing ($\Delta x_{n-1,n}$) is quite small [22]. The higher psychological pressure related to merging makes drivers accept smaller gaps as they arrive nearer the end of the auxiliary lane compared to cases where they can take an original gap near the beginning of the acceleration lane [22]. In other words, field data show that the driver of SV tried a forced merging maneuver at close to the end of the acceleration lane [18, 22]. When $v_n < v_{n+1}$ and the lag spacing ($\Delta x_{n,n+1}$) is quite small, the driver of SV waits until the LV passes the SV and then may merge using a backward gap. In Fig. 8, the calibrated stage game results show these behaviors in choosing an 'overtake (s_3)' and 'wait (s_2)' action according to the game location.

At near the beginning of the lane, as illustrated in Figure 4-10(a) to 4-10(d), the game results show that the driver of SV chooses the 'overtake (s_3)' action in conditions indicative of higher relative speed and short lead spacing. In contrast, the game results (as illustrated in Figure 4-10(f) to 4-10(i)) show that the driver of SV intentionally changes a lane due to a short remaining distance in the acceleration lane. For the 'wait (s_2)' action, differences in the results of the stage game for merging decision-making are revealed according to game location. These results prove that the forced merging utility works correctly when the SV is close to the end of the acceleration lane. Consequently, the stage game developed in this study accurately depicts realistic decisions made by human drivers according to game location.

As discussed in Section 3.3.3, TTC is critical in making lane-changing decisions. Since TTC is comprised of spacing (i.e., space headway) and relative speed, both are important in human drivers' decision-making for merging maneuvers at freeway merging sections. Hence, this study also analyzed the impacts of these factors. In Figure 4-10(c), blue lines parallel to the y-axis (as marked with ① to ③) and green lines parallel to the x-axis (as marked with A and B) denote test cases for sensitivity analysis on relative speed and spacing, respectively.

In the sensitivity analysis on relative speed, the PV and LV are supposed to drive at 80 km/h, and the SV's speed varies from 60 km/h to 100 km/h. Scenarios were prepared with three lag spacings: 10 m, 20 m, and 30 m, and the game results of all scenarios are shown in Figure 4-11. Game results clearly show that the relative speed affects decision-making. When lag spacing ($\Delta x_{n,n+1}$) is 10 m (as shown in Figure 4-11(a)), the drivers of the SV and LV decide on a 'wait

(s_2) and block (l_2)' action set if $\Delta v_{n,n+1} \leq -10\ km/h$. In addition, both drivers are willing to choose a 'change (s_1) and yield (l_1)' action set through the stage game if $\Delta v_{n,n+1} \geq -7\ km/h$. These cooperative action strategy sets are results of both drivers' common consent subject to safety. In a certain range, i.e., $-10\ km/h < \Delta v_{n,n+1} < -7\ km/h$, drivers' desired actions are competitive; in these conditions, the non-cooperative behaviors, 'change (s_1) and a block (l_2)' action, will be carried out.

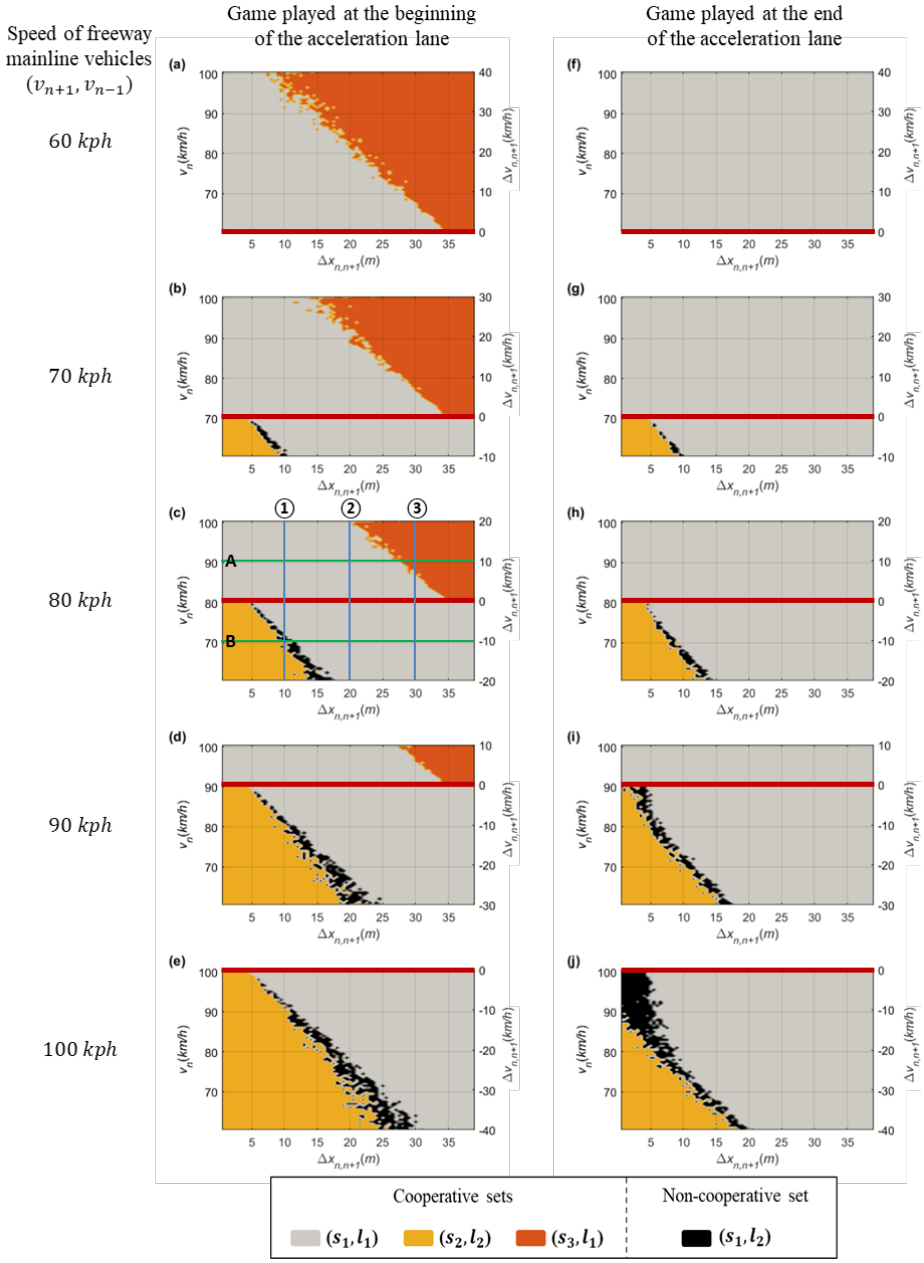

Note that a red line parallel to the x-axis on each graph indicates the speed of the freeway mainline vehicles (v_{n-1}, v_{n+1}).

Figure 4-10. Graphical representation of the one-shot game results depending on game locations, spacing between vehicles ($\Delta x_{n,n+1}$), and speed of the SV (v_n).

When $\Delta x_{n,n+1} = 20\ m$, in Figure 4-11(b), the driver of the SV and LV choose a cooperative action strategy (s_1, l_1) even if $\Delta v_{n,n+1} = -20\ km/h$. This means that the relative speed is largely irrelevant in influencing the driver of SV to choose a lane-changing action if there is sufficient spacing between vehicles. If there is enough space headway, real-life experience generally shows that a driver of a merging vehicle will change a lane upon reaching an acceleration lane even though a speed harmonization process is required. In response to the merging vehicle's lane change, the driver of LV decreases speed to adjust to the new preceding vehicle (i.e., the SV) or changes a lane to the left to maintain its speed. When $\Delta x_{n,n+1} = 30\ m$ (i.e., $\Delta x_{n-1,n} = 10\ m$), moreover, the game results show a distinct feature depending on the relative speed. The cooperative action strategy (s_1, l_1) is chosen by the stage game until v_n is slightly higher than v_{n-1}. If $\Delta v_{n,n-1} \geq 8\ km/h$, the driver of SV chooses an 'overtake (s_3)' action due to a relatively small TTC in order to avoid harsh braking. Of the overtaking vehicles, 97.7% were found to have a speed higher than the freeway mainline vehicles [22]. Thus, this game model can reasonably represent decision-making results according to relative speed.

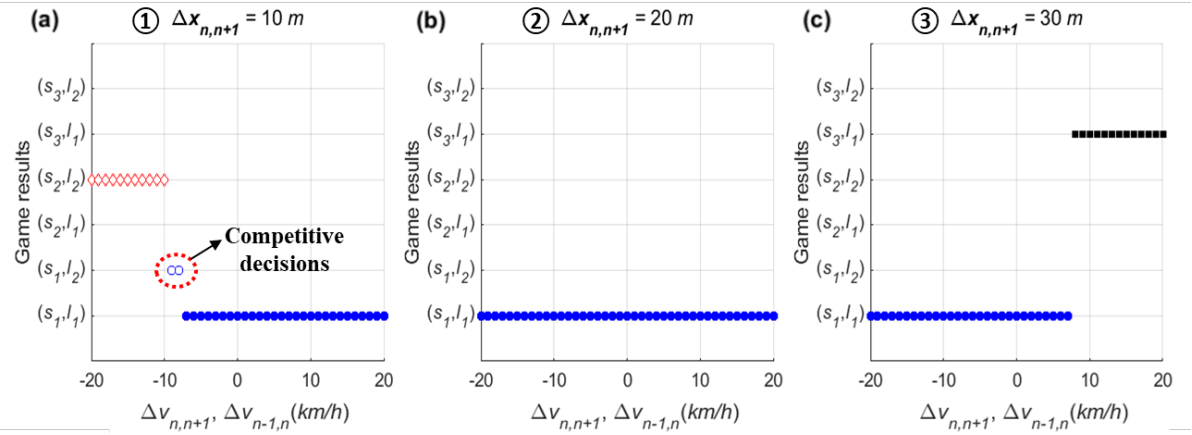

Figure 4-11. Game results on relative speed.

For the sensitivity analysis on spacing, the stage game was played with various lag spacing from 0 m to 40 m. The PV and LV are supposed to drive at 80 km/h, and the SV's speed is 70 km/h and 90 km/h. Game results of all scenarios are shown in Figure 4-12. In the figure, the x-axis indicates the lag spacing ($\Delta x_{n,n+1}$), and hence an increase of $\Delta x_{n,n+1}$ means a decrease of lead spacing ($\Delta x_{n-1,n}$).

When $v_n < v_{n-1}$, as shown in Figure 4-12(a), the stage game results show that the driver of SV decides on a 'wait (s_2)' action in cases in which lag spacing is less than 10 m. In other words, results indicate that a slower SV requires spacing of more than 10 m to choose a 'change (s_1)' action. Depending on the spacing, competitive decision-making is also expected. This trend is also found in choosing an 'overtake (s_3)' action when $v_n > v_{n-1}$. In Figure 4-12(b), the driver of SV

decides to overtake at $\Delta x_{n-1,n} \leq 12\ m$. Therefore, the sensitivity results indicate that the stage game reasonably explains the difference in drivers' choices according to spacing.

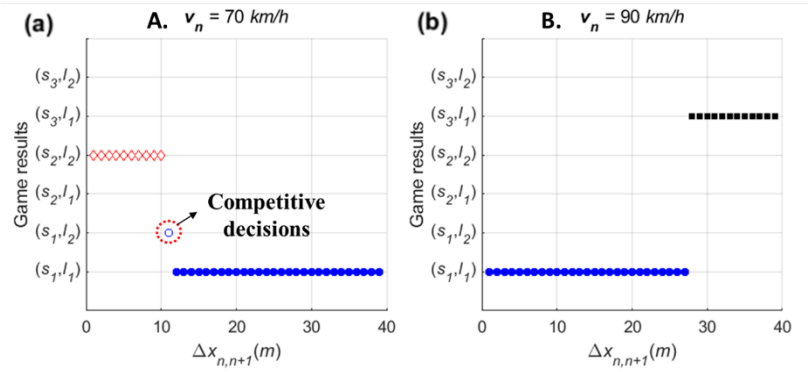

Figure 4-12. Game results on spacing.

In the results, decisions included in a non-cooperative action strategy set, i.e., (s_1, l_2), are found in a specific decision-making region, as colored black in Figure 4-10. This region implies that this strategy set, which is decided simultaneously by drivers, puts them into competition. This result means that the driver of SV wants to change a lane after trying to ensure a safe lead and lag gap and the driver of LV does not allow the SV to merge. During the game period, one driver should change their initial decision to avoid a potential collision, and the final decision set would be a cooperative set. In addition, due to an unbalance in the number of observations indicating each action strategy, the (s_2, l_1) action cannot be determined in this sensitivity analysis. From field data, including NGSIM data, it is clear that merging maneuvers are usually cooperative, as the driver of LV perceives the SV's lane-changing intention. Compared to cooperative merging, non-cooperative cases are only occasionally observed. The stage game results describe cooperative behaviors, and competition between drivers can be found at certain relative speed and spacing profiles. Consequently, the stage game model proposed in this study successfully explains rational human drivers' decision-making results.

4.6 Simulation Case Study

In this chapter, a simulation study is presented to demonstrate the performance of the game model based on the developed stage game for merging. For this case study, a microscopic simulation model based on an ABM method that included a vehicle acceleration controller was developed. To verify the performance of the ABM, a comparison between NGSIM data and simulation results is provided. The simulation setting is defined, and then various merging scenarios representing both cooperative and non-cooperative cases are explained. Next, simulation results for each scenario are presented.

4.6.1 Simulation model development

To investigate whether the repeated game model is efficient to use in microscopic traffic simulation, we used an ABM approach. ABM is a powerful method for making simulations that is widely applied across real-life problems [73-75]. This study developed a simulation model that was built on MATALB using the ABM method combined with the game model. ABM is a suitable approach for simulating the actions and interactions of intelligent entities, which includes individual people. Collaboration and competition, in particular, are major concerns in game theory; these are two typical types of human interactions addressed in several ABM methods [76]. One of the applicable situations for using ABM is when interactions among agents are heterogeneous and can lead to network effects [74, 77]. Thus, this study develops a simulation model to explain merging interactions.

According to Zheng et al. (2013) [75], the ABMs explored for the existing transportation system in today's literature, in general, have the distinguishing feature of integration combining three components: drivers' action decisions, drivers' route decisions, and microsimulation. As a microsimulation component, the simulation model developed in this study basically simulates vehicle movements based on position and by speed profile as determined by an acceleration controller at each time step. As shown in Figure 4-13, the controller consists of a game module and a car-following module. According to the game model for the drivers' action decision component, a driver of SV plays a stage game with a driver of LV in the target lane. Depending on the action strategies at each game time, both drivers determine the acceleration level to accomplish their own strategy. In the car-following module, in addition, the desired acceleration level is decided by the RPA car-following model. In this acceleration controller, neither the individual demographic nor travel characteristics of either agent are considered.

As the game results show, when the driver of SV chooses a 'change (s_1)' action, they evaluate lead and lag spacing for gap acceptance to satisfy sufficient spacing and collision avoidance. If the instantaneous gap is enough to change a lane, the SV begins merging onto the freeway, and the driver of LV determines the acceleration level to follow the SV in the car-following model in response to recognition of the SV's lane-change. In addition, a route decision module is not required because merging scenarios are tested on the one-lane freeway network, which includes a merging ramp.

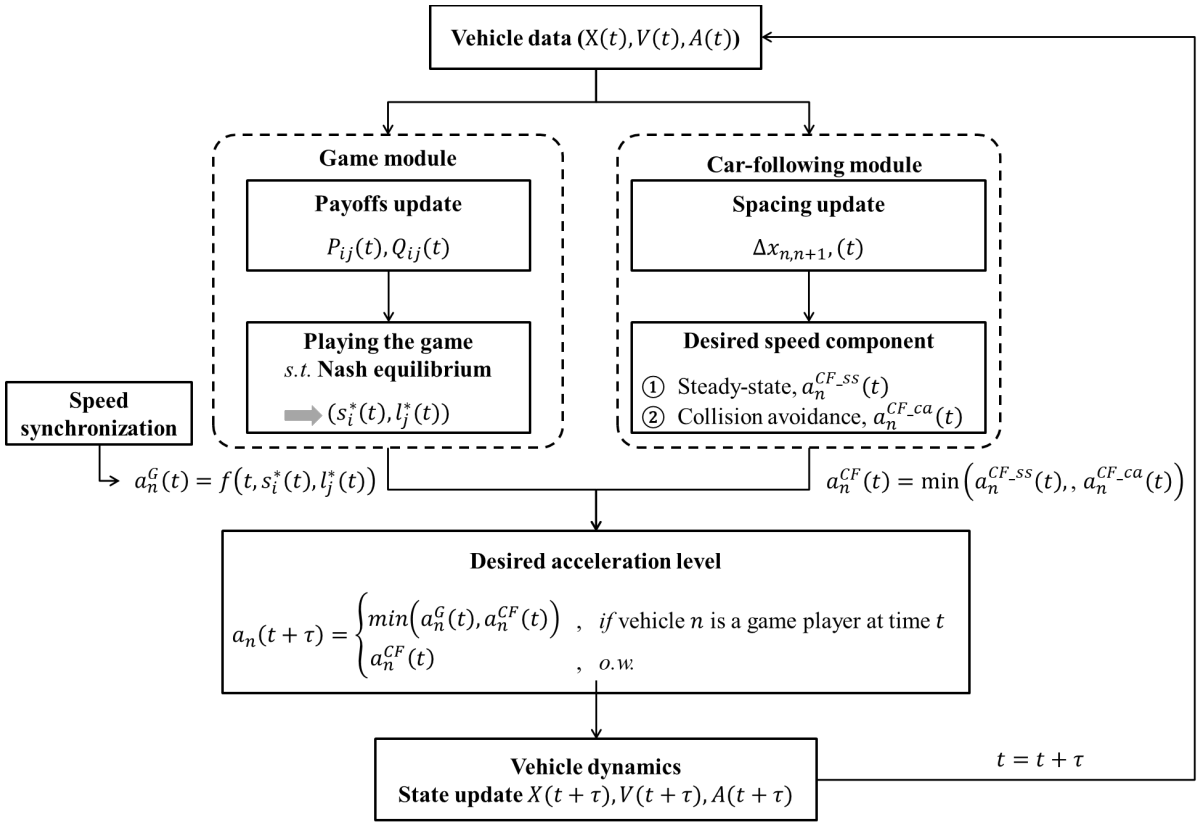

Figure 4-13. Vehicle acceleration controller structure in the developed simulation model.

Car-following module estimates an desired acceleration level based on instantaneous spacing between vehicles and speed at each time step t. This study used two components, i.e., steady-state and collision avoidance, of the RPA car-following model for the module [54]. The detailed definition and formulas of the components in the RPA model are described in [54]. Figure 4-14 shows performance of car-following module in a case which five vehicles formed a platoon. Vehicles decide an acceleration level to follow preceding vehicle by the RPA car-following model. Here, it was assumed that vehicles were located with shorter spacing than the steady-state spacing of Van Aerde's car-following model [67] at simulation time 0. As illustrated in Figure 4-14, therefore, following vehicles initially decreased speed to ensure proper spacing between vehicles. Then, they began to accelerate after ensuring the sufficient spacing by sequence in the platoon. In conclusion, acceleration level and speed were oscillated for a while, and then they were stabilized.

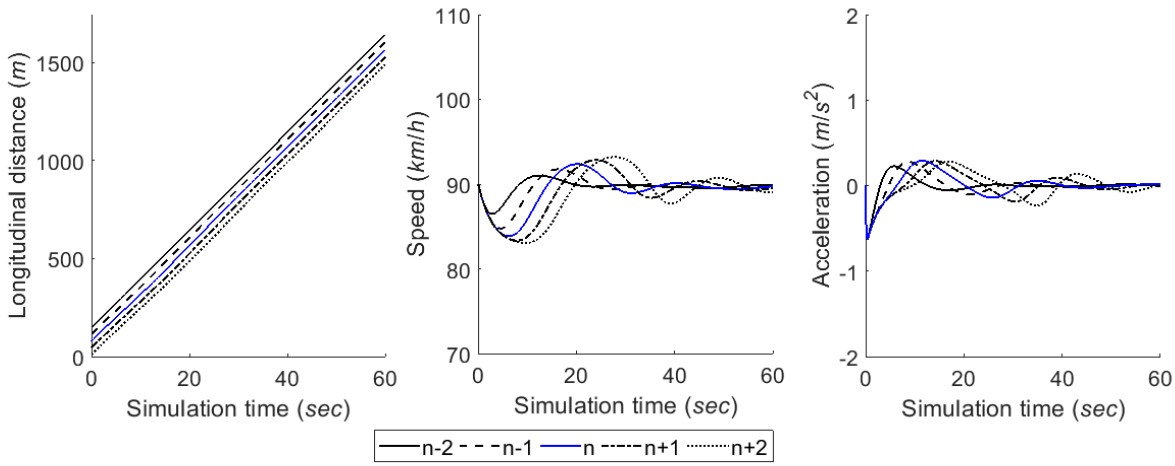

Figure 4-14. Performance of the car-following module.

The game module begins operating as soon as the SV enters the acceleration lane. The nearest following vehicle in the target lane becomes the opposite player. In this module, there are two types of merging game: (1) the one-shot game, in which a stage game between two drivers is independently played at each game time and (2) the repeated game, in which drivers play a game with consideration of the previous game's results. In detail, the one-shot game uses instantaneous payoffs, which are computed based on spacing and speed profile at time t, for each action strategy set, i.e., $P_{ij}(t), Q_{ij}(t)$. In the repeated game, on the other hand, the cumulated payoffs are utilized. Regardless of the game type, two players decide an action strategy set subject to the Nash equilibrium. Based upon the action chosen at time t, the desired acceleration level for each vehicle is calculated to execute that vehicle's individual action strategy. For the SV, the desired acceleration level is determined, as stated below.

- For 'change (s_1)' action, the driver of SV determines acceleration level in consideration of not only speed synchronization but also gap acceptance. If $v_n(t) \ll v_{n+1}(t)$, an acceleration level for speed harmonization is additionally calculated. Also, by gap acceptance rule, another acceleration level is calculated to ensure sufficient gap for lead and lag spacing.
- For 'wait (s_2)' action, a required acceleration level to wait in acceleration lane until the lag vehicle pass the SV is computed. Generally, waiting cases are observed when $v_n(t) \ll v_{n+1}(t)$ and $\Delta x_{n,n+1}$ is not sufficient. If $v_n(t) \ll v_{n+1}(t)$ and the remaining distance to the end of the acceleration lane at time t, $RD_n(t)$, is sufficient to not require deceleration, the SV slightly accelerates to harmonize the speed with freeway vehicles during waiting time.
- Lastly, it needs to calculate the required acceleration level to use the forward gap for 'overtake (s_3)' action. This case is observed when $v_n(t) \gg v_{n+1}(t)$ and $\Delta x_{n-1,n}$ is not sufficient. For this strategy, therefore, speed harmonization is exclude as an acceleration component.

In addition, the driver of LV decides the acceleration level for a 'yield (l_1)' action by accepting the SV's merging intention. To provide safe spacing for merging, the LV's acceleration level was calculated based on the car-following model with an assumption that the SV became a potential lead vehicle. For a 'block (l_2)' action, on the other hand, the driver of SV shows acceleration to pass the SV by decreasing spacing. This decrease in spacing is regarded as blocking intention.

4.6.2 Simulation model validation

Prior to conducting a case study, validation of the simulation model developed in this study was required to determine whether the conceptual model is a reasonably accurate representation of the real world [78] and whether the output of simulations is consistent with real world output [79]. To validate the simulation model, this study used the graphical comparison technique, in which the graphs of values derived from the simulation model over time are compared with the graphs of values collected in a real system. It is a subjective, yet practical approach, and is especially useful as a preliminary approach [80]. Since the objective of the case study was to verify the repeated game's efficiency, the simulation focuses on presenting microscopic vehicle movements based on rational drivers' decision-making without consideration of individual characteristics. Considering this objective, a mathematical approach, such as statistical testing of simulation results, was not selected for model validation. Therefore, this study provides a graphical comparison between NGSIM data and the results derived from the simulation model to investigate similarity of trend in vehicle position and corresponding spacing.

This study extracted game cases from NGSIM data in which there was no interference by other surrounding vehicles except for the three main vehicles (i.e., the SV, PV, and LV). Next, instantaneous vehicles' location and speed at prior to 1.0 seconds in each case were prepared as input data for simulation. The graphical comparison results are presented showing longitudinal vehicle position and spacing are shown in Figure 4-15. In an example to show changing situation (see Figure 4-15(a)), vehicle position and corresponding lead and lag spacing are almost identical. In an example in overtaking situation (see Figure 4-15(b)), furthermore, considerable similarity is observed. The results show that the simulation model based on the ABM represents values similar to those found in the NGSIM data in longitudinal vehicle position and spacing. Consequently, it was possible to conclude that the developed simulation model could be utilized in the case study.

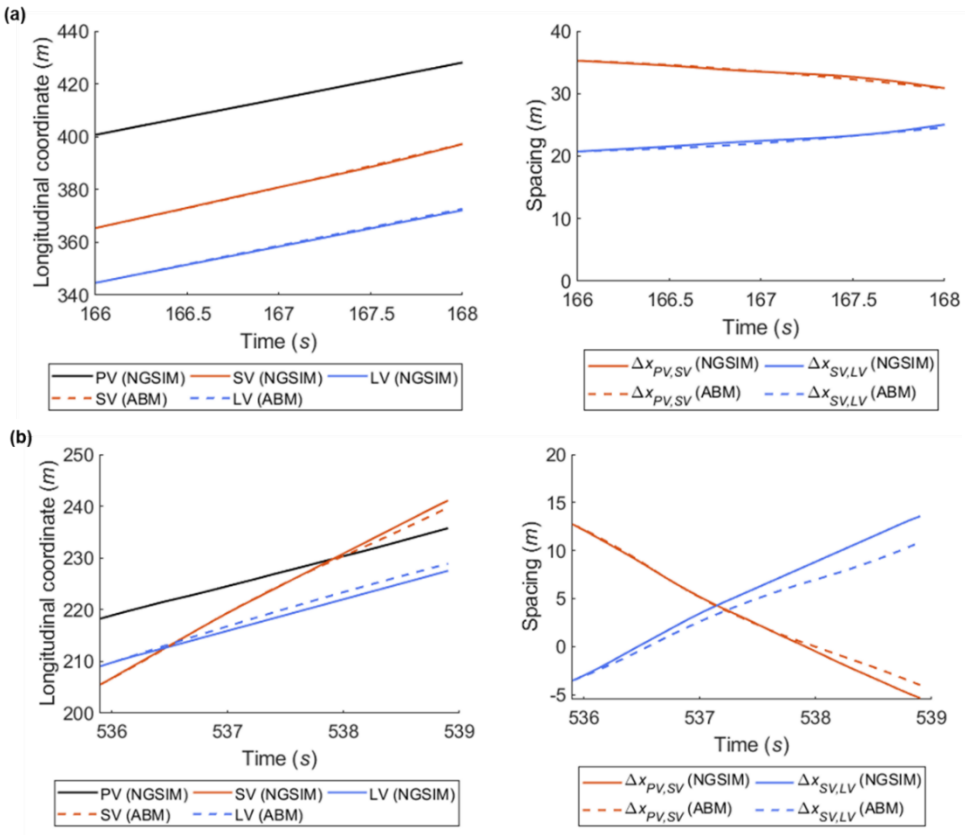

Figure 4-15. Simulation model validation results based on the graphical comparison method: (a) changing situation (SV ID: 268, PV ID: 258, and LV ID: 269 in the US101 data collected from 8:05 a.m. to 8:20 a.m.) and (b) overtaking situation (SV ID: 1108, PV ID: 1112, and LV ID: 1118 in the US101 data collected from 8:20 a.m. to 8:35 a.m.).

4.6.3 Case Study

1) Simulation setting and cases

This study conducted case studies in various merging scenarios simulated for a total of five vehicles, including a merging vehicle. Simulation experiments were executed using both the one-shot game model and the repeated game model. As described above, the one-shot game herein is played independently without consideration of previous results at every decision-making point. The repeated game is played based on the cumulative payoffs proposed in Section 3.4. In addition, a freeway segment, including one merging section, was modeled on MATLAB, as illustrated in Figure 4-16. The length of the freeway mainline was 1.0 km and the 250 m acceleration lane was located 80 m downstream of the beginning of the network. The details of the simulation settings are defined as follows.

- Link properties for the freeway are as follows. Saturation flow rate was 2,400 $veh/h/lane$. Jam density was 160 $veh/km/lane$. Free-flow speed and speed-at-capacity were 100 km/h and 80 km/h, respectively.
- Based on initial longitudinal coordination, vehicles on the network were designated as $n-2, n-1, n, n+1$, and $n+2$, respectively. Here the vehicle n denotes the SV.
- It was assumed that the average initial speed of freeway vehicles was v_{fwy}. The initial speeds of four vehicles on the freeway mainline (i.e., $n-2, n-1, n+1, n+2$) were randomly determined using the normal distribution with a mean of v_{fwy} and standard deviation of 0.2 at simulation start time.
- The initial spacing between freeway vehicles, i.e., $\Delta x_{n-2,n-1}, \Delta x_{n-1,n+1}, \Delta x_{n+1,n+2}$, was determined using the Van Aerde's steady-state model according to instantaneous speed of corresponding following vehicle at time step 0.
- With regard to the game, the time interval for playing the game was 0.5 s. The stage game would be newly formed if the LV or PV changed.
- Maximum and minimum accelerations are 3.4 m/s^2 and -3.4 m/s^2, respectively, as determined with reference to the NGSIM data. Length of all vehicles was assumed as constant as 4.8 m.
- In this simulation model, the freeway mainline vehicles' behaviors to avoid a potential collision with the merging vehicle, i.e., lane change to left or deceleration before arriving the merging section, were excluded. These behaviors could not be modeled for an individual vehicle's driving maneuvers in traffic simulator because they are a result of vehicles' independent decisions rather than any interaction with the merging vehicle after recognizing the merging vehicle.

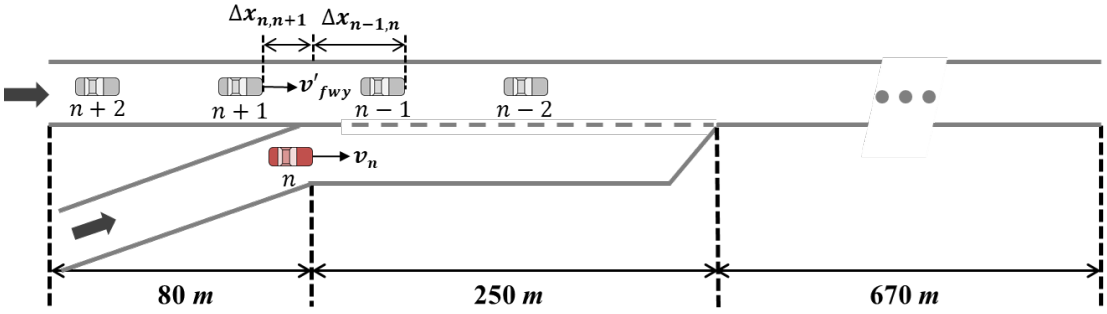

Figure 4-16. Simulation network configurations.

A total of five simulation cases were prepared, as summarized in Table 4-12, to represent plausible merging cases as defined by diverse input values of three factors: freeway mainline vehicles' average speed (v_{fwy}), initial SV's speed (v_n), and initial lag spacing ($\Delta x_{n,n+1}$). There are two main categories in merging: cooperative and competitive merging. Cooperative merging

cases, in which the drivers' decision set would be collaborative by common consent of both drivers, indicate typical cases to select a gap type among three types: a forward gap, an adjacent gap, and a backward gap. In contrast, a competitive merging case represents an example showing a conflict in both drivers' behavior. For example, the driver of SV who wants to use an adjacent gap is willing to prepare to merge onto freeway by turning a signal on, and then executing a lane change. In that time, the driver of LV decides not to allow the cut-in to avoid the expected considerable deceleration. One of the drivers should change their initial decision in order to avoid a potential collision. This competitive situation is not common, but many drivers may have had an experience of this type. Thus, we picked two cases in order to show not only the game model's performance in non-cooperative cases but also differences between the two game models in competitive scenarios.

Table 4-12. Initial Conditions of Merging Scenarios for Case Study

Index	Scenarios	Gap type used for merging	$\overline{v_{fwy}}$	$\overline{v_n}$	$\overline{\Delta x_{n,n+1}}$
1	Cooperative	Adjacent gap	90 km/h	75 km/h	20.0 m
2		Backward (lag) gap	90 km/h	65 km/h	15.0 m
3		Forward (lead) gap	50 km/h	65 km/h	15.0 m
4	Competitive	Adjacent gap or backward gap (Initial decision: non-cooperative)	85 km/h	72 km/h	14.0 m
5		Adjacent gap or backward gap (Initial decision: cooperative)	90 km/h	75 km/h	7.5 m

2) Case study results

Cooperative and competitive cases were tested using the developed simulation model. In order to validate the repeated game model's performance, the simulation results using the repeated model are compared with results using the calibrated stage game model played independently, i.e., one-shot game model at every decision-making point.

In cooperative scenarios, a dominant action strategy is found in rational decision-making due to the apparent situation. The simulation model using the repeated game model shows very close performance with that using the one-shot game as the game results are same in each game point. Since there is a mixed strategy Nash equilibrium in the competitive cases, both drivers decide an action strategy depending on the probability of actions. For case study results, this study provides the typical outcome of each scenario if there is no distinct difference in decision-making using the two game models. Otherwise, especially in the competitive scenario, the decision-making output simulation results of each game model are individually presented.

a) Case 1: cooperative merging scenario using an adjacent gap

As described in the sensitivity analysis, the developed game model has the ability to represent drivers' decisions in normal cooperative merging cases. According to the game results, as shown in Figure 4-18, drivers chose a 'change (s_1) and yield (l_1)' action set during the game period. The SV slightly accelerated by speed harmonization rules in preparation for merging while the LV decelerated in order to accept the SV's lane change. When a lead and lag gap was acceptable, the SV merged onto the freeway mainline. In simulation, the driver of SV controlled the vehicle's speed via the car-following rule as soon as executing the lane change and its following vehicles also showed oscillation in their speed profiles to ensure a safe gap.

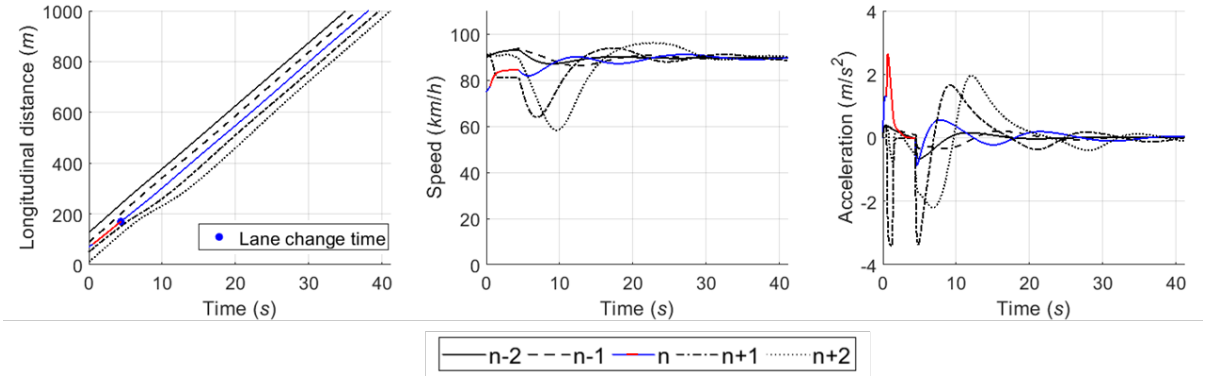

Note that a red solid line indicates simulation data of the SV (vehicle n) during game period, whereas a blue solid line shows the SV's data in simulation time except game period.

Figure 4-17. Graphical representation of simulation results in case 1.

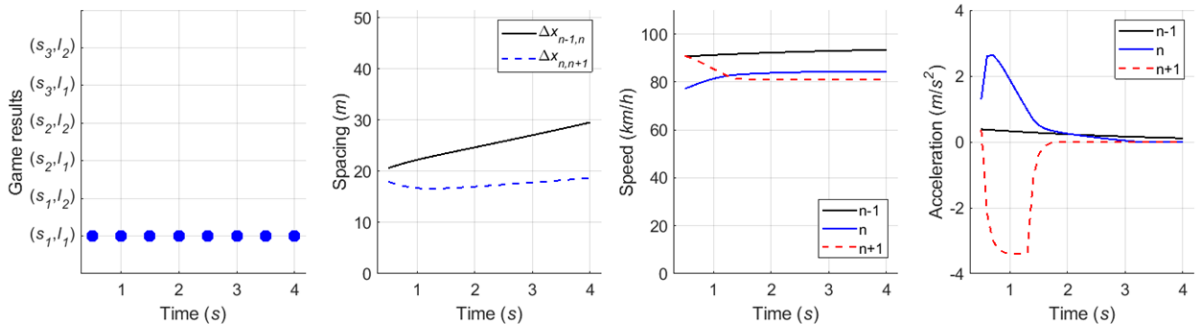

Figure 4-18. Decision-making game results in case 1.

b) Case 2: cooperative merging scenario using a backward gap

Simulation results for the second case, as shown in Figure 4-19, indicate that the driver of SV used the backward gap after the initial LV to overtake the SV. In Figure 4-20(a), the drivers decided on a 'wait (s_2) and block (l_2)' action strategy, respectively. The LV accelerated to block merging, and the SV also accelerated for speed synchronization even though the driver of SV decided to take a 'wait (s_2)' action. As soon as the initial LV overtook the SV, a new merging decision-

making game was identified in which the vehicle $n+2$ became the new LV. The results of the second game are shown in Figure 4-20(b). The SV continuously chose a 'change (s_1)' action until the gap acceptance rule was satisfied, then moved to the freeway mainline in consideration of gap size and relative speed. The LV, i.e., the vehicle $n+2$, in the second game decelerated in a yielding action in response to the SV's intention to merge. In conclusion, the merging decision-making model was shown to depict a typical waiting scenario for both game models.

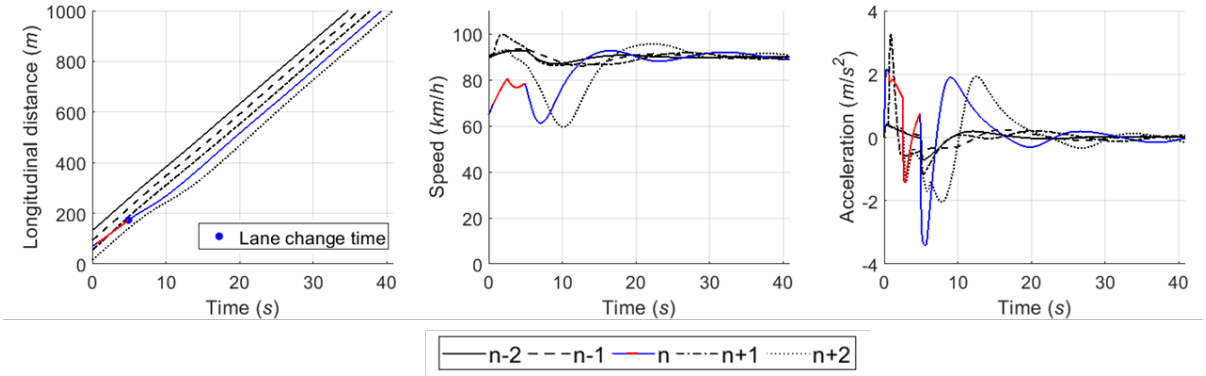

Note that a red solid line indicates simulation data of the SV (vehicle n) during game period, whereas a blue solid line shows the SV's data in simulation time except game period.

Figure 4-19. Graphical representation of simulation results in case 2.

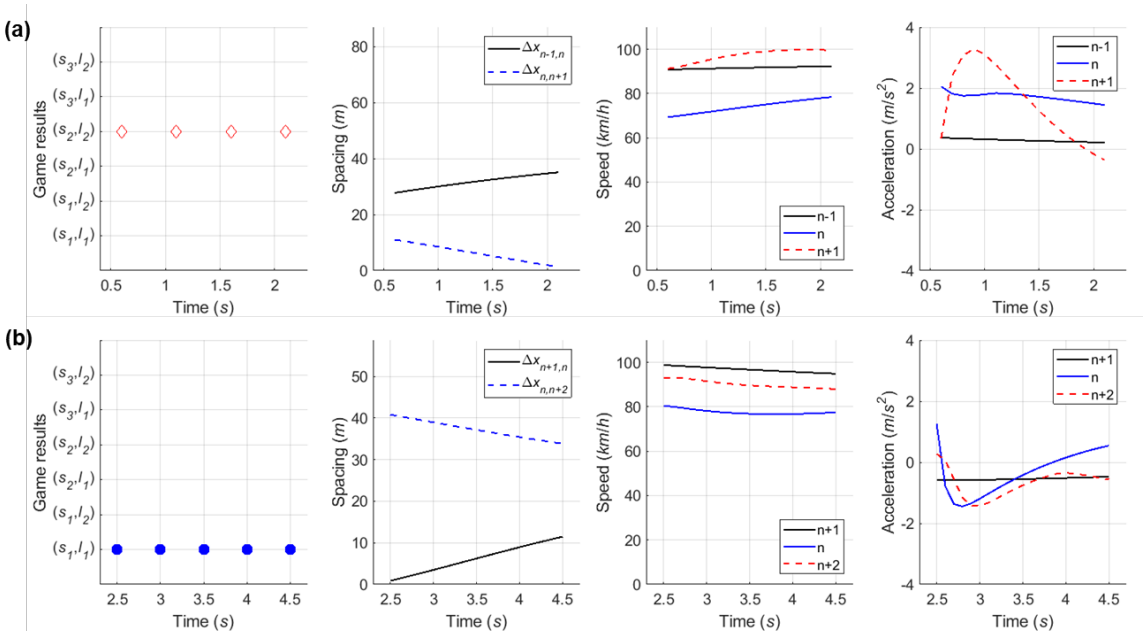

Figure 4-20. Decision-making game results in case 2.

c) Case 3: cooperative merging scenario using a forward gap

In overtaking scenario, time-space diagram in Figure 4-21 shows that the SV took the forward gap and then merge onto the freeway. When the SV entered the acceleration lane, the SV and LV

chosen the 'overtake (s_3) and yield (l_1)' action set. Although the LV decided the yielding action, it was observed that the LV maintained its speed during the first game period due to observing the SV's passing. After overtaking the lead vehicle, the SV began to decrease the speed to harmonize with that of freeway vehicles. New LV, i.e., it had been the lead vehicle in the first game period, selected the yielding action in interaction with the SV. So it showed the deep deceleration during the second game period. The SV maintained on the acceleration lane, then it changed a lane as soon as the gap acceptance rule was satisfied. As described in simulation setting, overtaking scenario is usually observed in congested traffic condition. Thus this lane-changing by overtaking action caused huge oscillation in speed profile because generally spacing between vehicles is small under congested traffic condition. It is concluded that this simulation model based on the proposed game model well represents inducing a backward forming shockwave by merging traffic in congested condition.

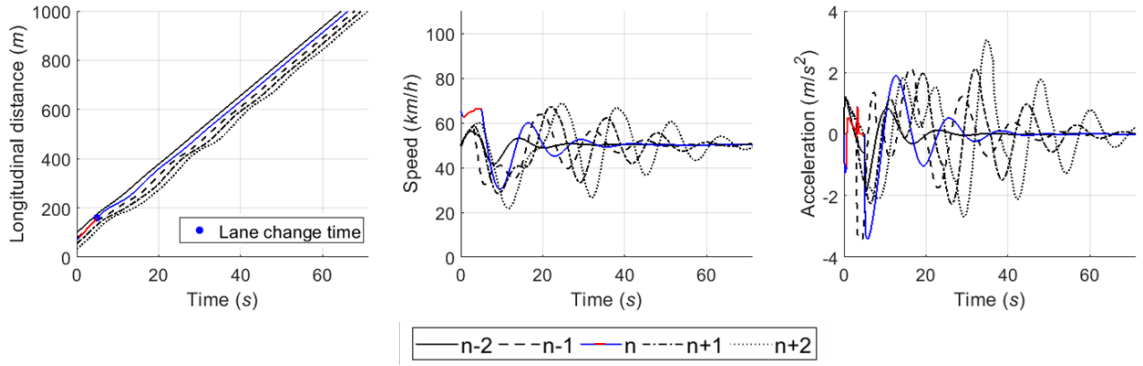

Note that a red solid line indicates simulation data of the SV (vehicle n) during game period, whereas a blue solid line shows the SV's data in simulation time except game period.

Figure 4-21. Graphical representation of simulation results in case 3.

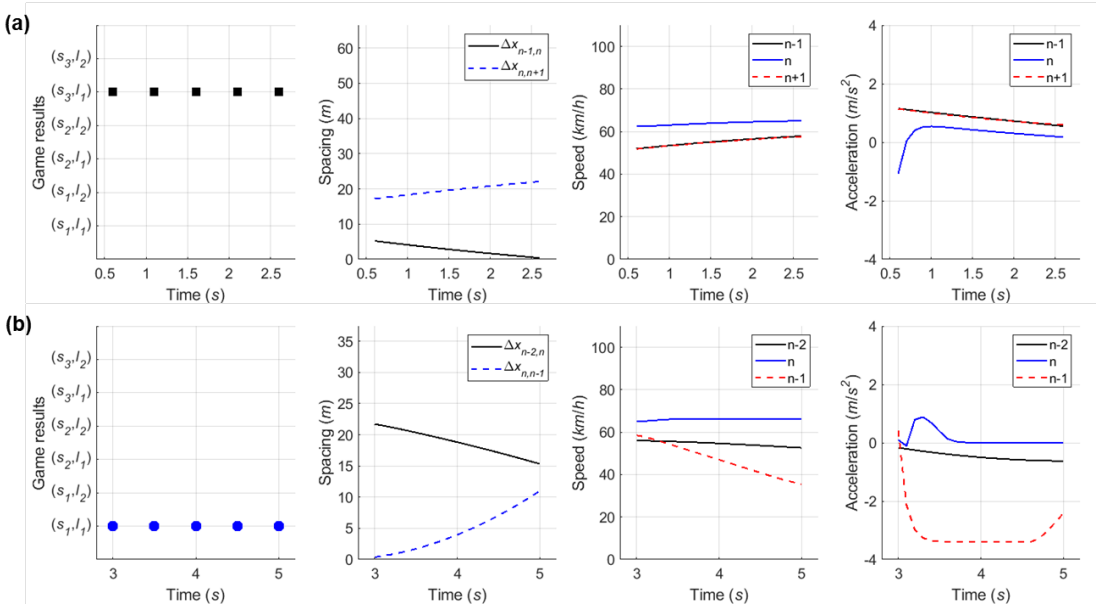

Figure 4-22. Decision-making game results in case 3.

d) Case 4: competitive merging scenario choosing an adjacent gap or a backward gap (1)

In the fourth competitive merging case, the initial game result of (s_1, l_2) is observed in Figure 4-24(a). As a non-cooperative action strategy set, it means that both drivers are in competition to achieve their own objective. At the third decision-making point, a decision they make becomes (s_2, l_2) as a cooperative action strategy set. Although the driver of SV initially wanted to change a lane using an adjacent gap as soon as entering an acceleration lane, they change the initial decision in order to avoid collision after recognizing the opposite driver's aggressive behavior. Thus the driver finally uses the backward gap for merging onto the freeway. By this case, this study conclude that the repeated game model enables to depict practical change of drivers' decision in competitive decision-making even using the cumulative function.

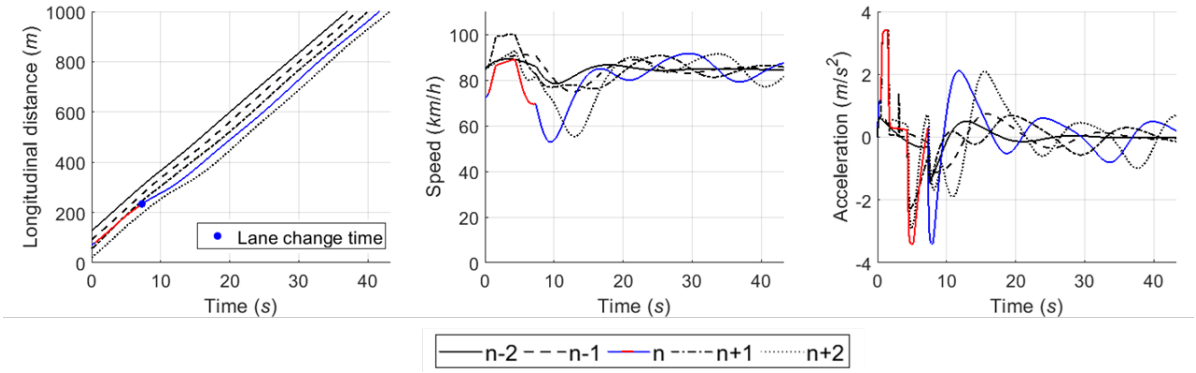

Note that a red solid line indicates simulation data of the SV (vehicle n) during game period, whereas a blue solid line shows the SV's data in simulation time except game period.

Figure 4-23. Graphical representation of simulation results in case 4.

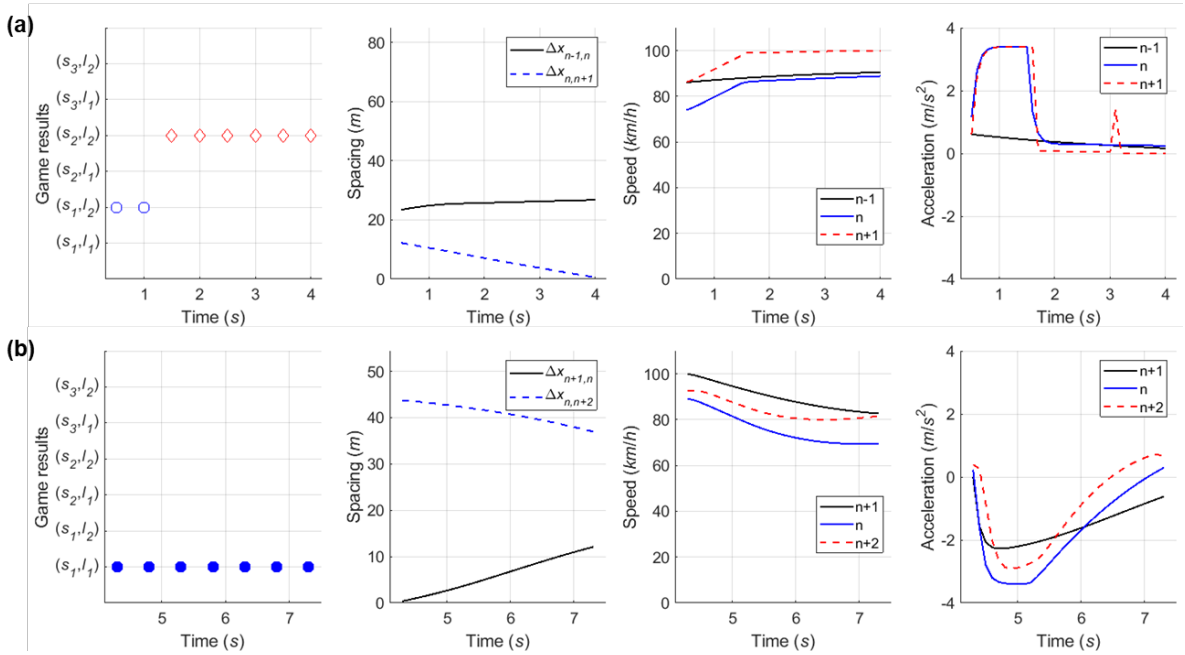

Figure 4-24. Decision-making game results in case 4.

e) Case 5: competitive merging scenario choosing an adjacent gap or a backward gap (2)

In Case 5, the simulation results show the SV used the backward gap for merging onto the freeway whichever game model is used, as illustrated in Figure 4-25 and Figure 4-26. This example shows competition to choose an adjacent gap or a backward gap, as in Case 4. However, there is a difference in that the initial decision is a cooperative action strategy in Case 5.

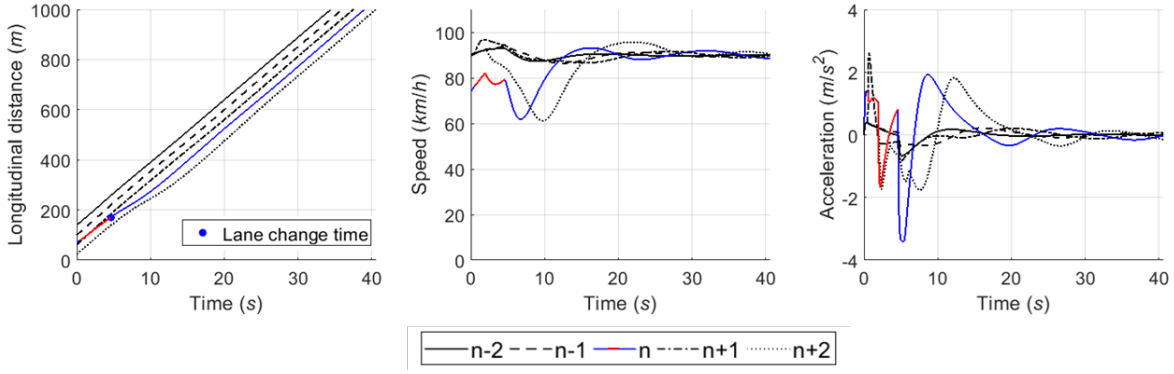

Note that a red solid line indicates simulation data of the SV (vehicle n) during game period, whereas a blue solid line shows the SV's data in simulation time except game period.

Figure 4-25. Graphical representation of simulation results in case 5 using the repeated game model.

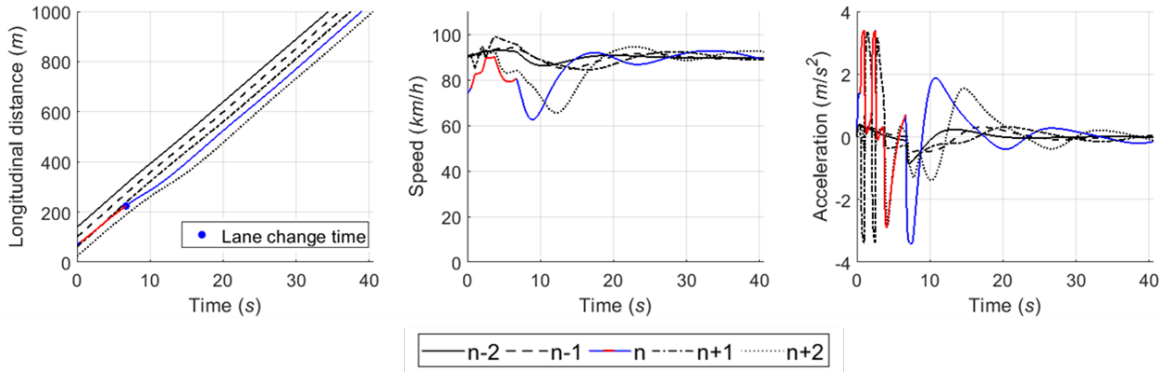

Note that a red solid line indicates simulation data of the SV (vehicle n) during game period, whereas a blue solid line shows the SV's data in simulation time except game period.

Figure 4-26. Graphical representation of simulation results in case 5 using the one-shot game model.

In Figure 4-27(a), when the repeated game model was used, the driver of SV chose a 'wait (s_2)' action during the first game period and then decided to change a lane in the second game period. While decision-making results were maintained using the repeated game model, oscillation in decision-making is revealed when the one-shot game is used, as shown in Figure 4-28(a). One reason why the one-shot game model causes unstable decision results is that the stage game decides a driver's action in a merging situation based on instantaneous vehicle location, speed, and acceleration data without consideration of previous game results (i.e., decisions made at previous game points). Considering the goal of each action, a change from a non-cooperative strategy set to

a cooperative strategy is required in order to avoid a collision (if (s_1, l_2) is chosen) or unnecessary deceleration (if (s_2, l_1) is selected). However, changes between cooperative action strategy sets (i.e., (s_1, l_1) and (s_2, l_2)) are not realistic except when there is a surrounding vehicle intervention. This case shows a distinct difference observed in simulation results depending on which type of the two game models is used. Oscillation in decision-making may reduce the performance of microscopic traffic simulation models even though it is only observed in specific competitive merging situations.

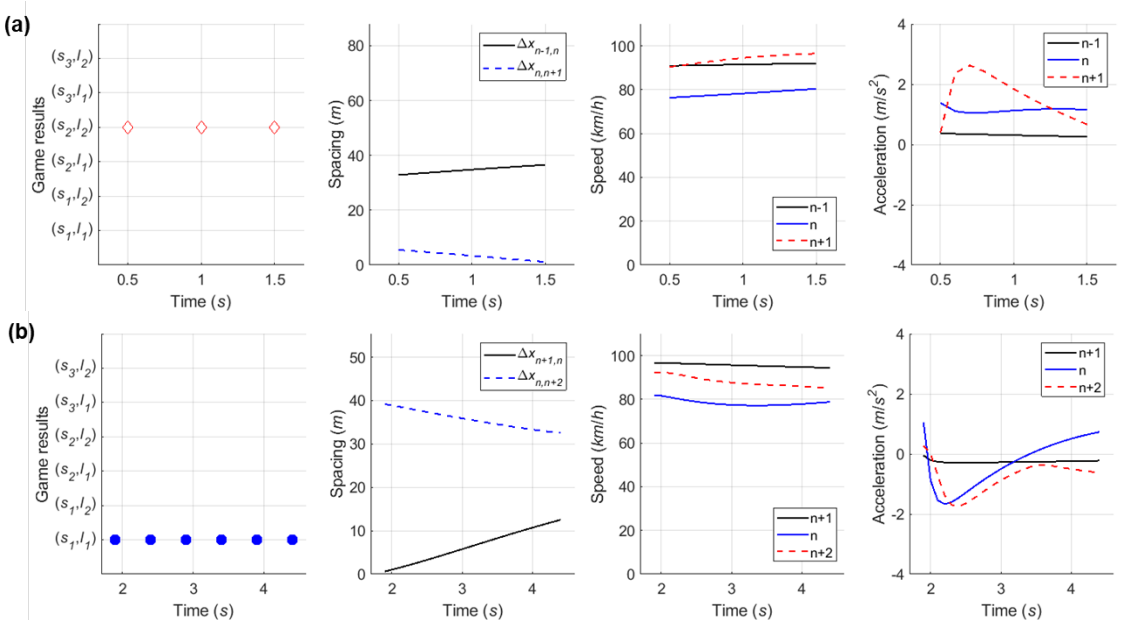

Figure 4-27. Decision-making game results in case 5 using the repeated game model.

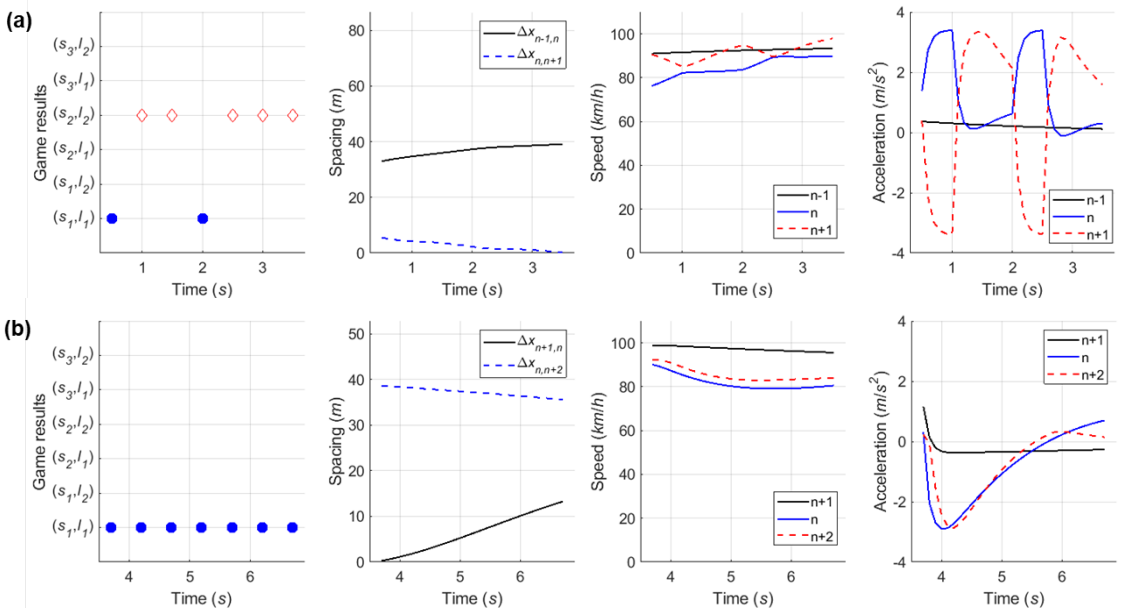

Figure 4-28. Decision-making game results in case 5 using the one-shot game model.

Chapter 5. Cooperative Maneuvers Planning based on a Game Model for CAVs

---

This study proposes a decision-making game structure for CAVs in merging, and expands it as cooperative maneuver planning in merging. In consideration of features of the CAVs, the cooperative game design is established and payoff functions are modified based on the third model described in Chapter 3. Next, explanation on how cooperative decision-making is performed is followed. To show the effectiveness of the proposed cooperative game model, a sensitivity analysis is provided and compared to the results using the non-cooperative game model. Lastly, a simulation study is conducted to prove the performance of the cooperative maneuver planning in the mixed traffic of traditional vehicles and CAVs.

5.1 Introduction

AVs have recently attracted increasing interest. Both the IT and the automobile industry are engaged in this transformation. According to the IEEE members, they predicted up to 75% of vehicles would be autonomous by 2040 [81]. AVs will coexist in traffic systems, and bring about potential benefits: enhancement of safety, mitigation of traffic congestion, increase of traffic flow, and reduction of environmental impacts. AV is expected to substitute a human-driven vehicle (HV), especially, can decrease serious crashes, which 94% of these crashes are due to dangerous decisions or human error [82].

Moreover, transportation systems will be transformed as the advanced transportation environment based on connected automated vehicles (CAVs), which enable to communicate with other transportation components through vehicle-to-everything (V2X) communication. In comparison to the dedicated short-range communication (DSRC), the evolution of long-range cellular communication, such as 5G or 4G LTE technology, motivates to develop efficient traffic management application and precise vehicle control. Especially, researchers are developing application based on vehicle-to-vehicle (V2V) and vehicle-to-infrastructure (V2I) communication.

Fundamental tasks of autonomous driving include car-following, lane keeping and lane-changing [83]. Car-following and lane keeping have been extensively studied. Cruise control, adaptive cruise control (ACC), lane-keeping assist and lane-centering have been developed [84]. Complicated tasks including lane-changing are usually realized through planning algorithms [85]. The algorithms can be divided into four hierarchical classes: route planning, path planning, trajectory planning, and maneuver planning [57]. In maneuver-based model, it relies upon interpreting the intention of surrounding traffic components (e.g., vehicles, pedestrians, and obstacles). Therefore, a game model which studies the interaction between vehicles is an appropriate approach to predict other vehicle's behavior and then decide a corresponding reaction as a maneuver.

As maneuver planning for CAVs' lane change, this study develops the merging decision-making game in which CAVs participate based on the third model developed in Chapter 3. A cooperative game design is presented including payoff functions. To show cooperative performance of the game, a sensitivity analysis is conducted and a result is compared with that of the non-cooperative game model. Last, a simulation study for the competitive cases is conducted using the simulation model, which was developed in Chapter 4, integrated with the proposed cooperative game model.

5.2 Cooperative Maneuver Planning of CAVs

5.2.1 Background

1) Stackelberg game model

A game theoretical approach can be applied into various decision-making situations using game characteristics. Especially, the *Stackelberg* games, which represents a sequential game, have been widely used to explain CAV (or AV)'s lane-changing process or vehicle control [57, 86-88]. This approach assumed that the leader decides their action first and then the follower move sequentially and that the leader knows the follower's reaction corresponding to the leader's choice. In order words, there is a prerequisite condition that the presence of a hierarchical decision order among players exists. This model is proper to model LC behaviors under perfect information. Therefore, this study proposes the game model based on the Stackelberg game concept in the mixed traffic which CAVs and HVs coexist.

For illustration purpose, an example is given with specific payoffs for imaginary lane-changing scenario, as shown in Figure 5-1. The first player SV is the CAV which is able to predict reaction of the opposite according to their decision and the other player is a driver of the nearest HV, denoted as the driver of LV, in the target lane who wants to maximize their own outcome. Both players have respective two action strategy as shown in the figure, and the corresponding payoffs for each action strategy set are shown in the parentheses; the number on the left indicates the payoff of the SV while the right-side number indicates the payoff of the driver of LV. If the Nash equilibrium is used in this example, they will choose the 'change and yield' action strategy set where there is no player has motivation to change their decision if other player maintain their action. However, in the Stackelberg model the optimal decision is chosen by predicting reactions of other player. According to the payoffs in Figure 5-1, the driver of LV will decide a yielding action to SV's lane-changing execution as it will bring higher payoff. If the SV decides to wait, the driver of LV will block SV's lane change. By comparison of payoffs between 'change and yield' and 'wait and block' action strategy set, therefore, it is recommended for the SV to stay in the current lane for getting the highest payoff by choosing 'wait' action. This approach to find an equilibrium is called as *backward induction*. In this manner, the Stackelberg model can be solved to find the *subgame perfect Nash equilibrium* (SPNE), i.e. the strategy profile that serves best each player, given the strategies of the other player. To apply this concept into the decision-making in merging, required assumptions and a difference with the Stackelberg equilibrium for finding the decision are described in the following subsection.

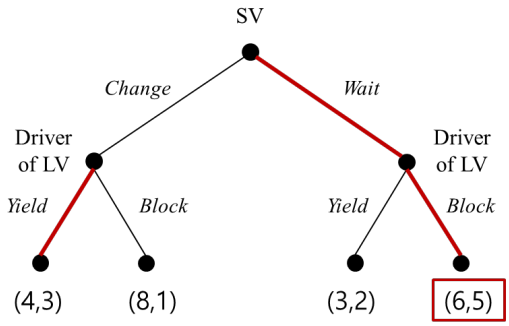

Figure 5-1. Decision tree in a lane-changing example.

2) Assumptions to model a decision-making game in the mixed traffic

The decision-making in which the CAV participated were modelled as a game under perfect information by several assumptions: a) the CAV can obtain precise data about surrounding vehicles via not only advanced sensors but also V2V communication; b) hence it can perceive whether a surrounding vehicle is a CAV or not in the mixed traffic (i.e., market penetration rate is not 100%.) by connection status between them; c) All the CAVs decide an action in merging by use of identical prediction strategy based on the proposed game model; and d) CAVs decide a cooperative action if it does not interfere in their safety, i.e., HV has a priority in decision-making in the mixed traffic. The CAV, in other words, can make a decision to avoid conflict based upon prediction of HV's expected action even though there is an expected loss in reward.

5.2.2 Game Design

In Chapter 3, indeed, this study defined the merging decision-making game is played simultaneously under imperfect information in traditional transportation environment. Since this merging decision-making game is played to decide the driver's maneuvers, not deciding whether they execute a lane change at every decision-making time period. Since this study assumed that the CAV has a role to substitute a human driver based on accurate data collection and decision-making without human error, game structure including the number of players and players' action strategies was considered as identical form defined in Chapter 3. A difference was that the error term to capture unobserved decision variables by human driver's subjective perception was excluded from the payoff functions.

1) Game structure

As shown in Table 5-1, games can be categorized into four games according to the vehicle types: $CAV^{SV} - CAV^{LV}$, $CAV^{SV} - HV^{LV}$, $HV^{SV} - CAV^{LV}$, and $HV^{SV} - HV^{LV}$. Note that a superscript SV and LV indicate the player's identification in the game. As a review of the game structure, the SV has three action strategies change a lane for merging (s_1), wait for the lag vehicle's overtaking maneuver in the acceleration lane (s_2), or overtake the lead vehicle to use a forward gap to merge

(s_3). The LV has two action strategies: yield to allow the subject vehicle's lane change maneuver (l_1) or block the subject vehicle's merging maneuver by decreasing the spacing to the subject vehicle (l_2). Let $S = \{s_1, s_2, s_3\}$ and $L = \{l_1, l_2\}$ denote the set of pure strategies for the S and L, respectively. In addition, $a_{ij} = (s_i, l_j)$ denotes a set of actions ($a \in S \times L$) where i and j indicate the index of action strategies of the S and L (i.e., $i = 1,2,3$ and $j = 1,2$). Thus, there are total six sets of action strategies in the proposed game. Payoff functions of each action a_{ij} for the HV are denoted as P_{ij} (for HV^S) and Q_{ij}(for HV^L), while these functions for the CAV are denoted as G_{ij} (for CAV^S) and H_{ij} (for CAV^L).

Table 5-1. Game Composition by Vehicle Types

Vehicles		Vehicle type of the LV	
		CAV^{LV}	HV^{LV}
Vehicle type of the SV	CAV^{SV}	Player and Actions: Lag Vehicle (LV) — Yield $[l_1(q_1)]$ / Block $[l_2(q_2)]$ Subject Vehicle (SV): Change $[s_1(p_1)]$: (G_{11}, H_{11}) / (G_{12}, H_{12}) Wait $[s_2(p_2)]$: (G_{21}, H_{21}) / (G_{22}, H_{22}) Overtake $[s_3(p_3)]$: (G_{31}, H_{31}) / (G_{32}, H_{32})	Player and Actions: Lag Vehicle (LV) — Yield $[l_1(q_1)]$ / Block $[l_2(q_2)]$ Subject Vehicle (SV): Change $[s_1(p_1)]$: (G_{11}, Q_{11}) / (G_{12}, Q_{12}) Wait $[s_2(p_2)]$: (G_{21}, Q_{21}) / (G_{22}, Q_{22}) Overtake $[s_3(p_3)]$: (G_{31}, Q_{31}) / (G_{32}, Q_{32})
	HV^{SV}	Player and Actions: Lag Vehicle (LV) — Yield $[l_1(q_1)]$ / Block $[l_2(q_2)]$ Subject Vehicle (SV): Change $[s_1(p_1)]$: (P_{11}, H_{11}) / (P_{12}, H_{12}) Wait $[s_2(p_2)]$: (P_{21}, H_{21}) / (P_{22}, H_{22}) Overtake $[s_3(p_3)]$: (P_{31}, H_{31}) / (P_{32}, H_{32})	Player and Actions: Lag Vehicle (LV) — Yield $[l_1(q_1)]$ / Block $[l_2(q_2)]$ Subject Vehicle (SV): Change $[s_1(p_1)]$: (P_{11}, Q_{11}) / (P_{12}, Q_{12}) Wait $[s_2(p_2)]$: (P_{21}, Q_{21}) / (P_{22}, Q_{22}) Overtake $[s_3(p_3)]$: (P_{31}, Q_{31}) / (P_{32}, Q_{32})

2) Payoff functions

This study basically uses the payoff functions formulated for the third model in Chapter 3. To decide like a human driver, this study assumed that the CAV makes a decision by the calibrated payoff functions in Chapter 4. As described earlier, in addition, the error term was not included. Table 5-2 shows the payoff functions for the $CAV^{SV} - CAV^{LV}$ game. Here G_{ij} and H_{ij} can be applied identically into the other games.

Table 5-2. Game Structure and Payoff Functions of the Merging Decision-Making Game between CAVs in Normal Form

Player and Actions		CAV^{LV}	
		Yield $[l_1(q_1)]$ [b]	Block $[l_2(q_2)]$
CAV^{SV}	Change $[s_1(p_1)]$ [a]	• $G_{11} = \alpha_{11}^1 + \alpha_{11}^2 U_{SV}^S(s_1) + \alpha_{11}^3 U_{SV}^{FM}$ • $H_{11} = \beta_{11}^1 + \beta_{11}^2 U_{LV}^S(l_1)$	• $G_{12} = \alpha_{12}^1 + \alpha_{12}^2 U_{SV}^S(s_1) + \alpha_{12}^3 U_{SV}^{FM}$ • $H_{12} = \beta_{12}^1 + \beta_{12}^2 U_{LV}^S(l_2)$
	Wait $[s_2(p_2)]$	• $G_{21} = \alpha_{21}^1 + \alpha_{21}^2 U_{SV}^S(s_2)$ • $H_{21} = \beta_{21}^1 + \beta_{21}^2 U_{LV}^S(l_1)$	• $G_{22} = \alpha_{22}^1 + \alpha_{22}^2 U_{SV}^S(s_2)$ • $H_{22} = \beta_{22}^1 + \beta_{22}^2 U_{LV}^S(l_2)$
	Overtake $[s_3(p_3)]$	• $G_{31} = \alpha_{31}^1 + \alpha_{31}^2 U_{SV}^S(s_3)$ • $H_{31} = \beta_{31}^1 + \beta_{31}^2 U_{LV}^S(l_1)$	• $G_{32} = \alpha_{32}^1 + \alpha_{32}^2 U_{SV}^S(s_3)$ • $H_{32} = \beta_{32}^1 + \beta_{32}^2 U_{LV}^S(l_2)$

5.3 Cooperative Maneuver Planning for Merging

5.3.1 Merging Maneuver Planning by Cooperative Decisions

This study proposes merging maneuver planning in the mixed traffic based on the game model. In the mixed traffic, a human driver rationally decides after perceiving the surroundings, but they generally want to achieve their own purpose in competition. Although CAVs are developed to have a maneuver by mimicking human driver's decision-making, furthermore, they can make a cooperative decision even in competitive situation to avoid conflicts.

The game models this study developed cannot avoid deciding a non-cooperative action strategy if pure strategy Nash equilibrium and mixed strategies are only considered. In Chapter 4, the field data have some competitive cases even though most merging situations are cooperative, and in the sensitivity analysis of the game model the non-cooperative decision cases were found. Before being fully automated transportation systems, non-cooperative driving maneuvers of human drivers will be continuously observed. To minimize inefficient competition between, thus this study proposes maneuver planning algorithm based on the decision-making game in the mixed traffic.

The basic idea is the CAV can plan the maneuver after predicting the opposite player's desired action, as illustrated in Figure 5-2. Prediction of action strategies is based on the decision-making game result at instantaneous time step. If the predicted result is one of non-cooperative action strategy sets, i.e., (s_1, l_2) or (s_2, l_1), the CAV changes its maneuver to be cooperative with other player's action. This approach was developed to take the Stackelberg game concept which makes a decision in consideration of the estimated reaction into account. Since this study still maintains this the decision-making game is simultaneous game due to no visual sign assigning decision-

making order even in the connected environment, only the CAV can change its action depending on the non-cooperative game results. Examples how the CAV changes the estimated non-cooperative decision by type of the game is presented in following subsections.

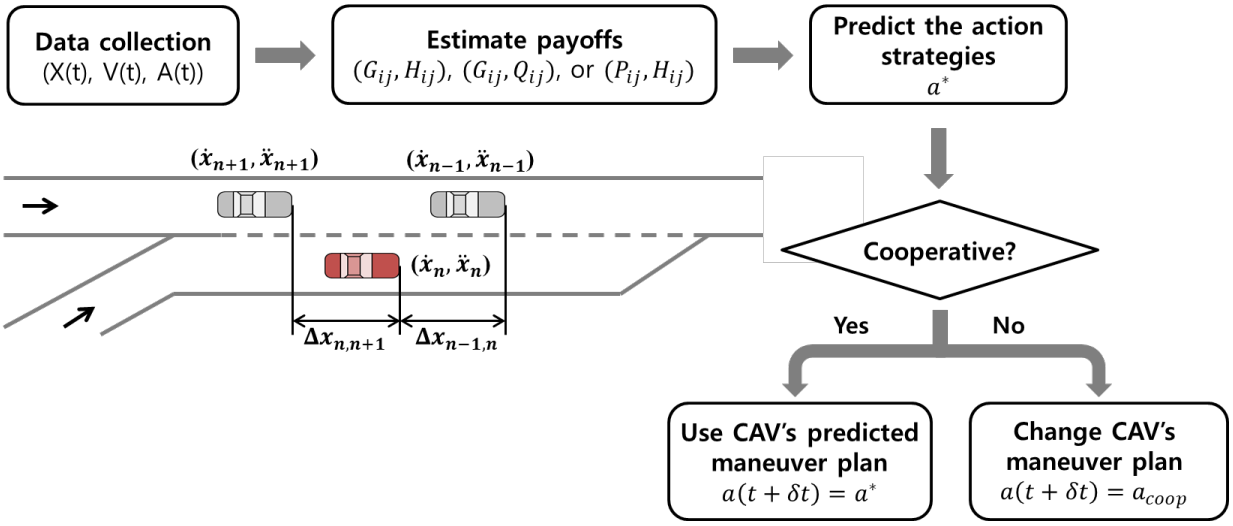

Figure 5-2. CAV's maneuver planning based on prediction by the game models.

5.3.2 Methodology of Cooperative Decision-making by Game Types

1) $CAV^{SV} - CAV^{LV}$ game

By assumptions described previously, when both players are CAVs, they can perceive the opposite is also the CAV, and plan maneuvers using same algorithm based on collected and shared data at every decision-making point. Hence their results will be identical cooperative decision even if they independently decide a maneuver. If the $CAV^{SV} - CAV^{LV}$ game result is a cooperative decision, set both vehicles just follows this maneuvers. Otherwise, the combined utility by corresponding probability and payoff for each cooperative action strategy set is specified as:

$$U_{ij}(a_{ij}) = p_i \cdot G_{ij} + q_j \cdot H_{ij} \qquad \forall\, a_{ij} \in \{a_{11}, a_{22}\} \tag{5.1}$$

They compare the combined utilities, then pick the one which has the higher payoffs. Therefore, the cooperative set which is applied until next decision-making time point is determined by:

$$a_{coop} = \begin{cases} (s_1, l_1) & if\ U_{11}(a_{11}) \geq U_{22}(a_{22}) \\ (s_2, l_2) & o.w. \end{cases} \tag{5.2}$$

where a_{coop} indicates the cooperative set required through the prediction of the non-cooperative game result.

Figure 5-3 shows an example of the maneuver planning where $a^* = (s_1, l_2)$ is expected as the desired action strategy through the game. There are two alternatives, i.e., (s_1, l_1) or (s_2, l_2), as shown in Figure 5-3(a). In the extensive form (see Figure 5-3(b)), dashed lines indicates that the decisions towards the non-cooperative sets are not allowed. Both CAVs choose the optimal maneuvers showing the highest rewards between alternatives.

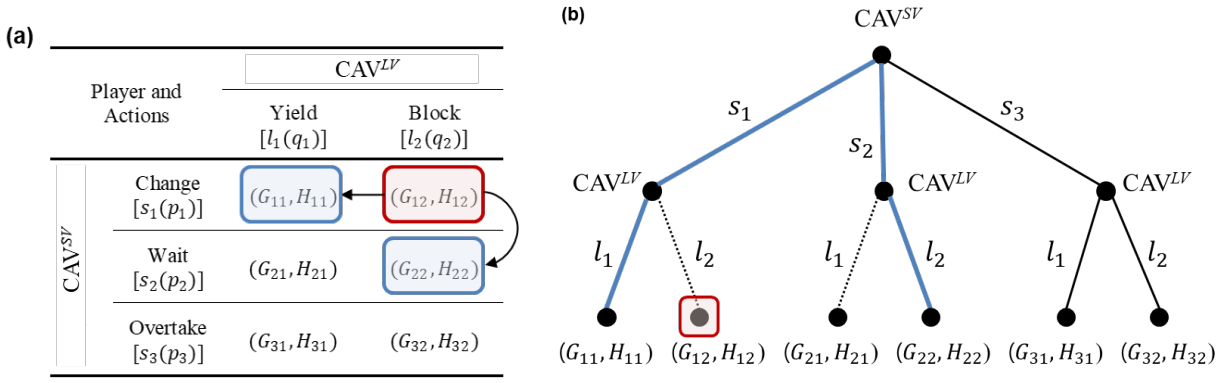

Figure 5-3. Cooperative maneuver planning in $CAV^{SV} - CAV^{LV}$ game with (s_1, l_2) action: (a) normal form and (b) extensive form.

To show the performance of the proposed maneuver planning in consideration of the CAVs, this study conducts the sensitivity analysis using the $CAV^{SV} - CAV^{LV}$ game. The sensitivity analysis was conducted by integrating the maneuver planning algorithm based on the game model and following the setting described in Section 4.5.1. Figure 5-4 shows the sensitivity analysis results, and there are two distinguished features. First, the payoff functions for the CAV reduce the uncertainty induced by the error term. At $v_{fwy} = 60\ km/h$, for instance, the results of the $HV^{SV} - HV^{LV}$ game (see Figure 4-10(a)) shows the unapparent boundary between regions indicating (s_1, l_1) and (s_3, l_1). In contrast, in Figure 5-4(a), there is a distinct boundary between two decision areas. In Figure 5-5, the yellow region illustrates that the difference of game results between the $CAV^{SV} - CAV^{LV}$ and $HV^{SV} - HV^{LV}$ game, i.e., indicating effect of the updated payoffs. In the $HV^{SV} - HV^{LV}$ game results, moreover, the non-cooperative decision set (s_1, l_2) was observed, indicating the human drivers compete at specific speed profile and spacing. However, the black region of Figure 5-5 indicates that the non-cooperative decision area in the $HV^{SV} - HV^{LV}$ game results changed to the cooperative sets by the proposed maneuver planning. It demonstrates that the proposed maneuver planning can increase the efficiency in merging section by reducing the non-cooperative behaviors if the CAVs exist.

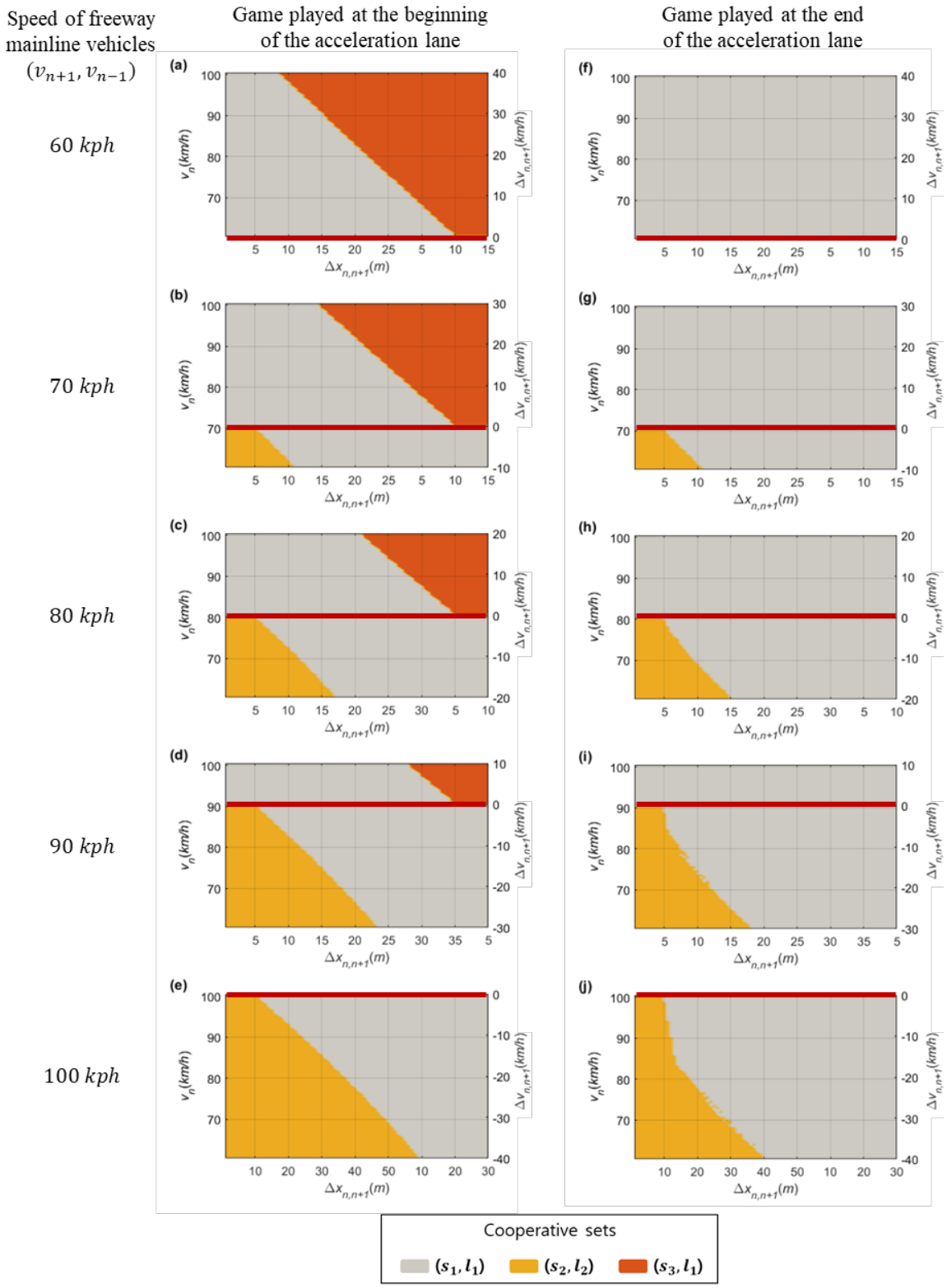

Note that a red line parallel to the x-axis on each graph indicates the speed of the freeway mainline vehicles (v_{n-1}, v_{n+1}).

Figure 5-4. Graphical representation of the one-shot game between CAV^{SV} and CAV^{LV} results depending on game locations, spacing between vehicles ($\Delta x_{n,n+1}$), and speed of the SV n (v_n).

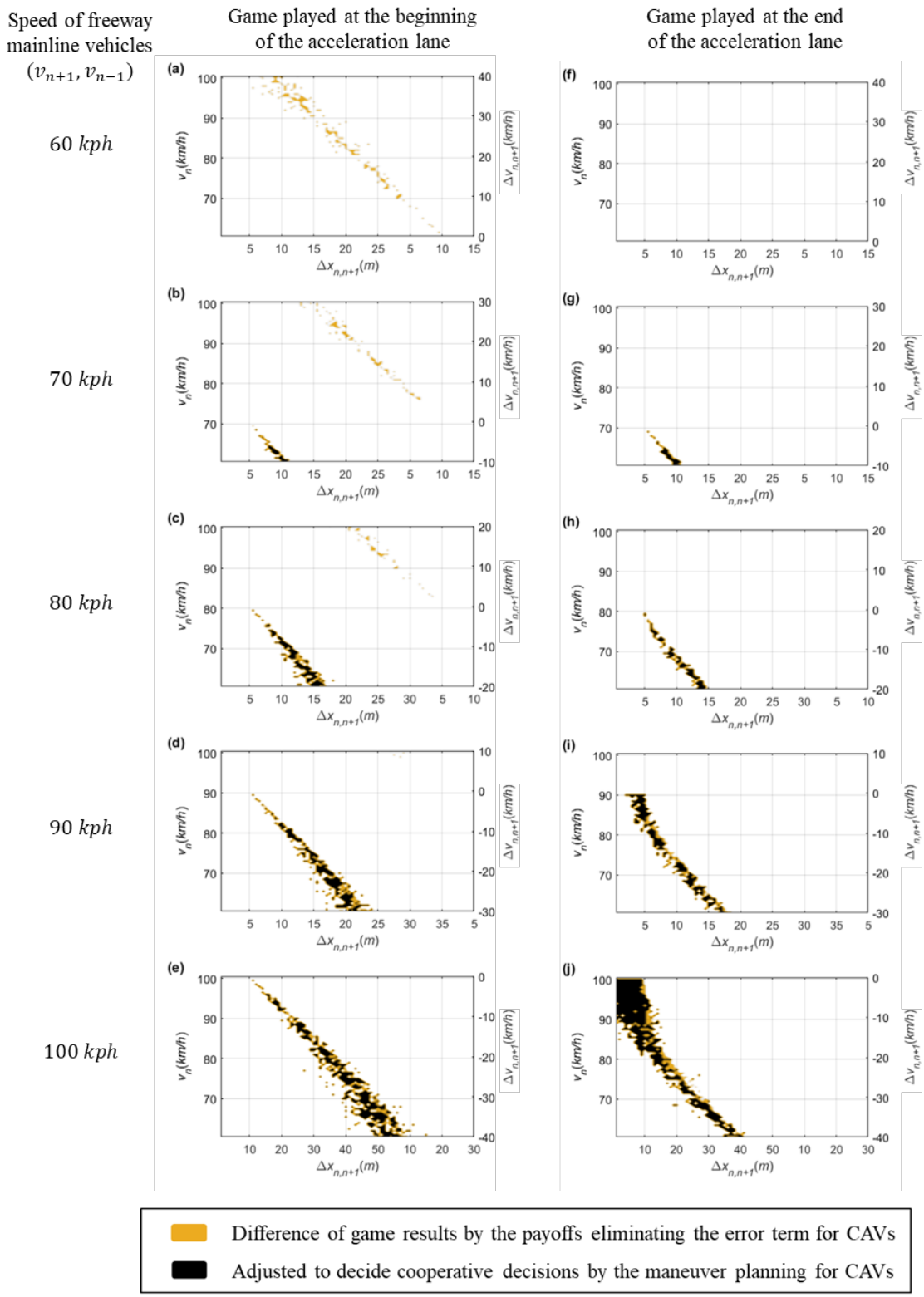

Figure 5-5. Graphical representation of the difference of game results between the $CAV^{SV} - CAV^{LV}$ and $HV^{SV} - HV^{LV}$ game.

2) $CAV^{SV} - HV^{LV}$ game

In the $CAV^{SV} - HV^{LV}$ game only the CAV^{SV} can predict the HV^{LV}'s decision through the game model. These is no way to request to show cooperative behavior on the CAV's maneuver. If the estimated action strategy is a non-cooperative set, hence the CAV^{SV} changes the action by Equation (5.3):

$$a_{coop} = \begin{cases} (s_1, l_1) & if\ a^* = (s_2, l_1) \\ (s_2, l_2) & if\ a^* = (s_1, l_2) \end{cases} \tag{5.3}$$

Figure 5-6 illustrates how this method works where $a^* = (s_1, l_2)$ is expected as the desired action strategy through the game. In consideration of the vehicle type, there is only one alternative (s_2, l_2), as shown in Figure 5-6(a). In the extensive form (see Figure 5-6(b)), it shows CAV^{SV} chooses the 'wait (s_2)' action when the HV^{LV}'s desired decision is the 'block (l_2)' action.

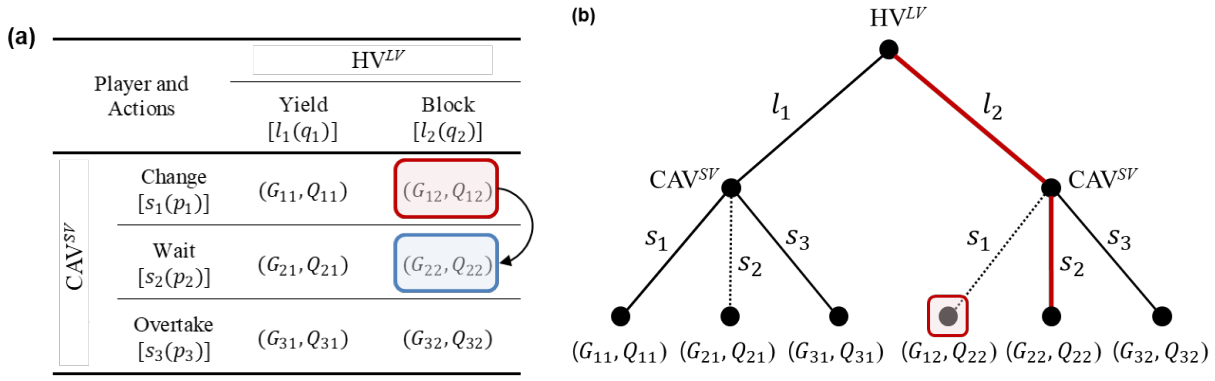

Figure 5-6. Cooperative maneuver planning in $CAV^{SV} - HV^{LV}$ game with (s_1, l_2) action: (a) normal form and (b) extensive form.

Figure 5-7 shows the sensitivity analysis results by the maneuver planning based on the $CAV^{SV} - HV^{LV}$ game. The apparent finding is that the CAV changes initial 'change (s_1)' action into the 'wait (s_2)' action in non-cooperative (s_1, l_2) decision area.

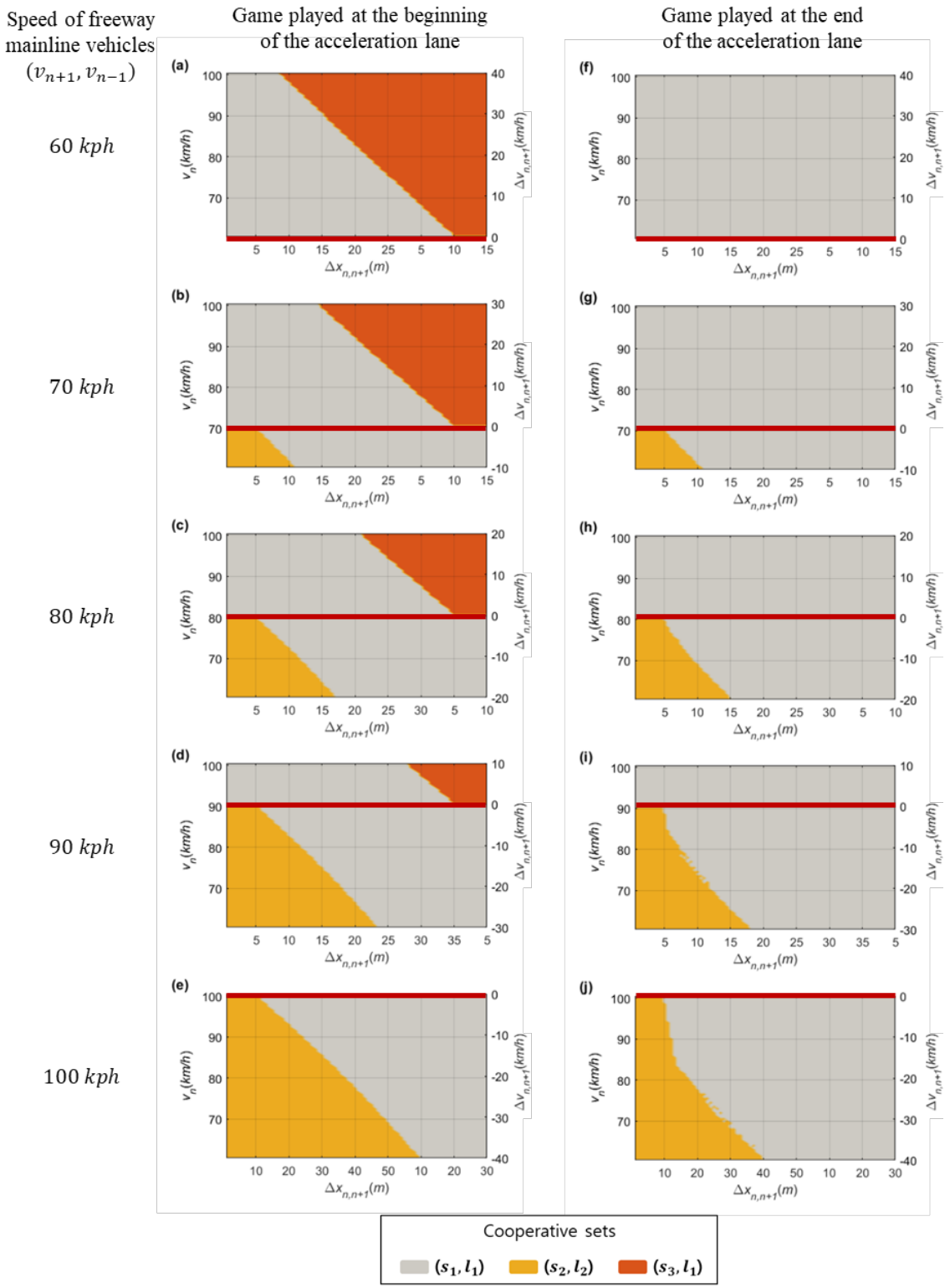

Note that a red line parallel to the x-axis on each graph indicates the speed of the freeway mainline vehicles (v_{n-1}, v_{n+1}).

Figure 5-7. Graphical representation of the one-shot game between CAV^{SV} and HV^{LV} results depending on game locations, spacing between vehicles ($\Delta x_{n,n+1}$), and speed of the SV n (v_n).

3) $HV^{SV} - CAV^{LV}$ game

Similarly, in the $HV^{SV} - CAV^{LV}$ game, only the CAV^{LV} can adjust its action to the HV^{SV}'s decision through the game model. The CAV^{LV} changes the action if the estimated action strategy is a non-cooperative set:

$$a_{coop} = \begin{cases} (s_1, l_1) & if\ a^* = (s_1, l_2) \\ (s_2, l_2) & if\ a^* = (s_2, l_1) \end{cases} \tag{5.4}$$

In the game between HV^{SV} and CAV^{LV}, the CAV^{LV} decides the 'yield (l_1)' action in consideration of HV^{SV}'s 'change (s_1)' action as illustrated in Figure 5-8. It reduces the unnecessary accelerating and decelerating between vehicles by avoiding competition.

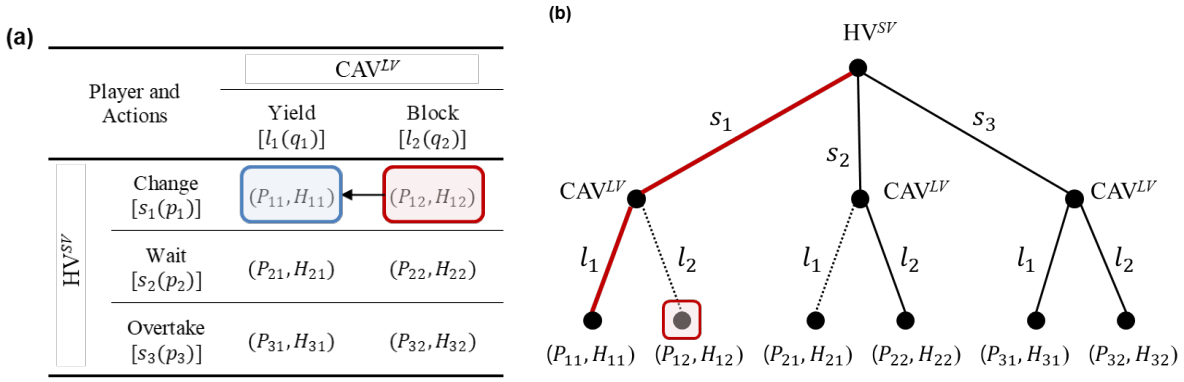

Figure 5-8. Cooperative maneuver planning in $HV^{SV} - CAV^{LV}$ game with (s_1, l_2) action: (a) normal form and (b) extensive form.

Figure 5-9 shows the sensitivity analysis results by the maneuver planning based on the $HV^{SV} - CAV^{LV}$ game. By the decision-making method, the CAV^{LV} decides an action to avoid the non-cooperative decision area. Especially, they choose the (s_1, l_1) action strategy in competitive situations, as marked with the black dashed box in Fig 5-9(j).

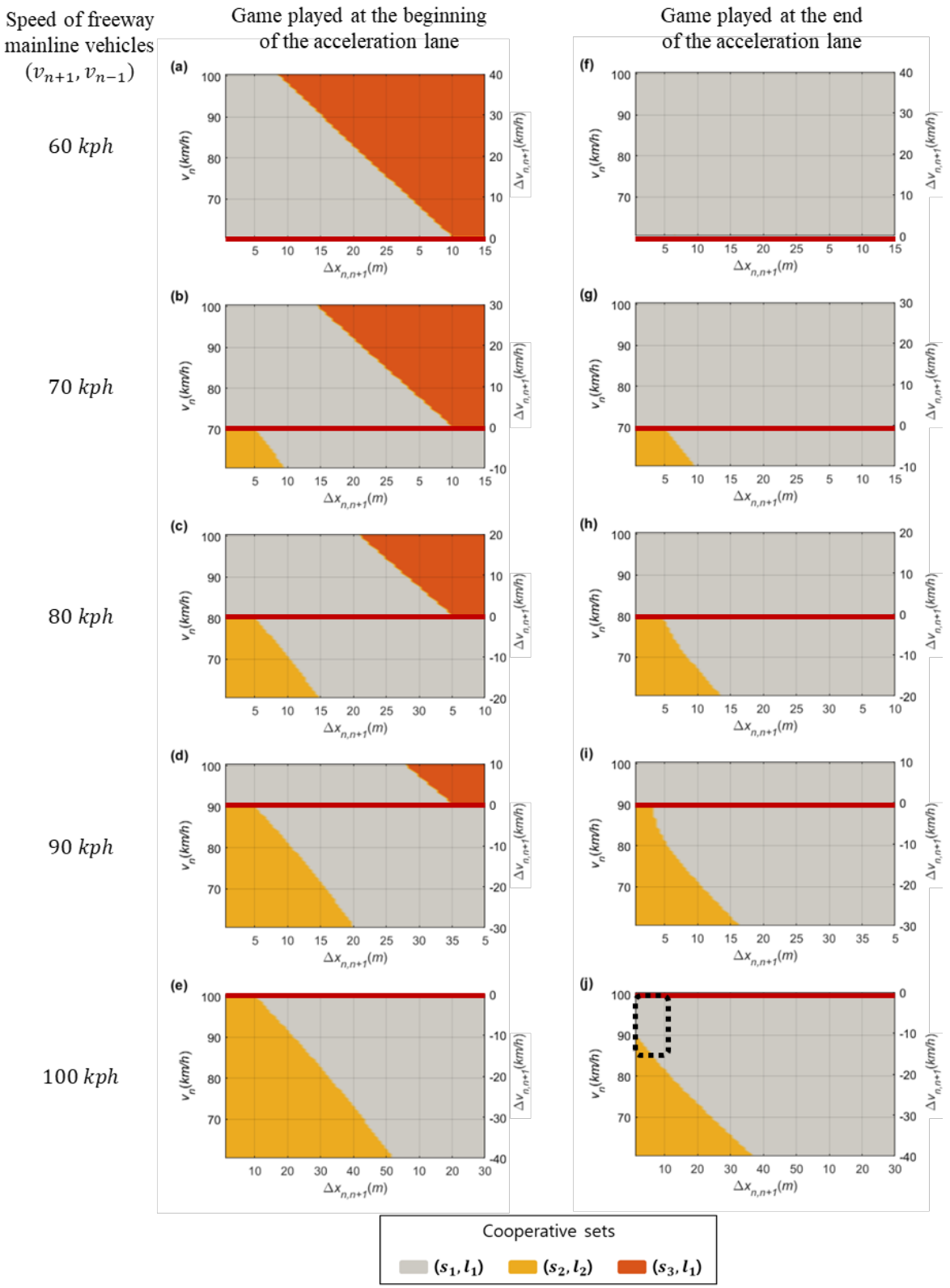

Note that a red line parallel to the x-axis on each graph indicates the speed of the freeway mainline vehicles (v_{n-1}, v_{n+1}).

Figure 5-9. Graphical representation of the one-shot game between HV^{SV} and CAV^{LV} results depending on game locations, spacing between vehicles ($\Delta x_{n,n+1}$), and speed of the SV n (v_n).

5.3.3 Case Study

1) Simulation setting

In cooperative merging situations, indeed, the cooperative maneuver planning algorithm cannot affect to the results as the game results are predicted as cooperative one. Thus this study used the non-cooperative case, as referred as the case 4 in Section 4.6.3, using the simulation model developed in Section 4.6.1. Testbed network was same as illustrated in Figure 4-16, and there are four freeway mainline vehicles and one merging vehicle. Note that initial spacing between vehicles and speeds of vehicles were constant by no consideration of a random distribution in order to verify the performance of the proposed algorithm only. In this competitive case, drivers chose the (s_1, l_2) action strategy set as the initial game result. For the case study, total four scenarios were prepared according to types of game structures: 1) $HV^{SV} - HV^{LV}$, 2) $HV^{SV} - CAV^{LV}$, 3) $CAV^{SV} - HV^{LV}$, and 4) $CAV^{SV} - CAV^{LV}$.

To compare the results, this study estimated the average total delay and the average number of vehicle stops by Equation (5.5) and (5.6), respectively, as defined in INTEGRATION manual [89]. The total vehicle delay D for all vehicles was formulated as:

$$D_{total} = \sum_{t=1}^{T} \sum_{i \in N(t)} \Delta t \left(1 - \frac{v_i}{v_f}\right) \tag{5.5}$$

where T and Δt indicate total simulation time and the time increment of data processing (= 1 deci-second), respectively; $N(t)$ is the number of vehicles at simulation time step t; and v_i and v_f indicate the instantaneous vehicle speed and free-flow speed, respectively. A partial stop is recorded at each time step when a vehicle decelerates, specified as:

$$S_i(t_i) = \frac{v_i(t - \Delta t) - v_i(t)}{v_f} \qquad \forall\ i \quad \ni v_i(t) < v_i(t - \Delta t) \tag{5.6}$$

where $S_i(t)$ denotes instantaneous partial stop of vehicle i estimated at time t_i. The sum of these partial stops provides a very accurate explicit estimate of the total number of stops that were encountered along that particular link [89].

2) Case study results

In the first scenario in which human drivers participated, there are two game periods as shown in Figure 5-10(a). At initial game point in the first game period, the (s_1, l_2) action strategy was selected and then the driver of SV changed their decision after perceiving the LV's blocking maneuver. The drivers of the SV and LV maintained the decision of (s_2, l_2) action strategy during the first period. In the second game period, the SV and new LV decided the (s_1, l_1) action strategy. In Figure 5-10(b), when the LV was the CAV, it changed to make a cooperative decision by

prediction of the game result. Thus, the (s_1, l_1) action strategy was observed as initial decision and maintained until the SV merged onto the freeway. Lastly, using both C$AV^{SV} - HV^{LV}$ and $CAV^{SV} - CAV^{LV}$ game showed the same results, as illustrated in Figure 5-10(c). In C$AV^{SV} - HV^{LV}$ game, the SV decided the 'wait (s_2)' action to be cooperative with the LV's desired action. In $CAV^{SV} - CAV^{LV}$ game, the combined utility (as defined in Equation (5.1)) of the (s_2, l_2) action is larger than that of the (s_1, l_1) action, thus they decided the former one.

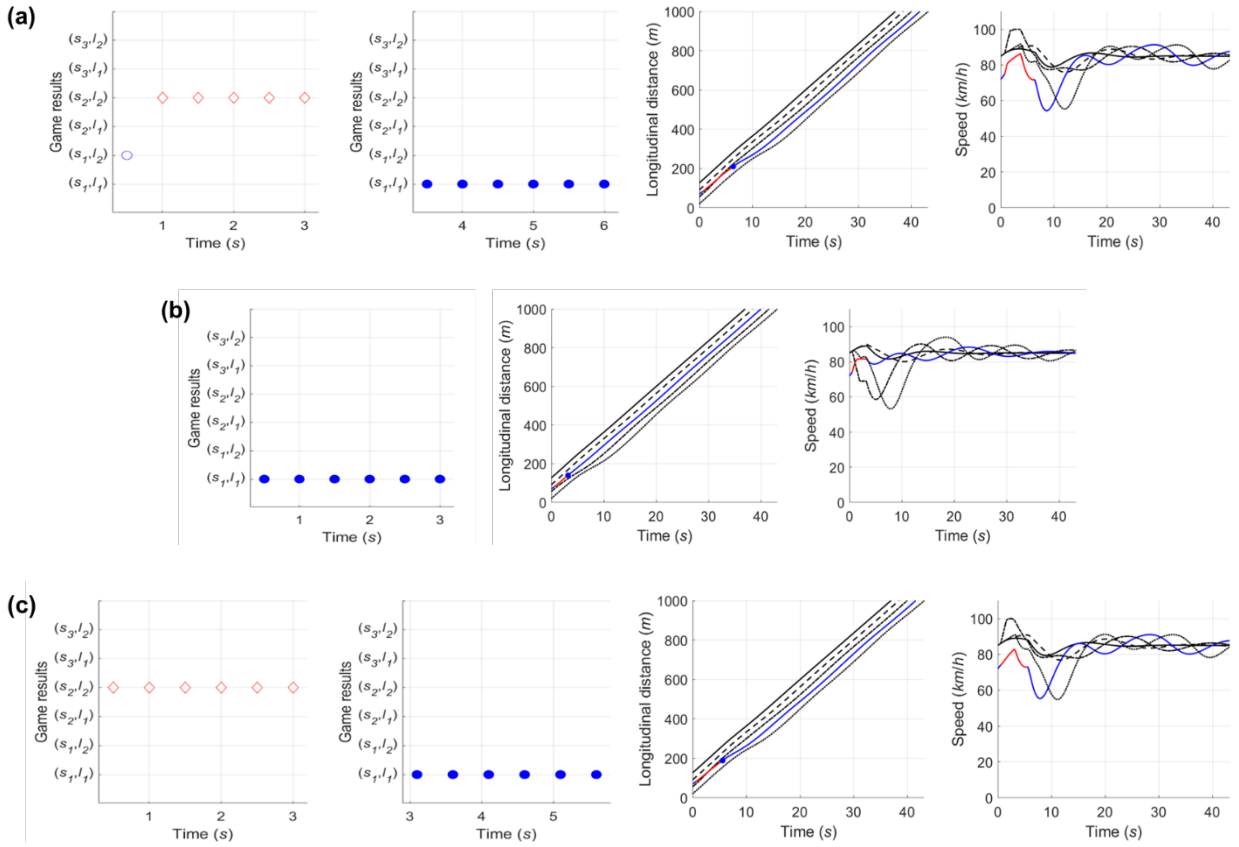

Figure 5-10. Game results and graphical representation of simulation results in the case study: (a) $HV^{SV} - HV^{LV}$ (b) $HV^{SV} - CAV^{LV}$, and (c) C$AV^{SV} - HV^{LV}$ and $CAV^{SV} - CAV^{LV}$ game.

The total delay and the number of stops were summarized in Table 5-3 and 5-4, respectively. Since the delay is related to the stops, both MOEs shows same trend in each scenario. In the second scenario, using $HV^{SV} - CAV^{LV}$ game provides the smallest total delay (D_{total}) and the number of stops (S_{total}) for all the vehicles. The sum of MOEs for both SV and LV in the second scenario is also less than that in the base scenario. However, the delay and stops of CAV^{LV} are greater than those of the other scenarios. It reveals that the CAV forcedly yield to allow the SV's merge, hence the delay and the number of stops of the LV on the target lane increased. However, it might be not observed if the simulation model is integrated with the advanced acceleration controller developed

for the CAVs (or AVs). For 'yield (l_1)' action, the LV would likely not decelerate if the distance to the expected merging point is far from current decision-making point. Thus, it should be evaluated using the advanced simulation models in further studies. In the scenarios using both $CAV^{SV} - HV^{LV}$ and $CAV^{SV} - CAV^{LV}$ games, all MOEs are smaller in comparison to the base scenario. It demonstrates that avoiding non-cooperative behavior improves network performance in mobility by decrease of conflicts.

Table 5-3. Total Delay (D) in the Case Study

Game type	D_{total} (sec)	D_{SV} (sec)	D_{LV} (sec)	Sum (= $D_{SV} + D_{LV}$)
$HV^{SV} - HV^{LV}$	38.74	1.19	0.52	1.70
$HV^{SV} - CAV^{LV}$	38.56 (-0.5 %)	0.52 (-55.9 %)	0.73 (+42.2 %)	1.26 (-26.1 %)
$CAV^{SV} - HV^{LV}$ and $CAV^{SV} - CAV^{LV}$	38.69 (-0.1 %)	1.15 (-3.4 %)	0.46 (-10.2 %)	1.61 (-5.5 %)

Number in parentheses indicates difference of total delay as comparison to the $HV^{SV} - HV^{LV}$ scenario.

Table 5-4. The Number of Stops (S) in the Case Study

Game type	S_{total}	S_{SV}	S_{LV}	Sum (= $S_{SV} + S_{LV}$)
$HV^{SV} - HV^{LV}$	1.720	0.154	0.103	0.258
$HV^{SV} - CAV^{LV}$	1.368 (-20.5 %)	0.003 (-98.1 %)	0.190 (+84.3 %)	0.193 (-25.0 %)
$CAV^{SV} - HV^{LV}$ and $CAV^{SV} - CAV^{LV}$	1.638 (-4.8 %)	0.107 (-30.6 %)	0.090 (-13.1 %)	0.197 (-23.6 %)

Number in parentheses indicates difference of the number of stops as comparison to the $HV^{SV} - HV^{LV}$ scenario.

5.4 Simulation Test and Discussion

This study evaluates the proposed maneuver planning through simulation study. The simulation model is developed, and then validated with comparison of the microscopic traffic simulator INTEGRAION. As the results, network performances are compared in order to prove how the cooperative behavior of vehicles by the maneuver planning affects to the freeway network.

5.4.1 Development of the Agent-based Simulation Model

To evaluate the proposed maneuver planning, this study integrated the planning algorithm into the developed simulation model in Section 4.6.1. The developed model consists of mainly four parts: a) putting vehicle into the network, b) calculation of acceleration level, c) vehicle motion control, and d) on-screen animation (see Figure 5-11) and summarization of simulation results. Vehicles

are randomly distributed and enter the network through mainline and on-ramp based on the volume-to-capacity (V/C) ratio. In the second part, acceleration level is determined by the car-following model, developed game models, and proposed maneuver planning for CAVs. As described in Section 4.6.1, the RPA car-following was used to model steady-state car-following and collision avoidance. In addition, game models were used at a merging section and type of the model is decided by the type of vehicles (i.e., players). It affects to determine an acceleration level to execute vehicle's maneuver decided by the game model in merging situation. Lastly, the maneuver planning is only applied when the CAV is one of players participated in the game and the expected action strategy is non-cooperative. Vehicle moves by the determined acceleration level at every simulation time step and the simulation results are summarized after end of simulation.

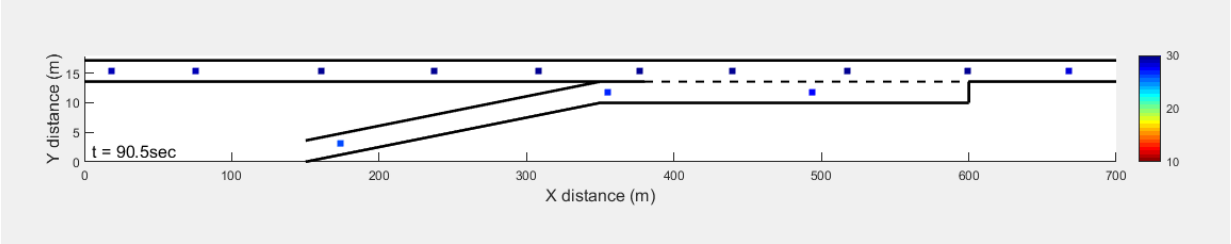

Figure 5-11. Graphic animation in the developed simulation model.

5.4.2 Simulation network and parameters

Simulation tests were conducted on a simplified freeway network extended over 700 *m* and included one merging ramp, as shown in Figure 5-12. In order to verify the proposed strategy only, the freeway with one lane was coded in the developed MATLAB simulation model. There are two scenarios according to the number of vehicles entering into the roadway. The simulation experiments were prepared as follows:

- Total simulation time was 70 minutes (= 4,200 seconds) including 10-minute cool-down time.
- The V/C ratios of the freeway mainline and on-ramp traffic are 0.6 and 0.2, respectively.
- There are total six cases according to the market penetration rates (MPRs) of the CAVs: 0.0 (the base case), 0.2, 0.4, 0.6, 0.8, and 1.0.
- Link properties for the freeway mainline: saturation flow rate was 2,400 *veh*/*h*/*lane*. Jam density was 160 *veh*/*km*/*lane*. Free-flow speed and speed-at-capacity were 100 *km*/*h* and 80 *km*/*h*, respectively.
- Link properties for the on-ramp: saturation flow rate was 1,800 *veh/h/lane*. Jam density was 160 *veh/km/lane*. Free-flow speed and speed-at-capacity were 80 *km/h* and 60 *km/h*, respectively.

- The vehicle randomly enters the network based on the normal distribution with a coefficient of variation (= standard deviation / mean) of 0.1. It is assumed that its initial speed is also normally distributed with a coefficient of variation of 0.1.

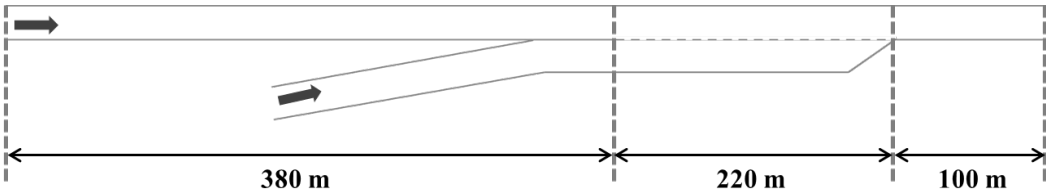

Figure 5-12. Road network for simulation test.

5.4.3 Simulation validation

1) Simulation validation approach and measure of simulation results

Simulation validation is required to verify the performance of the simulation model. Although the simulation model used the validated microscopic models (i.e., the RPA car-following model was validated in [54] and the game model was evaluated in Chapter 4), the developed simulation model should be verified to show whether it is a proper model for evaluating the proposed algorithm. However, there is a limitation on comparison with data obtained from the field having identical roadway design as this developed model is hard to represent the complicated behavior such as DLC. Therefore, this study compared the simulation performance derived from the developed model with the results of the microscopic traffic simulator INTEGRAION, which was validated and utilized in various studies.

INTEGRATION, an agent-based microscopic traffic assignment and simulation software, creates individual vehicle trip departures based on an origin-destination (O-D) matrix and moves vehicles along the network in accordance with the RPA car-following model [89]. It simulates the movement of individual vehicles every deci-second by modeling acceleration, lane-changing movements, and car-following behavior [89]. In a previous study, discretionary lane distribution was consistent with empirical data [90]. The mandatory lane-changing logic, moreover, was validated against empirical data from weaving sections in California [55]. In validation, simulation output were compared to the empirical data at several sites and the spatial variation in the lane flow distribution was also compared.

To compare the results, this study coded the identical freeway network as illustrated in Figure 5-11 onto INTEGRATION and used the same parameters as described in the previous section. In the base scenario without input of CAVs, the V/C ratios of freeway mainline and on-ramp are 0.6 and 0.2, respectively. As the measure of effectiveness (MOE), this study compares the average travel time, average total delay (as defined in Equation (5.5)), and the average number of vehicle stops (as defined in Equation (5.6)).

2) Simulation validation results

To validate the simulation model, this study ran the base scenario ten times in each simulator. Table 5-4 shows the comparison of MOEs (i.e., average travel time, average speed, average total vehicle delay, and average the number of vehicle stops) between the INTEGRATION model and the developed simulation model. The results showed difference of less than 10 % on average travel time and average travel speed. It indicates that, in the developed tool, all the traffic traveled slightly faster. In contrast, it could be interpreted that there are quite large differences on the average total vehicle delay and the number of vehicle stops between results of two simulation tools. Although the percentages of difference on both MOEs are relatively high value, the differences of both MOEs in total traffic are not huge from a quantitative point of view. The average total vehicle delay and average the number of vehicle stops in entire traffic are only one second per a vehicle and less than 0.5 vehicle-stops, respectively. However, there were apparent differences on the MOEs of the on-ramp traffic as the lane-changing logic based on the game model shows the dissimilar merging behaviors to the logic in INTEGRATION. In the simulation model based on the game model, the on-ramp traffic relatively merged earlier than the results in INTEGRAION. In other words, faster cut-in caused the larger delay and partial stops on the mainline traffic. Although this difference exists, the developed simulation model generated reasonable outputs. Therefore, this study concludes that the simulation model can be utilized for the proposed maneuver planning evaluation as a simulation tool.

Table 5-5. Simulation Model Validation Results

MOEs	Traffic	INTEGRATION	Developed Simulation Tool	Difference
Average travel time (sec)	Total	32.73	31.43	-4.0%
	Mainline	33.34	32.33	-3.0%
	On-ramp	30.29	27.85	-8.1%
Average speed (km/h)	Total	75.25	76.57	1.8%
	Mainline	75.34	77.95	3.5%
	On-ramp	64.93	71.09	9.5%
Average total vehicle delay (sec/veh)	Total	7.90	6.88	-12.9%
	Mainline	7.64	7.05	-7.7%
	On-ramp	8.94	6.18	-30.9%
Average the number of vehicle stops (veh-stops)	Total	0.48	0.88	84.0%
	Mainline	0.45	0.92	104.9%
	On-ramp	0.60	0.73	21.3%

5.4.4 Evaluation results of the cooperative maneuver planning

As mentioned previously, this study conducted simulations by MPRs at the mainline V/C ratio of 0.6 and on-ramp V/C ratio of 0.2. To evaluate the proposed application, first this study compared the MOEs and the number of games in various MPR cases, as summarized in Figure 5-13. The simulation tests clearly show that distinct improvement in network performance is observed when the cooperative merging maneuver is activated. When CAVs coexist with HVs, in other words, vehicles' travel time, total delay, and the number of vehicle stops decreased in comparison to the base case at the MPR of 0 %, as shown in Figure 5-13(a) to 5-13(c). Especially, the superior improvement is revealed in the fully connected and automated environment. In the MPR of 100 % case, vehicles on both traffic streams traveled faster by about 17 % compared to the base case. Both average of total vehicle delay and the number of vehicle stops for the entire vehicles reduced by about 78 %. It means that delays induced by competitions in merging situations significantly affect to upstream traffic even though only small amount of competitions occur. Since it was assumed that the games are played until the merging vehicle find an acceptable gap, moreover, the non-cooperative decisions causing competitions result in increasing the number of the game play times, as shown in Figure 5-13(d). It may occur the force merging situations as the merging vehicle cannot find the gaps, then it generates considerable delays.

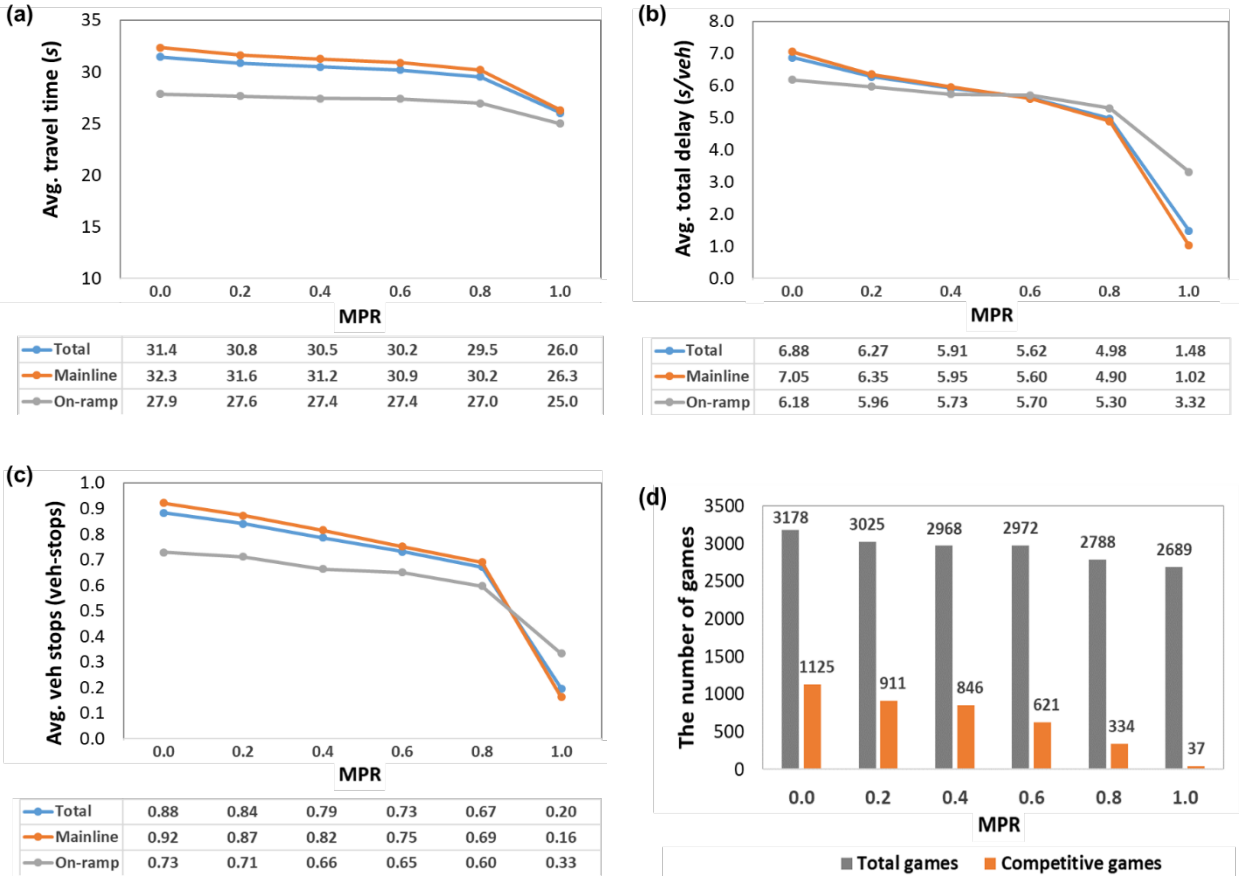

	0.0	0.2	0.4	0.6	0.8	1.0
Total	31.4	30.8	30.5	30.2	29.5	26.0
Mainline	32.3	31.6	31.2	30.9	30.2	26.3
On-ramp	27.9	27.6	27.4	27.4	27.0	25.0

	0.0	0.2	0.4	0.6	0.8	1.0
Total	6.88	6.27	5.91	5.62	4.98	1.48
Mainline	7.05	6.35	5.95	5.60	4.90	1.02
On-ramp	6.18	5.96	5.73	5.70	5.30	3.32

	0.0	0.2	0.4	0.6	0.8	1.0
Total	0.88	0.84	0.79	0.73	0.67	0.20
Mainline	0.92	0.87	0.82	0.75	0.69	0.16
On-ramp	0.73	0.71	0.66	0.65	0.60	0.33

Figure 5-13. Evaluation results of the cooperative maneuver planning.

These quantitative simulation results present that the cooperative behaviors at a merging section improve the system-wide network performance. The cooperative merging game between CAVs helps players choosing the best strategy without the impact of the uncertain payoffs induced by the error term. Thus, it is clear that the proposed cooperative maneuver planning is efficient if all the CAVs decide maneuvers based on the same prediction ability.

Figure 5-14 illustrates the screenshots captured in animation at around 500-second simulation time step at the respective MPR of 0 % and 100 %. Note that each box on the road network indicates the vehicle and its color shows the instantaneous speed of the vehicle based on the color bar indicating a range of the speed (in m/s) on the right side. At the MPR of 0 %, i.e., tradition transportation systems, the ramp vehicle's merge causes deceleration to following vehicles (see Figure 5-14(a)), whereas most vehicles travel at near the free-flow speed in the fully connected and automated environment (see Figure 5-14(b)). Since both the gap acceptance model and acceleration controller were identically operated without consideration of the vehicle type, this figure can be an evidence to indicate that the proposed cooperative maneuver planning can improve the network performance. In addition, time-space diagrams during 600 to 1,800-second simulation time in respective traditional vehicles (i.e. HVs only) environment and the CAVs environment are illustrated in Figure 5-15. Backward forming shock waves and forward recovery shock waves are observed several times in Figure 5-15(a). Competition between human drivers may result in extension of game period. It can induce the forced merging situations causing these shock waves. In contrast, in the CAVs environment, no shock wave is presented in Figure 5-15(b). Consequently, it reveals that the proposed cooperative maneuver planning contributes to improve traffic flow.

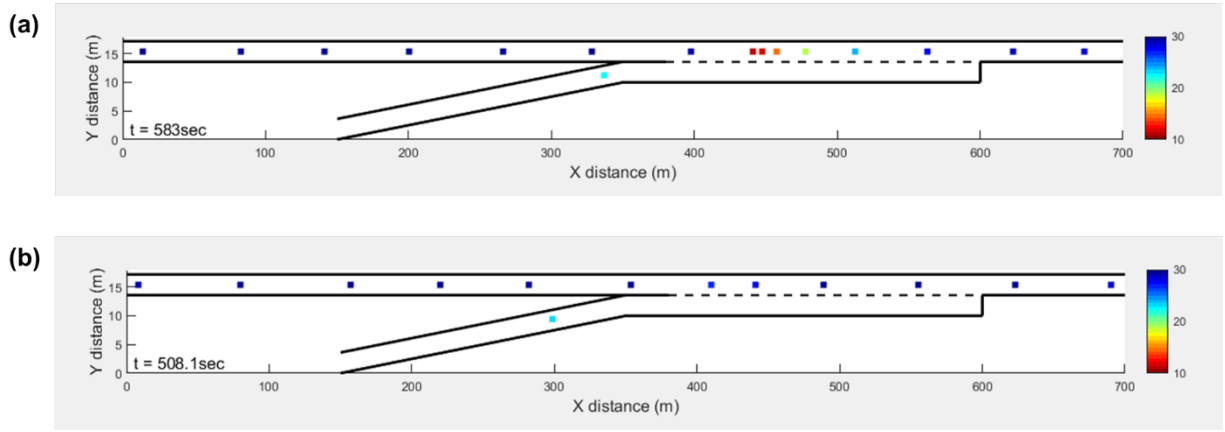

Figure 5-14. Comparison of animation between (a) the MPR of 0 % case and (b) the MPR of 100 % case.

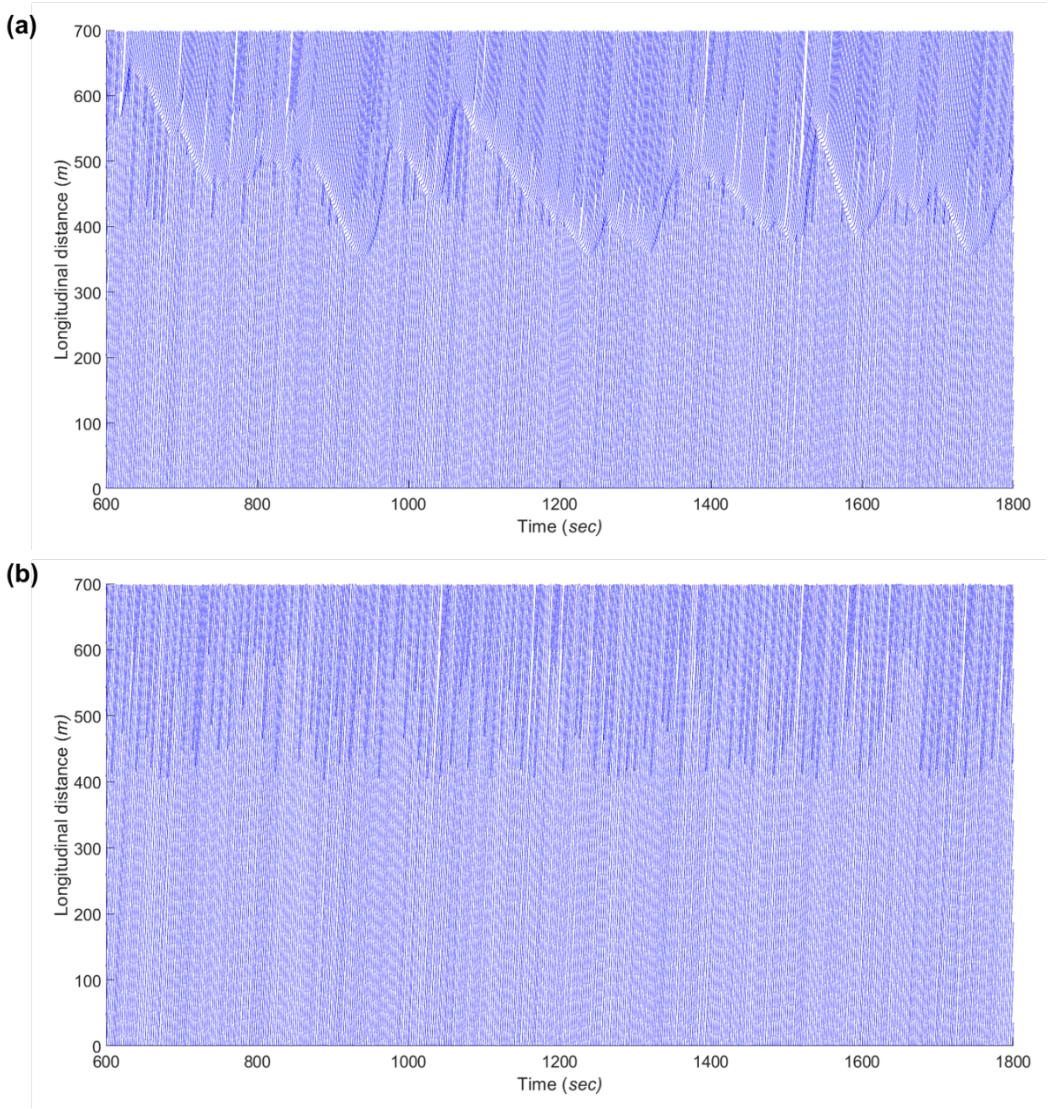

Figure 5-15. Time-space diagrams (in 600 to 1,800-second simulation time): (a) MPR of 0 % case and (b) the MPR of 100 % case.

5.4.5 Discussion

The well modeled and precisely validated game model can be applied into the algorithms or applications for the CAVs as a part of prediction of human driver's behavior. This study proposed the maneuver planning application based on the game model for merging decision-making, and proved that it has the potential benefits in mobility on a freeway. To further develop the proposed application, macroscopic traffic flow condition is should be considered to decide the control level. In the traffic stream traveling at the free-flow speed, for instance, forced control may induce unnecessary decelerations or delays. In other words, the additional algorithm to determine a control level (or activation of the cooperative maneuver planning) is necessary. It can be developed based on the simulation study conducted in various demand levels and conditions. Also, consideration

of physical features related to CAV system and sensors is required in order to integrate the developed model with the CAVs. As the preliminary study, this study concludes that the cooperative maneuver planning based on the game model has an ability to improve the transportation systems.

Chapter 6. Development of Optimal Lane Selection Algorithm

This study proposes an optimal lane selection (OLS) algorithm to consider the long-range connected environment on a freeway, which can be used an in-vehicle application based on real-time information. The study introduces the expanded connected environment and the OLS application is also described. Next, a utility function for the OLS algorithm is formulated. To evaluate the proposed application, a sensitivity analysis and case study are conducted using the INTEGRATION microscopic traffic simulator [89].

This chapter is based on the papers listed below:

1. Kang, K., Bichiou, Y., Rakha, H. A., Elbery A., and Yang, H. (2019, October). *Development and Testing of a Connected Vehicle Optimal Lane Selection Algorithm*. Accepted to present at 22nd International Conference on Intelligent Transportation Systems (ITSC) 2019, Auckland, New Zealand.
2. Kang, K., Elbery A., Rakha, H. A., Bichiou, Y., and Yang, H. (2018, November). Optimal Lane Selection on Freeways within a Connected Vehicle Environment. In *Proceedings of 21st International Conference on Intelligent Transportation Systems (ITSC) 2018*, Maui, HI, USA.

6.1 Introduction

Due to the continuous growth of travel demands and limited space for roadway facilities, traffic management agencies have been required to mitigate traffic congestion. In the present (traditional) transportation environment, intelligent transportation systems (ITS) have been utilized to improve road safety and traffic flow efficiency. Now, advanced information and communication technology (ICT) provides a chance to evolve the transportation system. Research efforts have been devoted to developing and testing connected vehicle (CV) technologies, which have the ability to exchange time-critical and safety-critical messages. Connected transportation systems enable cooperative control between vehicles and offer the potential benefits of improving safety and mobility.

Human driving behavior is critical to the safety and throughput of transportation systems. As drivers want to maintain their individual car-following status and minimize travel time, potential conflicts may occur, especially under congested traffic conditions. For example, drivers occasionally show non-cooperative behaviors in lane-changing to gain individual benefits. In lane-changing, lane selection is conducted using the limited information earned by sight view only, and drivers cannot communicate with each other. This causes excessive and unnecessary lane changes to avoid unexpected deceleration and improve the instantaneous driving condition. This results in turbulence, which triggers the formation of congestion and a capacity drop.

An in-vehicle CV system can provide beneficial advisories or warnings to drivers. The lane change warning application, for example, enhances safety by warning a driver of a potential collision with another vehicle or an object in the target lane [45]. In another study, cooperative lane-changing led to significant improvements in traffic flow efficiency [91]. Drivers can also increase traffic throughput by selecting lanes intelligently. Moriarty and Langley (1998) developed and evaluated an intelligent lane selection system, demonstrating that it produces higher speeds and reduces the number of lane changes [92]. Jin et al. (2014) proposed real-time optimal lane selection (OLS) algorithm with connected vehicle technology, and it reduced average travel time by up to 3.8% and the fuel consumption by around 2.2% [93]. Also, Tian et al. (2016) proposed a CV application to assist lane selection, and simulation study demonstrates that the application reduces travel time and the potential conflict risk [94].

6.2 Overview of an Optimal Lane Selection Application

This study designs an optimal lane selection (OLS) application that provides the driver with optimal lane information, as seen in Figure 6-1. The OLS algorithm is implemented in an in-vehicle CV system to determine which lane offers the most efficient freeway travel. CVs transmit their data, including speed profile, location (i.e., coordinates and lane identification), using V2V communication. The in-vehicle system of the subject CV uses the collected data to evaluate all lanes to choose the optimal one. The main purpose of the proposed application is to minimize

travel time for an individual CV, while also minimizing the turbulence resulting from selfish lane-changing. This study assumes that providing driver with the optimal lane advisory can improve traffic flow stability on freeways. In addition, the proposed in-vehicle application can be part of a lane-based path planning algorithm for lane selection in automated driving.

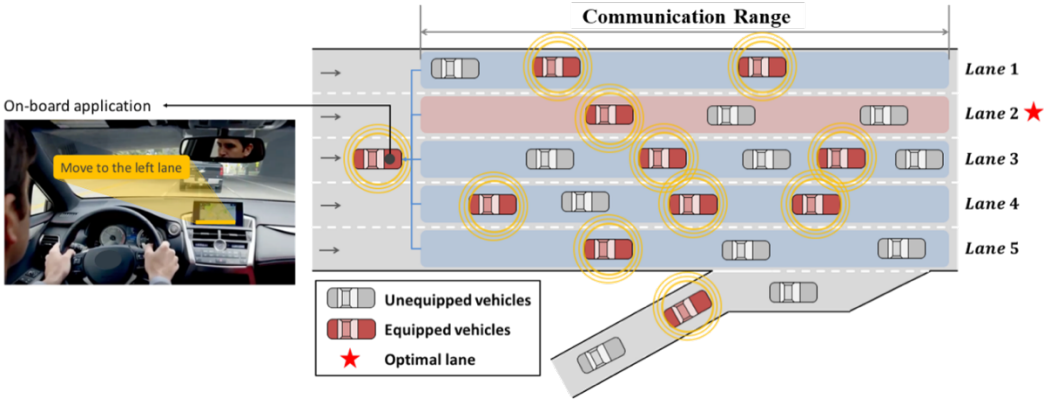

Figure 6-1. Concept of OLS application.

Based upon development of wireless communication technology, the advanced connected transportation environment is considered to develop and evaluate the OLS algorithm, as shown in Figure 6-2. This study assumes that existing Road Side Units (RSU) form a static cloud onto which the CV's data are transferred. In addition, a CV is able to transmit its own data through long-range communication. It has the ability to form a cloud for data sharing in areas not covered by RSUs. In order to decrease the number of data packets and to minimize communication failure, each cloud is divided into segments for aggregating raw speed data. It is also assumed that a CV in the cloud becomes an instant leader that gathers segment-based data within a short-communication range and can then transfer the data to a local server. It shares downstream data with other CVs in an assigned cloud. Following these assumptions, all CVs can obtain downstream data for use in the proposed OLS application.

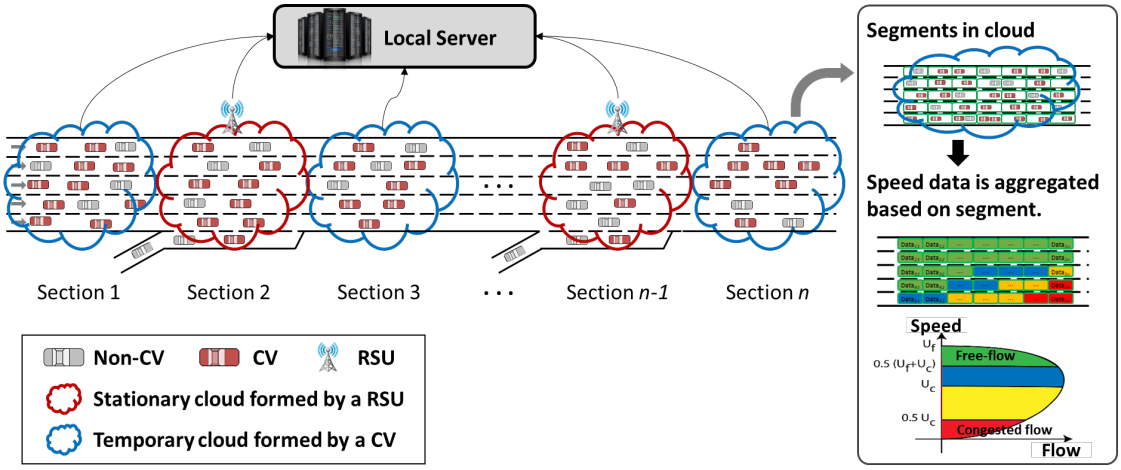

Figure 6-2. Concept of the advanced connected transportation environment.

6.3 Structure of the Utility Function

This study aimed at developing the OLS application, in consideration of the advanced connectivity between CVs. The subject CV_i suggests the optimal lane information to a driver based on a speed utility as illustrated in Figure 6-3. A lane showing the largest utility is chosen as the optimal lane. The speed utility of each lane l, $U_{i,l}(t)$, is defined as

$$U_{i,l}(t) = \left[\mu \cdot v_{i,l}^{P}(t) + (1-\mu) \cdot v_{i,l}^{S}\left(s_{i,l}(t)\right)\right] \cdot f_r \tag{6.1}$$

where, $v_{i,l}^{P}(t)$ is the prospective speed of a CV_i if it decides to travel in lane l, $v_{i,l}^{S}\left(s_{i,l}(t)\right)$ is the safety speed to explain safety computed by spacing headway between the subject vehicle and a preceding vehicle in each lane l $(s_{i,l}(t))$, μ is a weighting factor of each speed component ($\mu \in [0,1]$), and f_r is the lane-changing reduction factor.

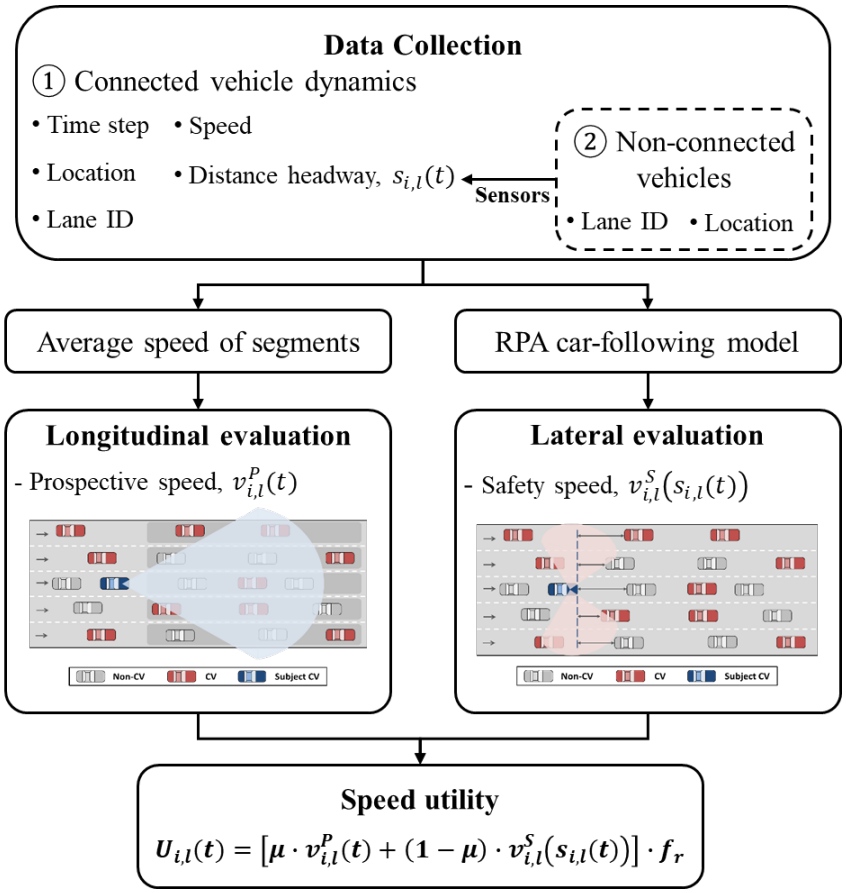

Figure 6-3. Structure of the speed utility function.

The first component, namely, the prospective speed, is a longitudinal evaluation to increase travel speed for an individual CV. This component allows the CV to choose the optimal lane to travel faster. The second component, the safety speed, was proposed based on an assumption that CVs can detect and monitor the location and speed of surrounding vehicles in all lanes via a multi-view camera or sensors. The safety speed allows the CV to take surrounding circumstances into account. Inclusion of the safety factor helps ensure OLS advisory reliability and helps provide efficient and safe travel. The final component, the lane-changing reduction factor, was proposed to minimize the number of consecutive lane changes and choose a lane change only if there are significant incentives. The speed utility including the three components—prospective speed, safety speed, and lane-changing reduction factor—was formulated as described in the following subsections.

6.3.1 Prospective Speed, $v_{i,l}^{P}(t)$

In Equation (6.1), the prospective speed, $v_{i,l}^{P}(t)$, provides the incentive to travel in lane l. Initially the OLS application was proposed in consideration of the short-range communication like V2V communication based on 802.11p DSRC, then this term was expanded in order to consider the long-range communication such as LTE or 5G cellular. A formulation for both communication environments is described as below.

1) Prospective speed based on the short-range communication environment, $v_{i,l}^{P\_SR}(t)$

The prospective speed based on the short-range communication $v_{i,l}^{P\_SR}(t)$ consists of a weighted average speed $\overline{u_l}$ and an anticipated average speed term, $\Delta u_l(\Delta\rho_l^*)$, as

$$v_{i,l}^{P\_SR}(t) = (\overline{u_l} + \Delta u_l(\Delta\rho_l^*)), \quad \forall\, l = 1, \cdots, L \tag{6.2}$$

where $\Delta\rho_l^*$ indicates the change in the lane density.

The weighted average speed of downstream CVs in each lane l, as defined in Equation (6.3), is calculated using the speed profile of downstream CVs within the transmission radius (R) of V2V communication (i.e., the V2V communication range for the collection of downstream CV data). The weighted average speed with normalized weights is one of the main factors for measuring lane performance and computes the expected driving speed in each lane. As defined in Equation (6.4), the weight θ_l^j is determined by the distance, $d_l^{i,j}$, between the subject CV_i and the CV vehicle j in each lane l that transmitted the data. The weight indicates that the contribution of data transmitted from closer vehicles is more important (or practical) to the estimate of the prospective speed than data of farther vehicles, as illustrated in Figure 6-4.

$$\overline{u_l} = \frac{\sum_{j=1}^{N_l} \theta_l^j v_l^j}{\sum_{j=1}^{N_l} \theta_l^j}, \qquad l = 1, 2, \cdots, L \tag{6.3}$$

$$\theta_l^j = 1 - \left(\frac{d_l^{i,j}}{R}\right)^2 \tag{6.4}$$

where j and N_l are the index of CVs in lane l and the total number of CVs downstream within the V2V communication range in lane l, respectively; and v_l^j is the speed of the CV j in lane l.

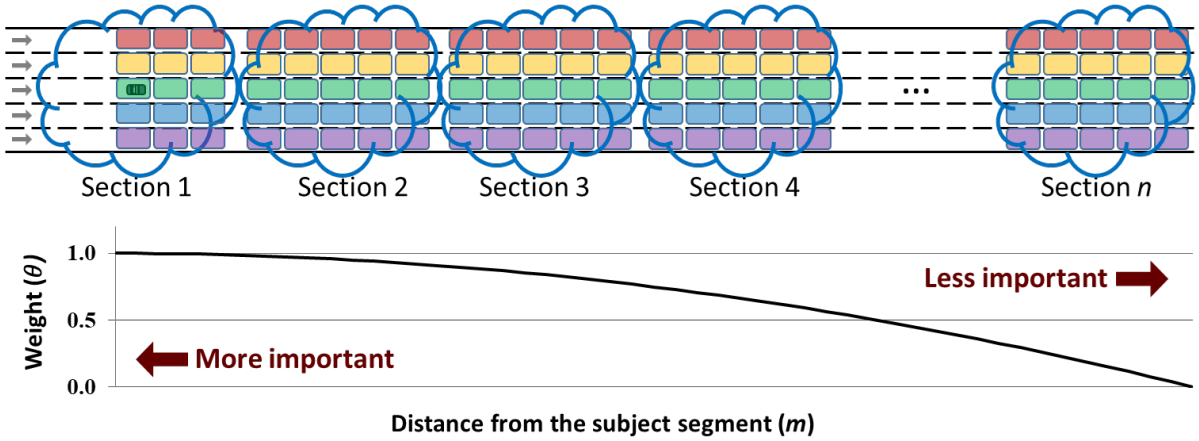

Figure 6-4. Weight factor (θ_l^j) value by distance for short-range-based OLS algorithm.

Using the weighted average speed based on real-time data collected on roadways illustrates one of the benefits that are achieved from CV technology. Tian et al. used the minimum speed and average speed of each lane as measurement of the current lane performance for the optimal lane selection [94]. However, considering only the current speed would result in most CVs choosing the identical lane when a lane shows a distinctly faster speed. This would cause excessive lane changes into the same lane, thereby decreasing the overall utility. As a result, real lane performance will be considerably different from the anticipated lane speed. To avoid this problem, an anticipated average speed term, $\Delta u_l(\Delta\rho_l^*)$, that describes the change in the lane density is simultaneously considered with the prospective speed as a correction to the estimated speed:

$$\Delta u_l(\Delta\rho_l^*) = u_l\left(\rho_l^*(t+\delta t)\right) - u_l\left(\rho_l^*(t)\right), \tag{6.5}$$

$$\rho_l{}^*(t) = \frac{N_l(t)}{R} \times \frac{1}{MPR}, \tag{6.6}$$

$$\rho_l{}^*(t+\delta t) = \frac{N_l{}^*(t+\delta t)}{R} \times \frac{1}{MPR} \tag{6.7}$$

where $N_l^*(t+\delta t)$, as shown in Figure 6-5, is the estimated number of CVs in lane l at time $t+\delta t$ $(= N_l(t) + q_l^{in} - q_l^{out})$ and *MPR* denotes market penetration rate.

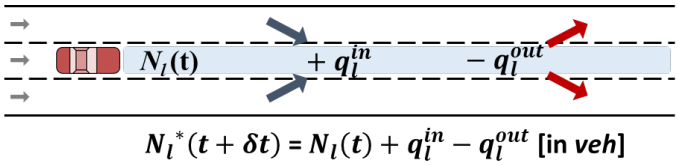

Figure 6-5. The estimated number of CVs in lane l at time $t+\delta t$.

This term is based on an assumption that CVs can share their target lane information through V2V communication. This means that a CV takes the lane selection of the other CVs downstream into consideration when computing their lane performance. This allows the selection be affected by changes in the traffic density, as seen in Figure 6-6. In addition, the traffic flow merging onto the freeway via an on-ramp is also considered as entering traffic flow for the rightmost lane. Consequently, the speed correction considering the density change is calculated using Equation (6.5). To estimate the traffic density of each lane at the current time t, the current number of CVs, $N_l(t)$, is considered. For the estimated density at time $t+\delta t$, in addition, $N_l(t)$ and the expected variation in the CV count, i.e., summation of entering vehicle count (q_l^{in}) and subtraction of exiting vehicle count (q_l^{out}) within the communication range R in the corresponding lane l, are simultaneously considered. As illustrated in Figure 6-6, correction of the estimated speed, $\Delta u_l(\Delta\rho_l^*)$, is estimated by a macroscopic speed-density relationship. This study uses the speed-density relationship in the steady-state traffic stream model that was proposed by Van Aerde (1995) and Van Aerde and Rakha (1995), which combines the Pipes and Greenshields models into a single- regime model as defined in Equation (6.8) [67, 68]:

$$k = \frac{1}{c_1 + \frac{c_2}{u_f - u} + c_3 u}. \tag{6.8}$$

The model coefficients can be computed as

$$c_1 = \frac{v_f}{k_j {v_c}^2}\left(2v_c - v_f\right), \tag{6.9a}$$

$$c_2 = \frac{v_f}{k_j {v_c}^2}\left(v_f - v_c\right)^2, \tag{6.9b}$$

$$c_3 = \frac{1}{q_c} - \frac{v_f}{k_j {v_c}^2} \tag{6.9c}$$

where v_f, k_j, v_c, and q_c indicate the free-flow speed, jam density, speed-at-capacity, and saturation flow rate.

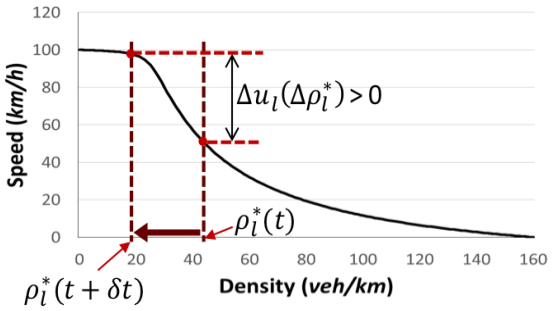

Figure 6-6. Correction of the estimated speed in speed-density relationship.

2) Prospective speed based on the long-range communication environment, $v_{i,l}^P(t)$

The prospective speed, $v_{i,l}^P(t)$, as defined in Equation (6.10), is the weighted average value of downstream segments' speed in each lane l. As description in section 6.2, speed of downstream segment k in lane l, $\overline{v_{k,l}(t)}$, is the average speed of aggregated CVs. In this work, the weight for segment k in each lane l (i.e., $\theta_{k,l}$) was always constant as 1.0, as illustrated in Figure 6-7. It causes that a CV which has an enough gap enables to change a lane for in order to avoid downstream congestion even if the CV is located far from the congestion area. If the weight by distance is considered, in contrast, only CVs near the congestion area would be induced to change a lane, but it is hard to follow the optimal lane advisory due to small spacing in high demand scenario. Because of consideration regarding the safety speed, in other words, CVs cannot choose the other lane if there is an insufficient gap to change lanes even if a lane change is highly recommended to efficiently traverse the congested area. To increase efficiency of this application, therefore, a CV even located far from the congested area has a chance to change lanes using the uniform weight. This ensures that farther downstream data be considered as important as closer data.

$$v_{i,l}^P(t) = \frac{\sum_{k=0}^{C} \theta_{k,l}\, \overline{v_{k,l}(t)}}{\sum_{k=0}^{C} \theta_{k,l}}, \qquad l = 1, 2, \cdots, L \tag{6.10}$$

where k and C are the index of segments and the total number of segments in downstream links that the OLS operates. In addition, $\theta_{k,l}$ and $\overline{v_{k,l}(t)}$ are the weight of each segment k and the average speed of the segment k in lane l.

Moreover, this study ignored a correction of the prospective speed which considers the predicted density change, as applied for the OLS algorithm based on the short-range communication, as it is not practical to apply into when considering communication technologies. In detail, this term had been intended to remove the possibility that all CVs choose the same lane when they consider only the average speed of CVs within a short-communication range. To make this term essential, two assumptions must be made: 1) that the CVs can share their OLS information and 2) that drivers always follow this advisory. In addition, there is a risk that

estimated density may cause significant error at low MPRs. Accordingly, this study only considers the average of speeds of downstream segments.

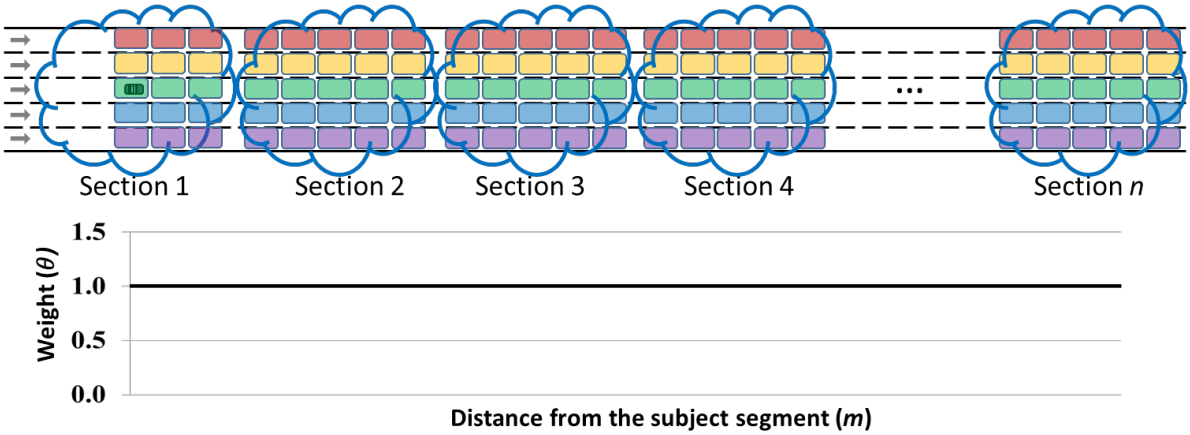

Figure 6-7. Weight factor ($\theta_{k,l}$) value by distance for long-range-based OLS algorithm.

6.3.2 Safety Speed, $v_{i,l}^{S}(s_{i,l}(t))$

The safety speed is calculated by spacing headway between the closest preceding vehicle and the subject CV_i, $s_{i,l}(t)$, in each lane l. To estimate the safety speed, this study used the RPA car-following model, which was first developed in [66]. It consists of the following three components: steady-state traffic stream behavior, collision avoidance, and vehicle dynamics [54]. Performance of the RPA car-following model was validated against naturalistic driving data [54].

First, the steady-state traffic stream model based on the Van Aerde's steady state car-following model [67, 68] is used as

$$s_i(t) = c_1 + c_3 \cdot v_i(t) + \frac{c_2}{v_f - v_i(t)} \tag{6.11}$$

where $v_i(t)$ signifies the speed of the vehicle i and time t, and $s_i(t)$ represents the spacing of the vehicle i at time t (i.e., the distance between the vehicle i and the vehicle ahead of it $i-1$).

The second component of the RPA model, collision avoidance, was modeled to avoid incidents at non-steady state conditions. The estimated speed by collision avoidance is defined as

$$v_{i,CA}(t) = \sqrt{v_{i-1}(t)^2 + 2a_{min}(s_i(t) - s_j)} \tag{6.12}$$

where a_{min} and s_j denote the minimum acceleration (i.e., maximum deceleration) and the jam spacing, respectively.

The last component, vehicle dynamics, is the acceleration based on the realistic acceleration capability of the vehicle, as described in Equation (6.13):

$$a_i(t) = \frac{F_i(t) - R_i(t)}{w_i} \tag{6.13}$$

where $a_i(t)$ is the acceleration of the vehicle i at time t, w_i is the mass of the vehicle i, and $F_i(t)$ and $R_i(t)$ represent the total tractive and resistive forces at time t, respectively. Both $F_i(t)$ and $R_i(t)$ are functions of the vehicle speed $v_i(t)$. The resistive force is proportional to the air resistance, grade resistance, and rolling resistance. The detailed formulas of the two forces are described in [54].

6.3.3 Lane-changing Reduction Factor, f_r

For optimal lane allocation in consideration of traffic flow, it is better for two CVs to make one lane change each rather than for one CV to make two lane changes. To avoid driver stress created by multiple lane-change requests, the driver's inertia factor should be considered to minimize the number of consecutive lane changes when there is feasible incentive. For the lane change reduction factor, f_r, the lower value is applied when a larger number of lane changes are required to reach the target lane. To discount the speed utility when multiple lane changes are required, as formulated in Equation (6.1), the utility is multiplied by the lane-changing reduction factor (f_r) which is proportional to the difference between the target lane and the index of the current lane, $|l - l_i(t)|$, as described in Equation (6.14):

$$f_r = 1 - \gamma|l - l_i(t)|, \qquad l = 1, 2, \cdots, L \tag{6.14}$$

where γ and $l_i(t)$ are the discount rate per lane change and the index of the current lane of CV_i at time t, respectively.

6.4 Sensitivity Analysis

In this section, a sensitivity analysis is presented to observe how changes of the factors related to the proposed OLS application impact the simulation results. For the analysis, connected environment was supposed as the advanced connected transportation environment, i.e., the long-range communication. The speed utility formulated for the long-range communication, therefore, was used here. The analysis was conducted with a microscopic traffic simulator, INTEGRATION

[89]. The analysis was conducted by varying several input factors: a) origin-destination (O-D) table, b) MPRs, c) OLS time step, d) ratio for prospective speed utility, f_s, and e) length of segment in cloud.

6.4.1 Integration of the OLS algorithm into the INTEGRATION

The proposed OLS algorithm was incorporated in the INTEGRATION software. In order to describe the connected transportation systems, the simulator identifies all CVs in each lane which have location, lane, speed, spacing data. At the OLS operation time t_{OLS}, they can transmit their data via the long-range communication. Then, the segment average speed is computed based on CVs' data. Each CV searches the optimal lane using the speed utility. The lane with the greatest speed utility is chosen as the optimal lane, $l_i^*(t)$; i.e.,

$$l_i^*(t) = \arg \max_{l \in \{1,2,\cdots L\}} \{U_{i,l}(t)\}. \tag{6.15}$$

The OLS application is executed for an individual CV with time interval, i.e., this lane selection process is repeated each time interval Δt. To execute the OLS application at each OLS execution time step, INTEGRATION defines the object group excluding CVs which have decided the optimal lane at previous OLS execution time steps. A CV, which selected previously the optimal lane, skips the OLS algorithm process during relaxation time, e.g., five seconds, and tries to reach the target lane. If there is sufficient spacing, the CV changes a lane to follow OLS advisory.

6.4.2 Simulation Setting for Sensitivity Analysis

Simulation experiments were conducted by comparing the connected transportation system using the OLS application and the traditional non-connected transportation system. In addition, a freeway segment, including one merging section, was modeled on INTEGRATION for sensitivity analysis, as illustrated in Figure 6-8. The length of the freeway mainline was 3.5 km and the 300 m acceleration lane was located 2.5 km downstream of the beginning of the network. The details of the simulation settings for the sensitivity analysis are described as follows.

- Link properties for the freeway mainline: q_c was 2,400 $veh/h/lane$. k_j was 160 $veh/km/lane$. v_f and v_c were 100 km/h and 80 km/h, respectively.
- Link properties for the on-ramp: q_c was 1,800 $veh/h/lane$. k_j was 160 $veh/km/lane$. v_f and v_c were 50 km/h and 40 km/h, respectively.
- There were two origin-destination (O-D) pairs—(1–3) and (2–3), as denoted using the node number in Figure 6-8—classified by entering the simulation network through the mainline and on-ramp, respectively.

- All vehicles were modeled as personal vehicles and the properties of vehicle dynamics were the basic properties set in INTEGRATION.
- The OLS application was applied on the upstream link of the merging section (i.e., OLS control region) as shown in Figure 6-8 and time interval Δt was 0.5 seconds.
- In addition, μ was 0.6 and the lane-changing reduction discount rate (γ) was 2% per lane change. Both were chosen as the optimal value via a feasibility study.
- A base segment length to aggregate lane performance data was set at 100 meters. The wireless communication was always successful and all CVs transmitted data with 0% noise.
- Simulation time for each scenario was an hour and 10 minutes, including 10 minutes warming-up time. In addition, this sensitivity analysis was conducted 10 times with various random seeds for each scenario.

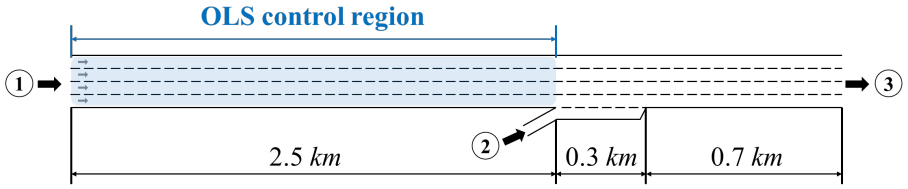

Figure 6-8. Simulation network for sensitivity analysis.

6.4.3 Sensitivity Analysis Results

1) Simulation analysis on traffic demands

As the first critical factor, a sensitivity analysis was conducted to understand the performance of the application at various traffic demand levels. The simulation settings are described in subsection B. In this analysis, the MPR of CVs was 100% and freeway traffic demand levels and the on-ramp traffic varied as follows.

- The volume-to-capacity (V/C) ratio (i.e. volume divided by capacity) of the freeway mainline traffic (1–3) varied from 0.6 to 0.9 with increment of 0.1. The much lower traffic demand cases were not considered because the OLS algorithm is not required in uncongested flow.
- The V/C ratio of the merging traffic via on-ramp (2–3) was 0.2, 0.4, 0.6, 0.8, and 1.0.
- Therefore, the total number of O-D sets, considering various demand levels for both traffic conditions, was 20 as summarized in Table 6-1.

According to the defined demand levels, the V/C ratios from both traffic conditions combined ranged from 0.64 to 1.09 against the freeway mainline capacity, as shown in Table 6-1. This study compared them with the level of service (LOS) criteria for basic freeway segments in highway capacity manual (HCM) 2010 [95]. Although the network for the sensitivity analysis is not the

basic freeway segments defined in HCM, this criteria was taken to simply show the magnitude of the combined traffic flows entering via freeway mainline and on-ramp. According to the manual, the maximum V/C for LOS C, D, and E at $v_f = 65\ mi/h$ is 0.71, 0.89, and 1.00. When the V/C is over 1.00, this condition would be classified as LOS F. As defined in Table 6-1, demand sets vary from LOS C to LOS F.

Table 6-1. Combined Demand (in veh/h) in Each Case for Sensitivity Analysis

Demand cases		On-ramp V/C				
		0.2	0.4	0.6	0.8	1.0
Mainline V/C	0.6	6,120 (0.64, C)	6,480 (0.68, C)	6,840 (0.71, C)	7,200 (0.75, D)	7,560 (0.79, D)
	0.7	7,080 (0.74, D)	7,440 (0.78, D)	7,800 (0.81, D)	8,160 (0.85, D)	8,520 (0.89, E)
	0.8	8,040 (0.84, D)	8,400 (0.88, D)	8,760 (0.91, E)	9,120 (0.95, E)	9,480 (0.99, E)
	0.9	9,000 (0.94, E)	9,360 (0.98, E)	9,720 (1.01, F)	10,080 (1.05, F)	10,440 (1.09, F)

Note: Number and alphabet in parentheses indicates the volume/capacity (V/C) ratio and the expected LOS, respectively.

For the sensitivity analysis, average of total delay of CVs was used as measure of effectiveness. Figure 6-9 illustrates the simulation results. At the mainline v/c ratio of 0.6 to 0.8, as shown in Figure 6-9(a) to 6-9(c), the OLS application was effective where the merging traffic was greater. The demand cases with a total V/C ratio between 0.75 and 0.99, with the exception of two cases—the total V/C ratio of 0.78 (the mainline V/C ratio of 0.7 and the on-ramp V/C ratio of 0.4) and of 0.84 (the mainline V/C ratio of 0.8 and the on-ramp V/C ratio of 0.2)—verified that the OLS application in the connected transportation system resulted in better network performance compared to the traditional system. Lastly, in high demand cases where the demand was over freeway capacity, the OLS did not work efficiently, as shown in Figure 6-9(d). When the demand level was over capacity due to severe traffic congestion, network performance was not improved even though the OLS application was active. In summary, if there is a quite amount of merging traffic and the total demand is not over the roadway capacity, the OLS application helps provide beneficial lane-changing advice and mitigates traffic congestion caused by merging traffic.

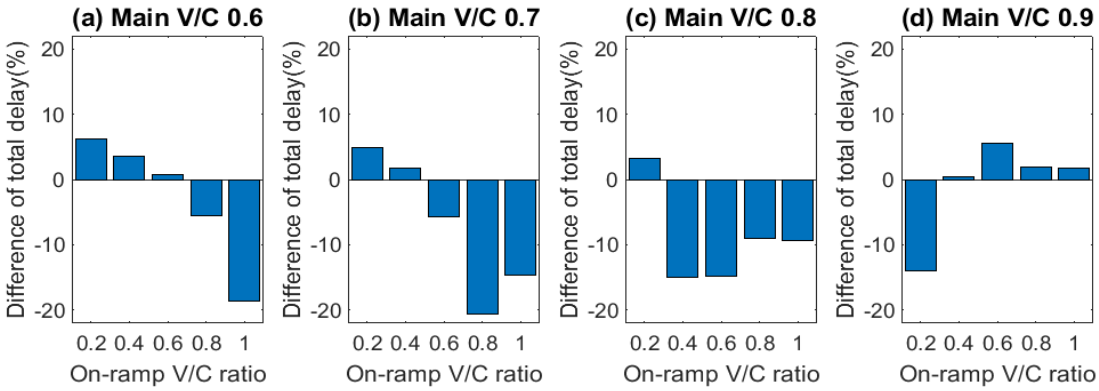

Figure 6-9. Difference of average total delay between the OLS-enabled CV scenario and the non-CV scenario in each demand set.

To demonstrate efficiency of the OLS algorithm, lane density in the non-connected and the connected transportation system was compared. Figure 6-10 was prepared to show the density of each lane on time-space diagram at the mainline V/C ratio of 0.8 and the on-ramp V/C ratio of 0.8. Figure 6-10(a) and 6-10(b) illustrates lane density in the traditional transportation system and connected transportation system with the OLS application, respectively. Lane 1 is the closest lane to the median and lane 4 is the rightmost lane. In both figures it is observed that turbulence occurred near merging section because of high demand. It caused traffic congestion, then backward forming shock wave is observed. Lane density was the highest in the rightmost lane (i.e., lane 4) and as going toward the lane 1 the density decreased. In comparison between two figures, however, there is a remarkable difference that the lane allocation performance by applying the OLS algorithm in the connected system is better that in the traditional transportation system. This advantage is described below.

Figure 6-11 shows the difference in lane density (i.e., $\rho_{CV} - \rho_{Non-CV}$). Here, ρ_{CV} is the density in the traditional transportation system (as shown in Figure 6-10(a)) and ρ_{Non-CV} is the density in the connected system with OLS control (as shown in Figure 6-10(b)). As the results illustrating comparison results between both systems, the red on the surface graph (in Figure 6-11) at a certain simulation time and location indicates an increased density, whereas a lower density in the connected systems is indicated where the surface is blue.

As Figure 6-11 shows, introducing the OLS application into the connected transportation systems resulted in a significant benefit in lane allocation. The density in lane 1 to 3 increased when using the OLS application, while the density in lane 4 decreased. In addition, the queue length was shorter in the connected systems as compared to the traditional systems. The distinct blue color surface in lanes 3 and 4 indicates a decrease in lane density, and therefore a shorter queue length. Hence, the lane density results indicate that the OLS application distributed traffic more evenly across lanes.

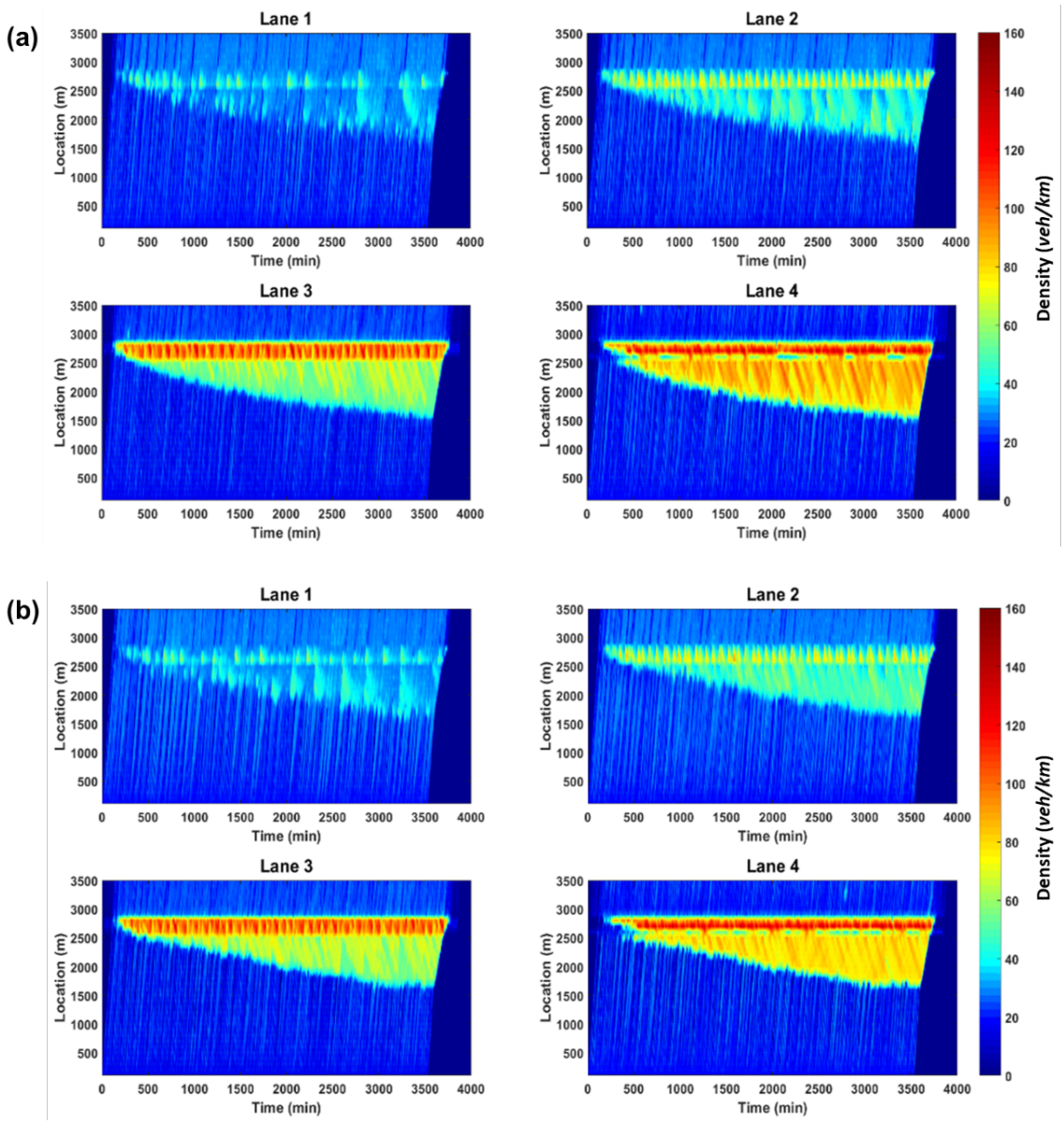

Figure 6-10. Density in each lane between (a) the non-CV scenario and (b) the OLS-enabled CV scenario.

This difference in lane density reveals that CVs changed a lane by following OLS-provided optimal lane advisories, making a lane change toward the left before arriving at the merging section to avoid congestion. Thus, the developed OLS application based on long-range wireless communication is shown to be effective in making travel more efficient in the connected system. Traffic management performance is therefore better in the CV system utilizing the OLS application.

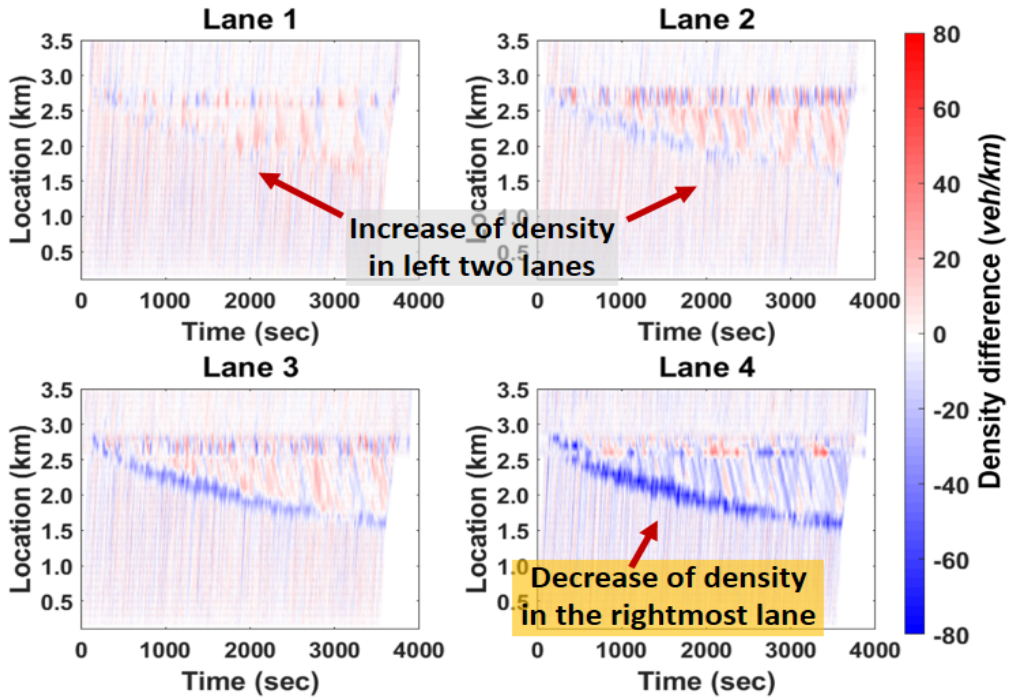

Note: Lane 1 and lane 4 indicate the closest lane to the median and the rightmost lane, respectively.

Figure 6-11. Density difference in each lane between the OLS-enabled CV scenario and the non-CV scenario.

2) Simulation analysis on market penetration rates (MPRs)

In this subsection, the impact of CV MPRs is assessed. For simulation, there were two demand sets. In the first demand set, the V/C ratios of the freeway mainline and ramp were 0.8 and 0.6, respectively. The second set used the V/C ratio of 0.8 for both O-D pairs entering through the mainline and ramp. Simulation cases with OLS control were set with MPRs from 0 % to 100 %. The other related parameter values are described in previous simulation setting.

Figure 6-12 shows total delay according to vehicle type in two demand sets. As the figure shows, CVs using OLS had better travel performance than traditional vehicles. In demand set 1, total system delay decreased with an increase in MPR. In a low MPR scenario, the difference in total delay between vehicle types was bigger. In demand set 2, on the other hand, total system delay in 20 % and 40 % MPR scenarios was higher than in the traditional vehicle system (i.e., 0 % MPR scenario). The OLS application leads CVs to travel faster than non-CVs by providing the appropriate optimal lane advisory. Since the v/c ratio of demand set 2 is close to capacity, however, a lane change prompted by the OLS advisory causes turbulence, which produces traffic congestion.

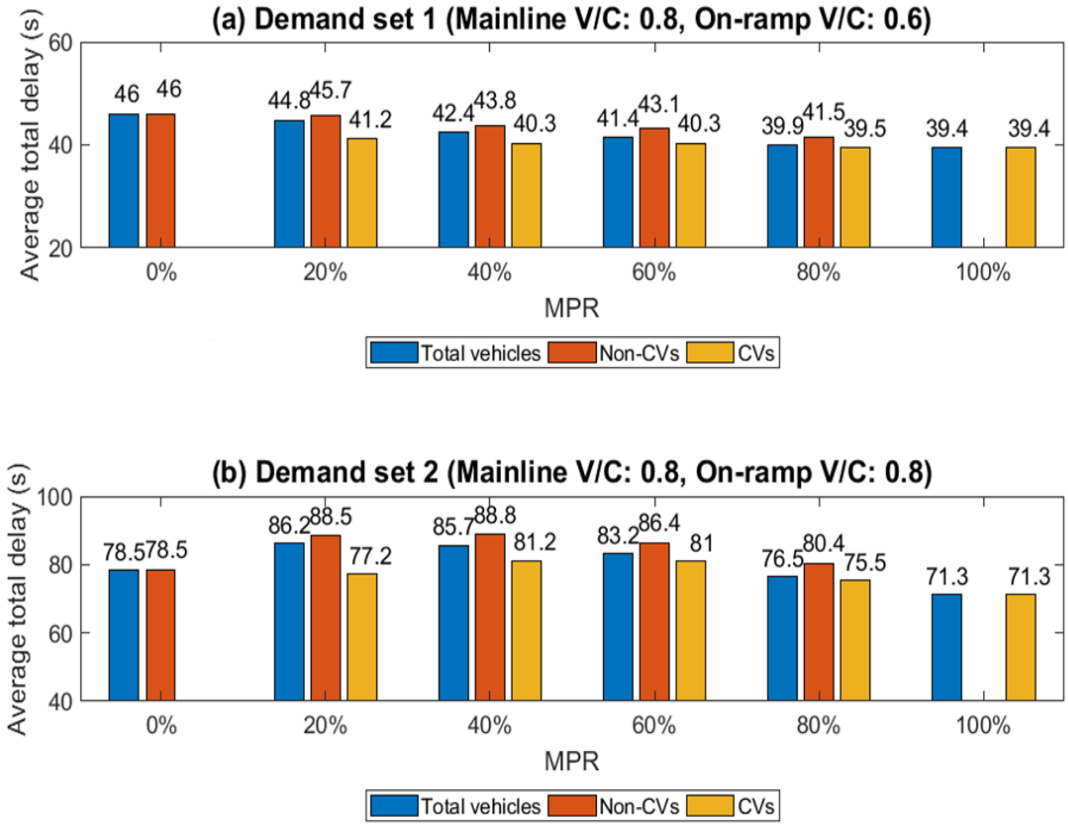

Figure 6-12. Comparison of total delay by MPRs.

3) Simulation analysis on OLS time step

This study additionally analyzes the impact of OLS time step which indicates how frequently the OLS algorithm is executed. Demand sets used here were same as the sets in analysis of MPR variation stated in previous subsection and for this test the MPR was 100 %. Table 6-2 shows total delay in various OLS time step with the range of 0.1 to 5.0 seconds. Other simulation parameters related to the OLS used here were same as defined in simulation setting.

In both demand sets the OLS algorithm demonstrates its performance improving traffic flow in comparison with the traditional transportation system which is not connected between vehicles. As the OLS is operated more frequently, the total delay decreased. It means that the OLS improves the transportation system performance when the OLS is often operated. In the demand set 1, i.e., mainline and on-ramp V/C were 0.8 and 0.6 respectively, total system delay decreased by 16.7 % and 14.9 % in scenario with frequency of 0.1 and 0.5 seconds, respectively. Other scenarios also show improvement on total delay even though the OLS application is operated every 5.0 seconds. In the second demand set which the V/C of both traffic streams are 0.8, total delay is also reduced when the OLS is executed. Only difference is that total delay in the 0.1 seconds frequency scenario

is slightly higher than that in the 0.5 seconds frequency scenario. The reason is that the OLS induces more lane changes by providing the optimal target information.

Table 6-2. OLS time step sensitivity on average delay

Scenarios / Demand set	Traditional system	Connected transportation system with OLS time step (s)				
		0.1 s	0.5 s	1.0 s	2.0 s	5.0 s
Demand set 1 (Mainline V/C: 0.8, Ramp V/C: 0.6)	45.97	38.27 (-16.7 %)	39.13 (-14.9 %)	41.36 (-10.0 %)	41.86 (-8.9 %)	42.87 (-6.7 %)
Demand set 2 (Mainline V/C: 0.8, Ramp V/C: 0.8)	78.45	72.63 (-7.4 %)	71.26 (-9.2 %)	73.47 (-6.3 %)	75.57 (-3.7 %)	76.31 (-2.7 %)

4) Simulation analysis on ratio for prospective speed utility (f_s)

One of critical parameter related to efficiency of the OLS is a ratio μ for the prospective speed utility, i.e., a weighting factor of each speed component. Due to direct impact on the utility it affects the utility to decide the target lane. To test the impact of this parameter, a range between 0.2 to 1.0 with increment of 0.2 was used. As described in utility formulation, the ratio of 1.0 means that the connected vehicle provides the optimal lane information selected by consideration of instant lane performance only. When this ratio is 1.0, in other words, the vehicle chooses the target lane to travel faster, but not consider the spacing with the preceding vehicle in each lane.

In the results, the ratio for prospective speed component has an important role on travel performance of the OLS in both demand sets. When the ratio is 1.0, in both demand sets the total delay extremely increased as shown in Table 6-3. Providing the optimal lane by the lane performance only induces that a driver of the CV tries to change a lane even if there is not sufficient spacing. It causes turbulence by forming a severe shockwave after forced lane-changing. Consideration of safety speed, therefore, is essential in order to avoid inefficient lane change. A driver of the CV should receive an advisory based on when there is sufficient gap to change into the target lane. Consequently, both prospective lane speed ($v_{i,l}^{P}(t)$) and speed based on headway ($s_{i,l}(t)$) should be considered simultaneously to choose the optimal lane.

In addition, when the ratio is less than 1.0, in the first demand set, the total delay in the connected transportation system with the OLS application is less than that of the traditional transportation system. In the second demand set, using the OLS application at $\mu < 0.8$ shows better performance in lane allocation even though the OLS using $\mu = 0.8$ in the connected system makes traffic flows worse in comparison to the traditional system. As the results, a scenario using the ratio of 0.6 in both demand sets shows the minimum delay during simulation. Thus, $\mu = 0.6$ is proposed as the optimal value for the OLS algorithm here.

Table 6-3. Ratio μ sensitivity on average delay

Scenarios / Demand set	Traditional system	Connected transportation system with ratio for prospective speed utility				
		0.1 s	0.5 s	1.0 s	2.0 s	5.0 s
Demand set 1 (Mainline V/C: 0.8, Ramp V/C: 0.6)	45.97	43.73 (-4.9 %)	41.17 (-10.4 %)	39.13 (-14.9 %)	39.78 (-13.5 %)	124.38 (170.6 %)
Demand set 2 (Mainline V/C: 0.8, Ramp V/C: 0.8)	78.45	76.31 (-2.7 %)	73.63 (-6.1 %)	71.26 (-9.2 %)	85.15 (8.5 %)	168.17 (114.4 %)

5) Simulation analysis on length of segment in cloud

Segment length indicates the data aggregation size to present instantaneous driving condition in each lane. As the results summarized in Table 6-4, dividing a cloud into more segments, i.e., using shorter segment length, showed smaller delay than using longer segments in all demand sets. When the segment length is 100 m, the average delay decreases by about 15 % and 9 % compared to the traditional system in the demand set 1 and 2, respectively. It implies that that using the OLS with the speed utility based on the short-length segment can provide the beneficial advice to the driver. If the OLS uses the traffic data aggregated in a short range of sections, however, the required number of instantaneous data would be increased. Consequently, using short length of the segment in utility calculation is recommended if long-range communication technology can support to transmit a huge amount of data without latency.

Table 6-4. Cloud segment length sensitivity on average delay

Scenarios / Demand set	Traditional system	Connected transportation system with length of segments in cloud		
		100 m	300 m	500 m
Demand set 1 (Mainline V/C: 0.8, Ramp V/C: 0.6)	45.97	39.13 (-14.9 %)	42.23 (-8.1 %)	43.42 (-5.5 %)
Demand set 2 (Mainline V/C: 0.8, Ramp V/C: 0.8)	78.45	71.26 (-9.2 %)	74.81 (-4.6 %)	75.87 (-3.3 %)

6.5 Case Study: I-66

In order to prove the OLS application's efficiency, it was evaluated in a real roadway network. Interstate 66 (I-66) and Virginia state route (SR) 267 located in northern VA, USA, as shown in Figure 6-13, were selected as case study roads. The segment along I-66 is about 6-miles long and

contains several on- and off-ramps. For the case study, this study used O-D data estimated in [96] to evaluate the developed OLS application. According to [96], observation data were collected between 2:00 p.m. and 8:00 p.m. on three consecutive days from March 12 to March 14, 2013, by five trailers installed on the test bed, as shown in Figure 6-14. The number of lanes changes from 4 at the Trailer 3 to 2 at the Trailer 4, and the average travel time from the entrance of I-66 or SR-267 to the exit of I-66 is about 10 minutes [96]. The O-D data were estimated by QueensOD [97]. Average error percentage on flow comparison between QueensOD and field observations every observed day is less than 1.5% error [96]. The total number of vehicles entering the simulation network for six hours was estimated as 31,105.

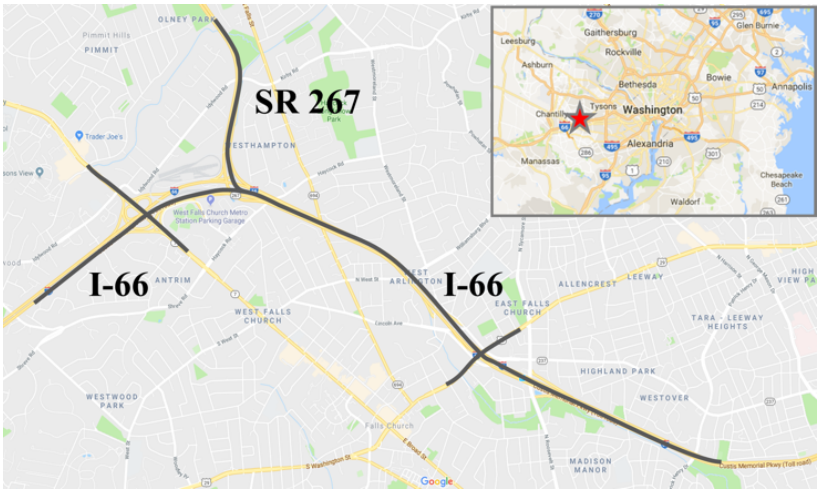

Figure 6-13. Network for case study: I-66 and Virginia SR 267 (source: [98]).

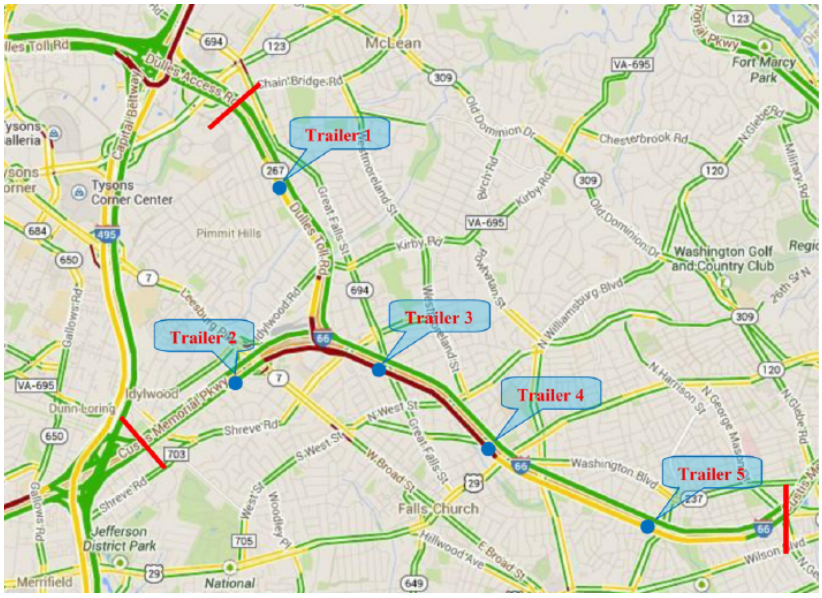

Figure 6-14. Location of trailers for data collection (in [96]).

Simulations were conducted for both a traditional transportation system and a connected transportation system in which CVs used the OLS application. In the OLS-enabled case, CVs suggested the optimal lane to a driver traveling the I-66 and SR 267 mainline. The case study was conducted with various MPRs of 0 %, 20 %, 40 %, 60 %, 80 %, and 100 %, and ran a simulation for each scenario 10 times with various random seeds. The other related parameter values are used same values described in simulation setting for the sensitivity analysis.

Prior to discussion about simulation results, this study provides simulation screenshots captured at every hour for total three hours, as shown in Table 6-5 below. There are two scenarios: a scenario in the traditional transportation system without using the OLS and a scenario using the OLS with MPR of 100 % in the connected transportation system. When simulation time is 3,600 seconds, congestion forms on I-66 eastbound in the traditional transportation system while there is no congestion in the connected transportation system. After additional an hour, congestion trend between the two cases is quite different at 7,200 seconds. Queue length on I-66, as shown in red dotted circle, in the traditional transportation system is longer than that in the connected system. When simulation time is 10,800 sec, I-66 is over-saturated and it affects traffic on SR 267 in the traditional transportation system. In the connected transportation system, congestion on I-66 is also observed, but there is no queue on SR 267. In conclusion, OLS application, which is an in-vehicle system application, is expected to contribute distinguished performance in traffic flow.

Simulation results are summarized in Table 6-6. System travel times decreased as MPRs of CV increased. At a MPR of 100%, travel time decreased by 16.6% compared to the traditional system with a MPR of 0%. As the results of this case study, it is expected that a traveler can travel faster by 106 seconds if the OLS application is activated. In addition, CVs' travel time is lower than that of traditional vehicles in all scenarios. This reveals that the OLS application is able to reduce travel time and provide a better driving experience. In conclusion, the OLS application based on advanced wireless communication will contribute to improve not only travel performance of individual vehicles but also entire network.

Table 6-5. Simulation screenshots in case study

Simulation time	Traditional transportation system	100% OLS-enabled in connected transportation system
3,600 seconds (1 hour)	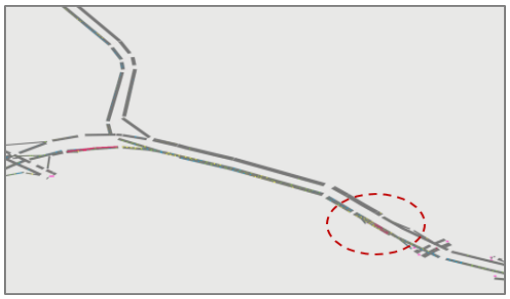	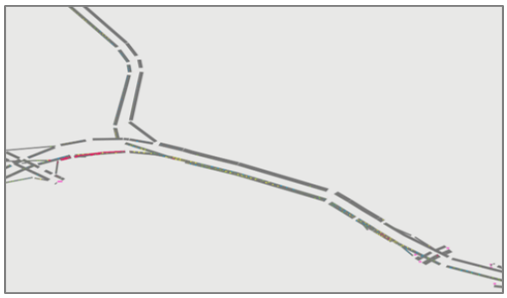
7,200 seconds (2 hour)	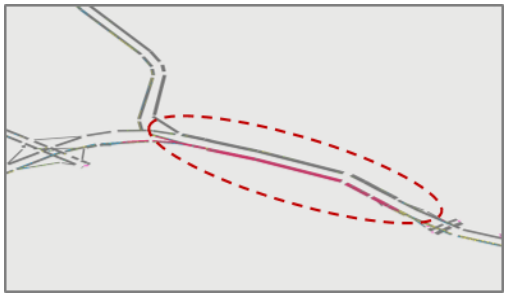	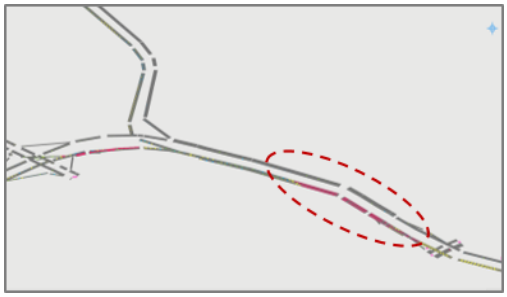
10,800 seconds (3 hour)	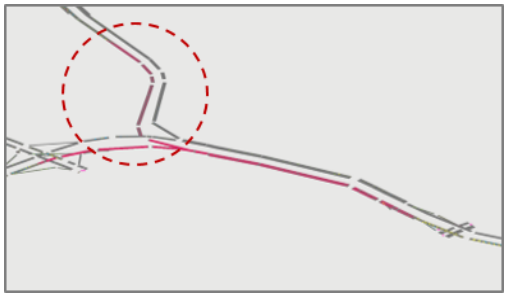	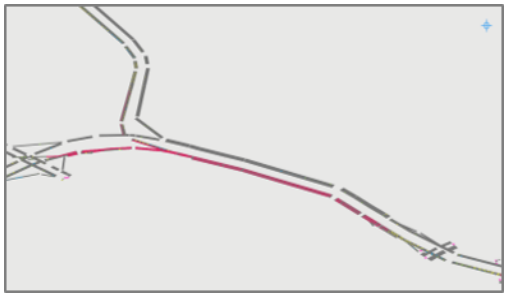

Table 6-6. Average travel time (in seconds) comparison results in case study

Index	MPRs					
	0 %	20 %	40 %	60 %	80 %	100 %
CVs	-	599.04	584.41	566.63	549.26	535.41
Non-CVs	641.98	605.97	601.92	581.67	543.97	-
Average	641.98	604.57 (-5.8%)[a]	594.91 (-7.3%)	572.64 (-10.8%)	548.21 (-14.6%)	535.41 (-16.6%)

[a] Number in parentheses indicates average travel time difference as comparison to the 0% MPR case.

Chapter 7. Conclusions and Recommendations

This chapter presents the conclusion found in the dissertation. Furthermore, the recommendations for future research are provided in terms of theoretical improvements and practical applications.

7.1 Main Findings and Conclusions

Drivers' behavior has a large effect on the safety and throughput of the transportation system. At a freeway merge section, traffic conflicts between merging and through vehicles induce shockwaves, which results in congestion. This dissertation, therefore, addressed on enhancing freeway merge section operations based on vehicle connectivity. The study initially focused on modeling human drivers' decision-making in merging situations thoroughly and accurately. To depict realistic drivers' decision-making process, non-cooperative behaviors for merging maneuvers was modeled based on a game theoretical approach. The developed model can be used to analyze traffic flow in a microscopic traffic simulator, and also be applied into the driving algorithm of an AV which substitutes a human driver. In addition, the cooperative maneuver planning was proposed based on a cooperative merging game, considering CAVs environment. Lastly, the optimal lane selection algorithm was also proposed to improve lane allocation by taking downstream traffic condition into account. In this study, each chapter demonstrate the following findings.

In Chapter 3, human drivers' decision-making process at a merging section on a freeway was modeled using a game theoretical approach. To describe the drivers' cooperative or non-cooperative decisions, the stage game structure for merging maneuvers was designed, then formulated payoff functions through three-phase development in order to not only enhance model performance but also eliminate the defects. Moreover, this study introduced the repeated game approach for practical decision-making conducted periodically and repeatedly until the merging vehicle enter onto the freeway mainline.

The research presented in Chapter 4 evaluated the developed game models using the NGSIM data. As a summary of the model evaluation, all the stage game models indicated the remarkable prediction capacity, more than 75%, of merging maneuvers in model validation. Among them, the third stage game model showed the excellent performance with 86% of prediction accuracy. To provide the performance of the repeated game model, the simulation model was developed, then the simulation study was conducted. As the results, both the one-shot game and repeated game model based on the third stage game identically presented reasonable decision-making performance in cooperative merging situations. In the competitive scenario, however, this study concluded that the repeated game model showed superior performance than the one-shot game model.

In Chpater 5, this study expanded the non-cooperative game model validated in the previous chapter as the part of the cooperative maneuver planning for CAVs. To enhance network performance based on the CAV's technological benefits, this study proposed that the CAV can choose a cooperative maneuver by responding to the predicted non-cooperative behavior. The simulation model was developed and then validated by comparison with the INTEGRAION on

network performances. The simulation results proved that the cooperative maneuver planning improve network performance on a freeway merge section.

Another lane-changing application, the OLS, was proposed in consideration of the advanced long-range wireless communication, which is expected to enhance transportation systems. To decide the optimal lane for an individual CV, the speed utility function was developed for a practical use considering both driving performance and safety. The sensitivity analysis of the OLS algorithm was conducted, and the results provided that the OLS application within the connected transportation system decreased delay and travel time. The application increased efficiency at certain higher demands that cause traffic congestion, though not at conditions over capacity, by inducing lane changes to allow CVs to avoid traveling in congested areas. Through the case study on I-66 and Virginia SR 267 this study concluded that the OLS application could contribute not only to travel efficiency for individual vehicles but also to system-wide performance.

7.2 Recommendations for Future Research

Regarding the game theory model, this study focused on modeling the actual decision-making at microscopic level, while other game theory-based models focused on lane-changing execution. Human driver's decision-making is very complicated and affected by individual perception on the surroundings, driving skill, and aggressiveness, roadway design, human error, and so on. To integrate it with acceleration controller of the microscopic traffic simulator, therefore, the game model should be calibrated using the field data obtained under various traffic conditions and roadway designs. Thereafter, the game model can be used as one of the important components determining acceleration level in microscopic simulation model.

In addition, as a new transportation paradigm, the AVs have attracted and the related industries, research institutes, and world-wide governments are looking forward that they coexist with human drivers. One of important issue is whether they can make a rational decision like human-being. To solve this problem, various approaches have been applied into the AV's decision-making algorithm. Game theory is also one of famous methodologies used for development of dynamic driving strategy for AVs. Thus use of the developed game model is recommended and it can be cooperated with the Machine learning, such as the reinforcement learning algorithm, to enhance decision-making ability by getting feedback in the form of reinforcement in a dynamic environment.

In the connected transportation environment, there are many potential benefits improving safety and mobility and reducing energy use and emissions. Following this trend, many algorithms have been proposed in consideration of the wireless communications. To use these algorithms in real transportation systems, these should follows the technical standards and specification and be integrated with other relevant algorithms and the vehicle systems. Therefore, the cooperative maneuver planning in this study should be developed to be one of applicable algorithm in the CAV

environment. To demonstrate its ability, in addition, it is required to test using the state-of-the-art simulation model, which has an ability to reasonably simulate based on the future environment, under various scenarios. This recommendation is useful for the OLS algorithm proposed in this study. More experiments are needed to verify the model's performance and increase the realism of the simulation. Finally, both the proposed cooperative maneuver planning and OLS application will be a part of lane-based path planning for CAVs.

References

[1] Rahman, M., Chowdhury, M., Xie, Y., & He, Y. (2013). Review of microscopic lane-changing models and future research opportunities. *IEEE transactions on intelligent transportation systems*, *14*(4), 1942-1956.

[2] Liu, H. X., Xin, W., Adam, Z., & Ban, J. (2007). A game theoretical approach for modelling merging and yielding behaviour at freeway on-ramp sections. In *17th International Symposium on* Transportation *and Traffic Theory, London, UK*.

[3] Roncoli, C., Bekiaris-Liberis, N., & Papageorgiou, M. (2017). Lane-changing feedback control for efficient lane assignment at motorway bottlenecks. *Transportation Research Record: Journal of the Transportation Research Board*, *2625*(1), 20-31.

[4] Cambridge Systematics, Inc. (2004). *Traffic Congestion and Reliability: Linking Solutions to Problems*. Cambridge, Massachusetts. Retrieved from https://ops.fhwa.dot.gov/congestion_report_04/congestion_report.pdf

[5] Cassidy, M. J., & Bertini, R. L. (1999). Some traffic features at freeway bottlenecks. *Transportation Research Part B: Methodological*, *33*(1), 25-42. doi: 10.1016/S0191-2615(98)00023-X

[6] Bertini, R. L., & Leal, M. T. (2005). Empirical study of traffic features at a freeway lane drop. *Journal of Transportation Engineering, 131*(6), 397-407.

[7] Laval, J. A., & Daganzo, C. F. (2005). Multi-lane hybrid traffic flow model: a theory on the impacts of lane-changing maneuvers. In *Proceedings of the 84th Annual Meeting of the Transportation Research Board*., *Washington*, *District of Columbia*.

[8] Chung, K., Rudjanakanoknad, J., & Cassidy, M. J. (2007). Relation between traffic density and capacity drop at three freeway bottlenecks. *Transportation Research Part B: Methodological, 41*(1), 82-95. doi: 10.1016/j.trb.2006.02.011

[9] Moridpour, S., Sarvi, M., & Rose, G. (2010). Lane changing models: a critical review. *Transportation letters*, *2*(3), 157-173.

[10] Kesting, A., Treiber, M., & Helbing, D. (2007). General lane-changing model MOBIL for car-following models. *Transportation Research Record: Journal of the Transportation Research Board*, *1999*(1), 86-94.

[11] United States. Department of Transportation. (2016). *Federal Automated Vehicles Policy*. Washington, DC. Retrieved from https://www.transportation.gov/sites/dot.gov/files/docs/AV%20policy%20guidance%20PDF.pdf

[12] U.S. DOT. (2018). *Comprehensive management plan for automated vehicle initiatives*. Washington, DC. Retrieved from

https://www.transportation.gov/sites/dot.gov/files/docs/policy-initiatives/automated-vehicles/317351/usdot-comprehensive-management-plan-automated-vehicle-initiatives.pdf

[13] Gipps, P. G. (1986). A model for the structure of lane-changing decisions. *Transportation Research Part B: Methodological*, *20*(5), 403-414.

[14] Toledo, T., Koutsopoulos, H. N., & Ben-Akiva, M. E. (2003). Modeling integrated lane-changing behavior. *Transportation Research Record: Journal of the Transportation Research Board*, *1857*(1), 30-38.

[15] Ahmed, K. I. (1999). *Modeling drivers' acceleration and lane changing behavior* (Doctoral dissertation, Massachusetts Institute of Technology).

[16] Halati, A., Lieu, H., & Walker, S. (1997). CORSIM—corridor traffic simulation model. In *Proceedings of Traffic Congestion and Traffic Safety in the 21st Century: Challenges, Innovations, and Opportunities*, *Chicago, Illinois*, 570–576.

[17] Lee, S. E., Olsen, E. C., & Wierwille, W. W. (2004). *A comprehensive examination of naturalistic lane-changes* (No. FHWA-JPO-04-092). U.S. National Highway Traffic Safety Administration.

[18] Kondyli, A., & Elefteriadou, L. (2012). Driver behavior at freeway-ramp merging areas based on instrumented vehicle observations. *Transportation Letters*, *4*(3), 129-142. doi: 10.3328/TL.2012.04.03.129-141

[19] Hidas, P. (2005). Modelling vehicle interactions in microscopic simulation of merging and weaving. *Transportation Research Part C: Emerging Technologies*, *13*(1), 37-62.

[20] Choudhury, C. F., Ben-Akiva, M. E., Toledo, T., Lee, G., & Rao, A. (2007, January). *Modeling cooperative lane changing and forced merging behavior*. In the 86th Annual Meeting of the Transportation Research Board, Washington, DC.

[21] Kondyli, A., & Elefteriadou, L. (2009). Driver behavior at freeway-ramp merging areas: focus group findings. *Transportation research record: Journal of the Transportation Research Board*, *2124*(1), 157-166. doi: 10.3141/2124-15

[22] Wan, X., Jin, P. J., Zheng, L., Cheng, Y., & Ran, B. (2013). Speed synchronization process of merging vehicles from the entrance ramp: empirical analysis. *Transportation Research Record: Journal of the Transportation Research Board*, *2391*(1), 11-21.

[23] Michaels, R. M., & Fazio, J. (1989). Driver behavior model of merging. *Transportation Research Record: Journal of the Transportation Research Board*, *1213*, 4-10.

[24] Yang, Q., & Koutsopoulos, H. N. (1996). A microscopic traffic simulator for evaluation of dynamic traffic management systems. *Transportation Research Part C: Emerging Technologies*, *4*(3), 113-129.

[25] Lee, G. (2006). *Modeling gap acceptance at freeway merges* (Doctoral dissertation, Massachusetts Institute of Technology).

[26] Xiao, H., Ambadipudi, R., Hourdakis, J., & Michalopoulos, P. (2005). *Methodology for selecting microscopic simulators: Comparative evaluation of AIMSUN and VISSIM* (No. CTS 05-05). Center for Transportation Studies, University of Minnesota, USA. Retrieved from https://conservancy.umn.edu/bitstream/handle/11299/944/CTS-05-05.pdf?sequence=1&isAllowed=y

[27] Daamen, W., Loot, M., & Hoogendoorn, S. P. (2010). Empirical analysis of merging behavior at freeway on-ramp. *Transportation Research Record: Journal of the Transportation Research Board*, *2188*(1), 108-118.

[28] The Federal Highway Administration. (1998). *CORSIM User Manual, Version 1.04*. U.S. DOT, McLean, Virginia.

[29] Myerson, R. (1991). *Game theory: Analysis of conflict*. Harvard University Press. Cambridge, MA.

[30] Toledo, T., Koutsopoulos, H. N., & Ben-Akiva, M. (2007). Integrated driving behavior modeling. *Transportation Research Part C: Emerging Technologies*, *15*(2), 96-112.

[31] Ma, X. (2004). Toward an integrated car-following and lane-changing model based on neural-fuzzy approach. In *Proceedings of Helsinki Summer Workshop*. Retrieved from http://citeseerx.ist.psu.edu/viewdoc/download?doi=10.1.1.527.9124&rep=rep1&type=pdf

[32] Hunt, J. G., & Lyons, G. D. (1994). Modelling dual carriageway lane changing using neural networks. *Transportation Research Part C: Emerging Technologies*, *2*(4), 231-245.

[33] FHWA (2006). *Freeway lane selection algorithm: Fact sheet* (No. FHWA-HRT-06-136). McLean, VA.

[34] Turocy, T. L., & Stengel, B. V. (2001). *Game theory*, Centre for Discrete and Applicable Mathematics (CDAM) Research Report (No. LSE-CDAM-2001-09). London School of Economics, London. Retrieved from http://www.cdam.lse.ac.uk/Reports/Files/cdam-2001-09.pdf

[35] Ross, D. (2019), Game theory. In E. N. Zalta (Eds.), *The Stanford Encyclopedia of Philosophy*.

[36] Barron, E. N. (2008). *Game theory: an introduction*. John Wiley & Sons., New Jersey.

[37] Kim, C., & Langari, R. (2014). Game theory based autonomous vehicles operation. *International Journal of Vehicle Design*, *65*(4), 360-383.

[38] Nash Jr, J. F. (1950). The bargaining problem. *Econometrica: Journal of the Econometric Society*, *18*(2), 155-162. doi: 10.2307/1907266

[39] Talebpour, A., Mahmassani, H. S., & Hamdar, S. H. (2015). Modeling lane-changing behavior in a connected environment: A game theory approach. *Transportation Research Procedia*, *7*, 420-440.

[40] Kita, H. (1999). A merging–giveway interaction model of cars in a merging section: a game theoretic analysis. *Transportation Research Part A: Policy and Practice*, *33*(3-4), 305-312.

[41] Smith, S. A. (1985). *Freeway data collection for studying vehicle interactions - technical report* (No. FHWA/RD-86/023). U.S. DOT, Washington, DC.

[42] Harsanyi, J. C. (1967). Games with incomplete information played by "Bayesian" players, I–III Part I. The basic model. *Management science*, *14*(3), 159-182.

[43] FHWA (2007). *Next generation simulation: US101 freeway dataset*. Retrieved from http://ops.fhwa.dot.gov/trafficanalysistools/ngsim.htm (accessed on Jan. 25, 2016)

[44] FHWA (2017). *An introduction to connected automated vehicles*. 2017 Advanced Technologies in Transportation Symposium. Retrieved from https://www.its.dot.gov/presentations/2017/CAV2017_AdvTechTransport.pdf

[45] U.S. DOT. *Intelligent transportation systems-joint program*. Retrieved from https://www.its.dot.gov/pilots/index.htm (accessed on January 12, 2018)

[46] NHTSA. *U.S. Department of Transportation releases request for comment (RFC) on vehicle-to-everything (V2X) communications*. U.S. DOT, Washington, DC. Retrieved from https://www.nhtsa.gov/press-releases/us-department-transportation-releases-request-comment-rfc-vehicle-everything-v2x (accessed on January 10, 2019)

[47] Campolo, C., Molinaro, A., Iera, A., & Menichella, F. (2017). 5G network slicing for vehicle-to-everything services. *IEEE Wireless Communications*, *24*(6), 38-45.

[48] Chen, S., Hu, J., Shi, Y., Peng, Y., Fang, J., Zhao, R., & Zhao, L. (2017). Vehicle-to-everything (V2X) services supported by LTE-based systems and 5G. *IEEE Communications Standards Magazine*, *1*(2), 70-76.

[49] Schakel, W. J., Knoop, V. L., & van Arem, B. (2012). Integrated lane change model with relaxation and synchronization. *Transportation Research Record: Journal of the Transportation Research Board*, *2316*(1), 47-57.

[50] Kang, K., & Rakha, H. A. (2017). Game theoretical approach to model decision making for merging maneuvers at freeway on-ramps. *Transportation Research Record: Journal of the Transportation Research Board*, *2623*(1), 19-28. doi: 10.3141/2623-03

[51] Kang, K., & Rakha, H. A. (2017, July). *Development of a decision making model for merging maneuvers: A game theoretical approach*. In the Conference on Traffic and Granular Flow, Washington DC.

[52] Kang, K., & Rakha, H. A. (2018). Modeling driver merging behavior: a repeated game

theoretical approach. *Transportation Research Record: Journal of the Transportation Research Board*, *2672*(20), 144-153. doi: 10.1177/0361198118792982

[53] Nash, J. (1951). Non-cooperative games. *Annals of Mathematics*, *54*(2), 286-295.

[54] Sangster, J., Rakha, H., & Du, J. (2013). Application of naturalistic driving data to modeling of driver car-following behavior. *Transportation Research Record: Journal of the Transportation Research Board*, *2390*(1), 20-33.

[55] Rakha, H., & Zhang, Y. (2004). INTEGRATION 2.30 framework for modeling lane-changing behavior in weaving sections. *Transportation Research Record: Journal of the Transportation Research Board*, *1883*(1), 140-149.

[56] Wang, M., Hoogendoorn, S. P., Daamen, W., van Arem, B., & Happee, R. (2015). Game theoretic approach for predictive lane-changing and car-following control. *Transportation Research Part C: Emerging Technologies*, *58*, 73-92.

[57] Yu, H., Tseng, H. E., & Langari, R. (2018). A human-like game theory-based controller for automatic lane changing. *Transportation Research Part C: Emerging Technologies*, *88*, 140-158.

[58] Wang, Z., Wu, G., & Barth, M. (2018). *Distributed consensus-based cooperative highway on-ramp merging using V2X communications* (No. 2018-01-1177). SAE Technical Paper. doi:10.4271/2018-01-1177

[59] Lee, S. E., Olsen, E. C., & Wierwille, W. W. (2004). *A comprehensive examination of naturalistic lane-changes* (No. FHWA-JPO-04-092). U.S. NHTSA.

[60] Brackstone, M., McDonald, M., & Sultan, B. (1999). Dynamic behavioral data collection using an instrumented vehicle. *Transportation Research Record: Journal of the Transportation Research Board*, *1689*(1), 9-16.

[61] Kusano, K. D., & Gabler, H. (2011). Method for estimating time to collision at braking in real-world, lead vehicle stopped rear-end crashes for use in pre-crash system design. *SAE International Journal of Passenger Cars-Mechanical Systems*, *4*(1), 435-443. doi: 10.4271/2011-01-0576

[62] Vogel, K. (2003). A comparison of headway and time to collision as safety indicators. *Accident Analysis & Prevention*, *35*(3), 427-433.

[63] National Safety Council. *Maintaining a Safe Following Distance While Driving*. Driveit HOME: digital driving coach lessons, 48. Retrieved from https://www.nsc.org/Portals/0/Documents/TeenDrivingDocuments/DriveItHome/Lesson48-English.pdf

[64] Marczak, F., Daamen, W., & Buisson, C. (2013). Key variables of merging behaviour: empirical comparison between two sites and assessment of gap acceptance theory. *Procedia-Social and Behavioral Sciences*, *80*, 678-697.

[65] Hwang, S. Y., & Park, C. H. (2005). Modeling of the gap acceptance behavior at a merging section of urban freeway. In *Proceedings of the Eastern Asia Society for Transportation Studies*, *5*, 1641–1656.

[66] Rakha, H., Pasumarthy, P., & Adjerid, S. (2009). A simplified behavioral vehicle longitudinal motion model. *Transportation Letters*, *1*(2), 95-110.

[67] Van Aerde, M. (1995, January). *Single regime speed-flow-density relationship for congested and uncongested highways*. In 74th Annual Meeting of the Transportation Research Board, Washington, DC.

[68] Van Aerde, M., & Rakha, H. (1995, August). Multivariate calibration of single regime speed-flow-density relationships. In *Proceedings of the 6th International Vehicle Navigation and Information Systems Conference*, Seattle, Washington, 334-341.

[69] Gardner, R. (2003). *Games for Business and Economics*, 2nd Edition. John Wiley & Sons, Inc., New Jersey.

[70] FHWA (2007). *Fact Sheet: Next Generation Simulation US101 Dataset* (No. FHWA-HRT-07-030). Retrieved from https://www.fhwa.dot.gov/publications/research/operations/07030/

[71] Chatterjee, B. (2009, December). An optimization formulation to compute Nash equilibrium in finite games. In *2009 Proceeding of International Conference on Methods and Models in Computer Science* (ICM2CS), 1-5.

[72] Rakha, H., & Arafeh, M. (2010). Calibrating steady-state traffic stream and car-following models using loop detector data. *Transportation Science*, *44*(2), 151-168.

[73] Bonabeau, E. (2002). Agent-based modeling: Methods and techniques for simulating human systems. In *Proceedings of the National Academy of Sciences*, *99*(3), 7280-7287.

[74] Macal, C. M., & North, M. J. (2006, December). Tutorial on agent-based modeling and simulation part 2: how to model with agents. In *Proceedings of the 38th Conference on Winter Simulation*, 73-83.

[75] Zheng, H., Son, Y. J., Chiu, Y. C., Head, L., Feng, Y., Xi, H., Kim, S., & Hickman, M. (2013). *A primer for agent-based simulation and modeling in transportation applications* (No. FHWA-HRT-13-054). FHWA, McLean, VA.

[76] Elliott, E., & Kiel, L. D. (2002). Exploring cooperation and competition using agent-based modeling. In *Proceedings of the National Academy of Sciences*, *99*(3), 7193–7194.

[77] Ljubović, V., (2009). Traffic simulation using agent-based models. In *Proceedings of 2009 XXII International Symposium on Information, Communication and Automation Technologies*. doi: 10.1109/ICAT.2009.5348417

[78] Law, A. M., & Kelton, W. D. (2000). *Simulation modelling and analysis*. Second edition, McGraw-Hill, New York.

[79] Xiang, X., Kennedy, R., Madey, G., & Cabaniss, S. (2005, April). Verification and validation of agent-based scientific simulation models. In *Agent-directed Simulation Conference*, 47-55.

[80] Balci, O. (1998). Verification, Validation, and Testing. In *Handbook of Simulation: Principles, Methodology, Advances, Applications, and Practice*, John Wiley & Sons, New York, 335-393.

[81] IEEE News Releases (Nov. 1, 2012). "Look Ma, No Hands!." Retrieved from http://www.ieee.org/about/news/2012/5september_2_2012.html (accessed on May 12, 2019)

[82] Singh, S. (2015). Critical reasons for crashes investigated in the national motor vehicle crash causation survey (No. DOT HS 812 115). NHTSA.

[83] Khodayari, A., Ghaffari, A., Ameli, S., & Flahatgar, J. (2010, September). A historical review on lateral and longitudinal control of autonomous vehicle motions. In *2010 International Conference on Mechanical and Electrical Technology*, 421-429.

[84] Ozguner, U., Stiller, C., & Redmill, K. (2007). Systems for safety and autonomous behavior in cars: The DARPA Grand Challenge experience. In *Proceedings of the IEEE*, *95*(2), 397-412.

[85] Zhang, S., Deng, W., Zhao, Q., Sun, H., & Litkouhi, B. (2013, October). Dynamic trajectory planning for vehicle autonomous driving. In *2013 IEEE International Conference on Systems, Man, and Cybernetics*, 4161-4166.

[86] Yoo, J. H., & Langari, R. (2014). A stackelberg game theoretic driver model for merging. In *Proceedings of the American Society of Mechanical Engineers (ASME) 2013 Dynamic Systems and Control Conference*, *2*. Palo Alto, California, USA. doi: 10.1115/DSCC2013-3882

[87] Fisac, J. F., Bronstein, E., Stefansson, E., Sadigh, D., Sastry, S. S., & Dragan, A. D. (2019, May). Hierarchical game-theoretic planning for autonomous vehicles. In *2019 International Conference on Robotics and Automation (ICRA)*, 9590-9596.

[88] Wang, X. Y., Liu, Y. Q., Wang, F., Liu, Z. G., Zhao, H. X., & Xin, J. F. (2019). Driver's lane selection model based on multi-player dynamic game. *Advances in Mechanical Engineering*, *11*(1).

[89] Van Aerde, M., & Rakha, H. (2015). INTEGRATION© Release 2.40 for Windows: User's Guide-Volume I: Fundamental Model Features. M. Van Aerde & Assoc., Ltd., Blacksburg, VA.

[90] Carter, M., Rakha, H., & Aerde, M. V. (1999). Variability of traffic-flow measures across freeway lanes. *Canadian journal of civil engineering*, *26*(3), 270-281.

[91] European Commission (2017). *Cooperative Intelligent Transport Systems (CITS)*

Platform Final Report Phase II. Retrieved from https://ec.europa.eu/transport/sites/transport/files/2017-09-c-its-platform-final-report.pdf

[92] Moriarty, D. E., & Langley, P. (1998). Learning cooperative lane selection strategies for highways. In *Proceedings of the 15th National Conference on Artificial Intelligence*, Madison, Wisconsin, 684-691.

[93] Jin, Q., Wu, G., Boriboonsomsin, K., & Barth, M. (2014, June). Improving traffic operations using real-time optimal lane selection with connected vehicle technology. In *Proceedings of 2014 IEEE Intelligent Vehicles Symposium*, 70-75.

[94] Tian, D., Li, W., Wu, G., Boriboonsomsin, K., Barth, M., Rajab, S., & Bai, S. (2016, November). Evaluating the effectiveness of V2V-based lane speed monitoring application: a simulation study. In *2016 IEEE 19th International Conference on Intelligent Transportation Systems (ITSC)*, Rio de Janeiro, Brazil, 1592-1597.

[95] Transportation Research Board (2010). *Highway Capacity Manual 2010*. Transportation Research Board, Washington, D.C. 2010. ISBN 978-0-309-16077-3

[96] Rakha, H., & Yang, H. (2016). *Connected Vehicle Freeway Speed Harmonization Systems*. Advanced Operations Focused on Connected Vehicles/Infrastructure (CVI-UTC), Final research report, U.S. DOT.

[97] Rakha, H. (2010). *QueensOD Rel. 2.10-User's Guide: Estimating Origin-Destination Traffic Demands from Link Flow Counts*. M. Van Aerde & Assoc., Ltd.

[98] Google Map, https://www.google.com/maps (accessed on January 22, 2018)